NPS 69-79-014

NAVAL POSTGRADUATE SCHOOL
Monterey, California

THESIS

AN EXPERIMENTAL STUDY OF FILMWISE
CONDENSATION ON HORIZONTAL
ENHANCED CONDENSER TUBING

by

Huseyin Ciftci

December 1979

Thesis Advisor: P.J. Marto

Approved for public release; distribution unlimited.

Prepared for:

Naval Sea Systems Command
Washington, D. C.

NPS 69-79-014

NAVAL POSTGRADUATE SCHOOL
Monterey, California

THESIS

AN EXPERIMENTAL STUDY OF FILMWISE
CONDENSATION ON HORIZONTAL
ENHANCED CONDENSER TUBING

by

Huseyin Ciftci

December 1979

Thesis Advisor: P.J. Marto

Prepared for:

Naval Sea Systems Command
Washington, D. C.

Unclassified

SECURITY CLASSIFICATION OF THIS PAGE (When Data Entered)

REPORT DOCUMENTATION PAGE		READ INSTRUCTIONS BEFORE COMPLETING FORM
1. REPORT NUMBER NPS 69-79-014	2. GOVT ACCESSION NO.	3. RECIPIENT'S CATALOG NUMBER
4. TITLE (and Subtitle) An Experimental Study Of Filmwise Condensation On Horizontal Enhanced Condenser Tubing		5. TYPE OF REPORT & PERIOD COVERED Master's Thesis December 1979 6. PERFORMING ORG. REPORT NUMBER
7. AUTHOR(s) Huseyin Ciftci		8. CONTRACT OR GRANT NUMBER(s)
9. PERFORMING ORGANIZATION NAME AND ADDRESS Naval Postgraduate School Monterey, California 93940		10. PROGRAM ELEMENT, PROJECT, TASK AREA & WORK UNIT NUMBERS 62543N,19814 N0002479WR9G078
11. CONTROLLING OFFICE NAME AND ADDRESS Naval Postgraduate School Monterey, California 93940		12. REPORT DATE December 1979 13. NUMBER OF PAGES 169
14. MONITORING AGENCY NAME & ADDRESS(if different from Controlling Office)		15. SECURITY CLASS. (of this report) Unclassified 15a. DECLASSIFICATION/DOWNGRADING SCHEDULE

16. DISTRIBUTION STATEMENT (of this Report)

Approved for public release; distribution unlimited.

17. DISTRIBUTION STATEMENT (of the abstract entered in Block 20, if different from Report)

18. SUPPLEMENTARY NOTES

19. KEY WORDS (Continue on reverse side if necessary and identify by block number)

Filmwise Condensation
Augmented Heat Transfer
Condenser

20. ABSTRACT (Continue on reverse side if necessary and identify by block number)

Heat transfer and hydrodynamic performance of eight different geometrically enhanced tubes of different metals was determined. Results were compared to a 25.4 mm (1.0 in.) OD, smooth stainless steel tube.

Steam at about 21 kPa (3 psia) was condensed on the outside surface of each enhanced tube, horizontally mounted in the center of a dummy tube Bank. Each tube was cooled on the inside by water.

DD FORM 1 JAN 73 1473 (Page 1)

EDITION OF 1 NOV 65 IS OBSOLETE
S/N 0102-014-6601

Unclassified

SECURITY CLASSIFICATION OF THIS PAGE (When Data Entered)

The overall heat transfer coefficient was determined directly from experimental data. The inside and outside heat transfer coefficients were determined using the Wilson plot technique. The cooling water pressure drop was measured inside the tube and converted to the friction factor in the enhanced section.

The overall heat transfer coefficients of the enhanced tubes were increased as much as 1.9 times, and the corrected pressure drops of the enhanced tubes were as large as 4 times the corresponding smooth tube value for the same cooling water velocity.

The helix angle should be 45° to 60° on the inside surface and 90° on the outside surface of the tube to obtain maximum inside and outside heat transfer coefficients.

Approved for public release; distribution unlimited.

An Experimental Study Of Filmwise Condensation On Horizontal Enhanced Condenser Tubing

by

Huseyin Ciftci
Lieutenant, Turkish Navy
B.S.M.E., Naval Postgraduate School, June 1979

Submitted in partial fulfillment of the
requirements for the degree of

MASTER OF SCIENCE IN MECHANICAL ENGINEERING

from the

NAVAL POSTGRADUATE SCHOOL

ABSTRACT

Heat transfer and hydrodynamic performance of eight different geometrically enhanced tubes of different metals was determined. Results were compared to a 25.4 mm (1.0 inch) OD, smooth stainless steel tube.

Steam at about 21 kPa (3 psia) was condensed on the outside surface of each enhanced tube, horizontally mounted in the center of a dummy tube bank. Each tube was cooled on the inside by water. The overall heat transfer coefficient was determined directly from experimental data. The inside and outside heat transfer coefficients were determined using the Wilson plot technique. The cooling water pressure drop was measured inside the tube and converted to the friction factor in the enhanced section.

The overall heat transfer coefficients of the enhanced tubes were increased as much as 1.9 times, and the corrected pressure drops of the enhanced tubes were as large as 4 times the corresponding smooth tube value for the same cooling water velocity.

The helix angle should be 45° to 60° on the inside surface and 90° on the outside surface of the tube to obtain maximum inside and outside heat transfer coefficients.

TABLE OF CONTENTS

LIST OF TABLES

LIST OF FIGURES

NOMENCLATURE

A	Area (m^2).
A_c	Cross sectional area of test section (m^2), [volume/length].
A_n	Nominal surface area (m^2), [$A_n = \pi D_o L_{ts}$] .
c_p	Specific heat ($kJ/kg \cdot {}^oC$).
D	Diameter (m).
e	Tube groove depth (mm).
f	Friction factor.
G	Flow rate per unit area (kg/m^2 sec).
g_c	Gravitational constant (kg m/N sec^2).
h	Heat transfer coefficient ($W/m^2\ {}^oC$).
HA	Helix angle.
h_{fg}	Latent heat of vaporization (W sec/kg).
j	j factor in Colburn Analogy [$j=StPr^{2/3}$].
k	Thermal conductivity ($W/m{}^oC$).
K	Pressure loss coefficient due to abrupt entrance and exit area changes.
L	Length of test tube (m).
LMTD	Log mean temperature difference (^oC).
$\dot{m}$	Mass flow rate of cooling water (kg/sec).
M	Slope of Wilson Plot output from linear regression program.
Nu	Nusselt number [$Nu=hD/k$].
p	Tube spiral pitch (mm).
P	Pressure (kPa).

Pr Prandtl number ($\mu c_p/k$).

P_w Wetted perimeter (m).

Q Heat flow rate (W)

$\dot{Q}$ Volumetric flow rate (m^3/sec).

R Thermal resistance ($m^{2o}C/W$).

Re Reynolds number (DG/μ).

St Stanton number (Nu/RePr).

t Wall thickness (mm).

T Temperature (^oC).

T_c Temperature of cooling water (^oC).

TPF Tube performance factor (2j/f).

TRAN1 Heat transfer rate from condensation flow rate (kW).

TRAN2 Heat transfer rate from cooling water mass flow rate (kW).

U Overall heat transfer coefficient ($W/m^{2o}C$).

u Water velocity (m/sec).

V Volume (m^3).

Wp Pumping power (kW)

X x axis input to linear regression program.

Y y axis input to linear regression program.

Greek Symbols

Δ Differential.

μ Dynamic viscosity (kg/m hr).

ρ Fluid density (kg/m^3)

Subscripts

a	Augmented.
b	Fluid at the bulk temperature in ^{o}C.
br	Fluid at the bulk temperature in ^{o}K.
c	Corrected.
con	Condensation.
cn	Contraction.
e	Expansion.
ext	External.
h	Hydraulic.
i	Inside or inlet.
l	Liquid.
m	Measured.
n	Nominal.
o	Outside or outlet.
s	Smooth.
sat	Saturation.
ts	Test section.
v	Vapor.
w	Wall.

ACKNOWLEDGMENTS

The work herein has been supported by Mr. Charles Miller, Naval Sea Systems Command, Code 05R.

The author wants to express his grateful appreciation to Professor Paul J. Marto for his continuing encouragement and suggestions during the course of this study.

The author also wishes to thank Mr. Ken Mothersell, Mr. "Junior" Dames and Mr. Ron Longueira for their technical advice.

Finally, I would like to express my appreciation to my wife, Serpil, for her moral support, understanding and encouragement.

I. INTRODUCTION

A. BACKGROUND INFORMATION

Heat exchangers can be designed to be smaller in size which can result in a savings in costs by using enhanced heat transfer surfaces. Enhanced heat transfer methods would also permit lower condenser pressures to be achieved, thus reducing operating costs by saving fuel.

Search [1] conducted an investigation into present condenser design processes and into the feasibility of enhancing heat transfer in Naval condensers. He found that the design of condensers is very conservative. Search also concluded that size and weight savings on the order of 40 percent could be realized depending on the heat transfer enhancement method used.

In recent years many research efforts have been directed to the study of heat transfer enhancement techniques and their application to heat exchanger design. Bergles [2, 3] has summarized extensive works in both single phase and two phase heat transfer enhancement.

Palen, Cham and Taborek [4] published a report for Heat Transfer Research in which they compared the steam condensing performance characteristics of Turbotec tubing and plain tubing. The test tubes were 25.4 mm outside diameter with the plain tube made out of 90-10 copper-nickel and the Turbotec tube made out of 97.5 percent copper. The test condenser had a total of 196 horizontal tubes with 16 vertical rows. The steam pressure was varied between 379 kPa and 724 kPa. The cooling

water velocity varied between 0.457 and 1.219 m/sec. To insure filmwise condensation, all tubes were baked in a large oven at 260° for one hour to remove residue. The experimental results show that for a given Reynolds number the friction factor for a Turbotec tube is from 10 to 15 times that of a smooth tube. On the basis of total bundle performance, the overall heat transfer rate was increased by a factor of 2.5 using the Turbotec tubes compared to the plain tubes.

Eissenberg [5], performed an extensive study of condenser tube heat transfer coefficients using a multi-tube bundle. Watkinson et al. [6] conducted tests on 18 Noranda Forge Fin tubes. Catchpole and Drew [7] conducted experiments on five radially grooved tubes.

Young, Withers and Lampert [8] conducted bundle comparison tests of smooth tubes versus Korodense tubes manufactured by the Wolverine Division of Universal Oil Products. These tests were conducted at two different steam temperatures of 37.8°C and 100°C. Two sizes of tubes were tested: 15.9 mm outside diameter copper tubes and 25.4 mm outside 90-10 copper-nickel tubes. The cooling water velocity through each tube was varied from about 0.91 m/sec to 1.98 m/sec. The overall heat transfer coefficient for the 25.4 mm Korodense tube was 2.2 times that of the smooth tube, while the 15.9 mm Korodense tube's value was 2.7 times that of the smooth tube.

Beck [9] designed a test facility at the Naval Postgraduate School that permits the testing of a single, horizontally mounted, condenser tube. Completion of construction

and testing of this facility was done by Pence [10]. He conducted his tests using a smooth copper-nickel tube. The results of Pence's tests indicated that the facility was technically sound.

Reilly [11] conducted tests on enhanced tubes manufactured by General Atomic Company. Three different spirally fluted aluminum tubes were tested. The tubes were 15.9 mm in nominal outside diameter. Results were compared to 15.9 mm outside diameter smooth copper-nickel and aluminum tubes. Steam at a pressure of 20.7 kPa was supplied to the test condenser. The test tube was cooled by water on the inside at velocities of 0.91 to 7.62 m/sec. The overall heat transfer coefficients of the enhanced tubes were as large at 1.75 times the corresponding smooth tube value for the same mass flow rate of cooling water. The inside heat transfer coefficients were observed to increase by about a factor of 3 while the outside heat transfer coefficients decreased by 10 to 29 percent when compared to smooth tube values.

Fenner [12] conducted tests on ten enhanced tubes of different alloys. The test tubes were 15.9 mm in nominal outside diameter. Results were compared to 15.9 mm outside diameter smooth copper-nickel tubes. Steam at about a pressure of 20.7 kPa was condensed on the outside surface of each enhanced tube, horizontally mounted in the center of a dummy tube bank. Each tube was cooled on the inside by water at velocities of 2.7 to 7.6 m/sec. The overall heat transfer coefficients

of the enhanced tubes were as large as 2 times the corresponding smooth tube value for the same mass flow rate of cooling water.

B. GOALS OF THIS WORK

In view of the developments previously discussed, the purpose of this thesis was then:

1. To determine the heat transfer and performance characteristics of larger diameter enhanced tubes,
2. To determine the pressure drop characteristics of these tubes,
3. To compare each type of enhanced tube's performance to smooth tube operation.

II. EXPERIMENTAL FACILITY

A. TEST FACILITY

The test facility is shown in Figure 1. The layout was designed by Beck [9] and built and tested by Pence [10]. A detailed description of the components used in the various systems may be found in these reports. Only a general description of the various systems will be found within this report. Rotameters, thermocouples and the pressure transducer were calibrated. The calibration procedures of components requiring calibration are outlined by Reilly [11].

B. STEAM SYSTEM

The steam system is shown in Figure 2. For these tests the steam was provided from the house-steam supply. Steam at 34.5 kPa was used for all runs. Steam could be routed around the test condenser to the secondary condenser via the bypass valve (MS-4). The water contained in the steam is removed by the steam separator. The steam continues through the throttle valve (MS-3) where the pressure is reduced. The steam next passes through the desuperheater wherein water from the feed system in injected in order to remove some of the sensible heat from the steam. The steam continues into the test condenser where part of it is condensed on the test tube. The steam not condensed is collected in the vapor outlet and sent to the secondary condenser wherein the latent heat of vaporization is removed. If the house steam fails or if less steam

is required, the boiler can be used to provide steam. The boiler is an electrically heated Fulton Boiler which produces saturated steam at 45.4 kg/hr (13.8 kPa). The steam leaves the boiler through the boiler-isolation valve (MS-1). All steam lines (except the section downstream of MS-3) were insulated with 25.4 mm thick fiberglass insulation.

C. TEST CONDENSER

The test condenser is shown in Figures 3, 4, and 5. Steam enters via the top. It then passes through the expansion section over the baffle separators, and through three layers of 150 mesh screen and a flow straightener into the tube bundle. The condensate collects at the bottom of the test condenser where it flows through two 12.7 mm diameter lines to the test condenser hotwell. The viewing windows, shown in Figures 3 and 4, allow viewing of the condensation process. Pyrex glass windows 12.7 mm thick were used during the experiments.

The tube sheet arrangement is as shown in Figure 5. There are six 25.4 mm OD, stainless steel (AISI 304) tubes arranged in a typical condenser configuration, with a spacing-to-diameter ratio (S/D) of 1.5, around a single test tube.

The test tube is the only tube with water passing through it. This arrangement was selected to best simulate the steam flow conditions in an actual condenser. The test condenser is insulated with a 51 mm thick sheet of Johns-Manville Aerotube insulation.

D. CONDENSATE AND FEEDWATER SYSTEMS

The condensate and feedwater systems are shown in Figure 6. The test condenser hotwell collects the condensate from the test tube, while the secondary condenser hotwell collects the condensate from the secondary condenser, test condenser hotwell and desuperheater. Valve C-1 allows isolation of the test condenser hotwell from the secondary condenser hotwell. The condensate is pumped from the secondary condenser hotwell to the feedwater tank or house-steam return. When using house-steam, the feed pump should be closed.

If the boiler is used, the feed pump is operated. The feed pump routes the water from the feedtank to the boiler via a solenoid-controlled valve, a hot-water filter and a boiler isolation valve. The feedwater temperature is maintained between 54.4°C and 60.0°C by thermostat controlled heaters. This reduces fluctuations in the boiler output and provides a source of water at a temperature near saturation for the desuperheater. The condensate and feedwater lines are insulated with 25.4 mm thick Johns-Manville Aerotube insulation.

E. COOLING WATER SYSTEM

The cooling water system is shown in Figure 7. The water is pumped from the supply tank via a 5.6 kW pump through a filter and cooling tower. The cooling water for the test condenser also is pumped via a 6.7 kW pump. The water is routed to the test tube via two rotameters. The bypass valve CW-4 is provided to permit an increased volume of water to flow through the supply tank.

The dry cooling tower was constructed using four large plate/fin radiators connected in series. The water was directed through the radiators and outside air was forced over the cooling surface by a centrifugal fan.

The system piping was reduced from 63.5 mm to 25.4 mm diameter at a distance of approximately 1.5 m ahead of the test condenser to insure fully developed flow at the test-tube entrance. The cooling water lines were not insulated.

F. SECONDARY SYSTEMS

1. Desuperheater

The desuperheater removes sensible heat from the superheated steam by injecting feed water at between about 40°C and 60°C. The feedwater flow into the desuperheater is controlled by valve FW-4 and measured by a rotameter. The excess water is collected in the secondary condenser hotwell.

2. Vacuum System

The vacuum system is shown in Figure 8. The vacuum in the test condenser is maintained by a mechanical vacuum pump and a vacuum regulator which induces an air leak into the vacuum line. A cold trap at the inlet of the vacuum pump forces incoming vapor to pass over a system of refrigerated copper coils. This is to remove entrained water from the vacuum line and prevent moisture contamination of the vacuum pump oil. The vacuum pump outlet is vented through a root exhaust fan to avoid a health hazard from breathing any oil vapor that may be exhausted by the pump.

G. INSTRUMENTATION

1. Flow Rates

Fulton rotameters were used to measure the flow rate of water in the cooling water system and the desuperheater.

2. Pressure

Several different types of pressure measurement devices were used in this facility. They were: a Bourdon tube pressure gage which was used to measure boiler pressure, a compound gage which was used to measure the house steam pressure, an absolute pressure transducer and a 1.0 m mercury manometer which were used to measure the test condenser pressure, and a 3.6 m mercury manometer which was used to measure the cooling water pressure drop across the test tube.

3. Temperature

There were two types of thermocouples used in this facility. Stainless steel sheathed, copper-constantan thermocouples were used as the primary temperature monitoring devices. Table 1 lists the locations monitored. Teflon coated, copper-constantan thermocouples were used as secondary measuring devices. Table 2 lists the locations monitored using these thermocouples.

4. Data Collection

An autodata collection system was utilized to record and display the temperatures in degrees Celsius obtained from the primary thermocouples and to record and display the pressure in cm.Hg inside the test condenser. See Table 1 for channel numbers of the temperature monitoring devices.

A 28 channel digital pyrometer was utilized to display the temperatures obtained from the secondary thermocouples. See Table 2 for channel numbers.

H. TEST TUBES

The enhanced tubes tested during this study were manufactured by several companies. Two special tubes were manufactured by General Atomic Co. They are made of stainless steel and have helical flutes on both the inside and outside surfaces, which are formed by running a flat strip through rollers which cause the flat surface to become wavy. The wavy strip is then spirally wound and seam-welded to form a tube.

Two types of Turbotec tubing were made by the Spiral Tubing Corporation. These tubes are three-start, helically fluted, with flute pitch determining tube type. All Turbotec tubes were manufactured of copper. One of these tubes was manufactured with micro grooves.

Two tubes were manufactured by Yorkshire Imperial Metals Co. These tubes are three-start, and were manufactured of 90-10 copper-nickel.

Also one special Hitachi tube and a special German tube were tested during this study.

The test tubes which were tested are shown in Figures 9, 10, and 11.

III. EXPERIMENTAL PROCEDURES

A. INSTALLATION AND OPERATING PROCEDURES

1. Preparation Of Condenser Tubes

Prior to any run, the condenser tubes had to be properly prepared to insure filmwise condensation. The cleaning procedures are listed in Appendix A. The wall thermocouples also had to be prepared and installed in such a manner as to reduce the possibility of introducing errors.

2. System Operation And Steady State Conditions

Pence [10] developed and Reilly [11] modified a detailed set of operating procedures for this system. They are included, with minor changes in this report as Appendix B.

In general it takes about two hours from initial light off until steady-state conditions are established. After installation of the test tube is complete, the vacuum system can be activated. The data collection system is programmed, including setting the date and time in accordance with Reference [13]. The cooling water system is placed in operation. Both rotameters are set at about 50 percent flow to allow adequate venting of both legs of the 3.66 meter manometer. The rotameters are then reset to the lowest flow point for system operation. The steam system can now be placed into operation.

Steady-state conditions must be established prior to data collection. To determine this, two parameters were monitored. They were the cooling water inlet temperature and

the steam vapor temperature. The cooling water inlet temperature did not rise more than 0.6°C/hr. The steam vapor temperature did not vary more than 3.3°C between the six vapor thermocouples in the condenser. The change in temperature of an individual thermocouple never exceeded 0.3 °C/min. The steaming conditions and cooling water flow conditions remained constant while establishing steady-state conditions. The time for the system to stabilize was generally about one hour which is in agreement with that reported by Reilly [11] and by Fenner [12].

3. Maintenance Procedures

The condenser glass window, the inside surface of the condenser and the dummy tubes of the condenser required cleaning after each run to insure filmwise condensation. The secondary condenser hotwell required cleaning after approximately five runs.

B. DATA REDUCTION PROCEDURES

Data obtained in this thesis were evaluated using the smooth inside diameter and hydraulic diameter. As mentioned in Reilly [11], in evaluating the data obtained from the heat transfer runs, two objectives were established. The first of these was to present the data in such a way as to make it immediately useful to the designer. The second objective was to establish a reduction scheme that would allow the comparison of enhanced tubes based on their actual internal surface areas.

1. Reduction Based On The Smooth End Diameter, D_i

As mentioned above, to meet the condenser designer's needs, it was felt that the data should be reduced using the smooth end diameter. This would allow a direct substitution of an enhanced tube for a smooth tube and is especially important when considering the comparison of a wide variety of tube types. In addition, a nominal area was defined. The nominal area was based on the outside surface area of a smooth tube $\left[\bar{A}_n = \pi D_o L_{ts}\right]$.

Appendix C, the sample calculations, is a complete listing of the equations used to evaluate the data. Appendix D is a derivation of the probable error in the data reduction equations, followed by a sample error analysis for the 45^o helix angle (HA) General Atomic tube, Run 10.

a. Overall Heat Transfer Coefficient

The method employed to arrive at the overall heat transfer coefficient is straightforward and similar to that employed by many researchers in the past.

The heat transfer rate to the cooling water is given by

$$Q = \dot{m} c_p \, (Tc_o - Tc_i) \qquad (1)$$

The heat transfer rate from the steam is given by

$$Q = \dot{m}_{con} \left[c_{pv} \, (T_v - T_{sat}) + h_{fg} + c_{p(con)} (T_{sat} - T_{con}) \right] \qquad (2)$$

The heat transfer rate can also be found from the overall heat transfer coefficient by

$$Q = U_n A_n LMTD \tag{3}$$

where

$$LMTD = \frac{(T_v - Tc_i) - (T_v - Tc_o)}{\ln\left[\frac{T_v - Tc_i}{T_v - Tc_o}\right]} \tag{4}$$

After combining equations (1), (3), and (4) it is found that

$$U_n = \frac{\dot{m} c_p}{A_n} \ln \left[\frac{T_v - Tc_i}{T_v - Tc_o}\right] \tag{5}$$

A schematic illustration of the procedures to arrive at Un is shown in Figure 12.

To remove the effect of the tube wall material, a corrected heat transfer coefficient is found from

$$U_c = \frac{1}{\frac{1}{U_n} - Rw} \tag{6}$$

where

$$Rw = \frac{A_n \ln (r_o/r_i)}{2\pi k_w L_{ts}} \tag{7}$$

b. Inside Heat Transfer Coefficients

The Nusselt number on the inside is found from the Sieder Tate relationship, found in Holman [14] as:

$$Nu = \frac{h_i D_i}{k_b} = C_i Re^{0.8} Pr^{1/3} (\mu/\mu_w)^{0.14} \tag{8}$$

In the above equation, C_i is referred to as the Sieder Tate constant. The remainder of the right hand side of the above equation $[\ Re^{0.8}Pr^{1/3}\ (\mu/\mu_w)^{0.14}\ ]$ will be referred to as the Sieder Tate parameter, and the procedure for arriving at this value is illustrated schematically in Figure 13. The Wilson plot is used to arrive at the value of the Sieder Tate constant. The Wilson plot was developed in 1915 by Wilson [15], and has been modified by several researchers. The procedure used in this research was developed by Briggs and Young [16].

The Wilson plot is merely a plot of $1/U_n$ versus the inverse of the Sieder-Tate parameter which should be a straight line when varying the cooling water velocity. The reasoning behind the Wilson plot can be seen in the following development.

The overall heat transfer coefficient can be written as:

$$U_n = \frac{1}{\frac{D_o}{D_i h_i} + Rw + \frac{1}{h_o}} \qquad (9)$$

The inverse of this equation (9) is:

$$\frac{1}{U_n} = \frac{D_o}{D_i h_i} + Rw + \frac{1}{h_o} \qquad (10)$$

If $(Rw + \frac{1}{h_o})$ is assumed to be constant* and equation (8) is solved for h_i in terms of the Sieder-Tate parameter,

---

* Actually, h_o is not constant. As cooling water velocity (v) increases then h_o decreases slightly.

equation (10) can be rewritten as:

$$\frac{1}{U_n} = \frac{Do}{C_i k_b} Re^{-0.8} Pr^{-1/3} (\mu/\mu_w)^{-0.14} + B \qquad (11)$$

where $B = R_w + \frac{1}{h_o}$

The form of equation (11) is then exactly that of a straight line,

$$Y = Mx + B \qquad (12)$$

where:

$$Y = \frac{1}{U_n} \qquad (12a)$$

$$X = \frac{1}{\text{Sieder Tate parameter}}, \text{ and} \qquad (12b)$$

$$M = \frac{D_o}{C_i k_b} \qquad (12c)$$

The values of $1/U_n$ and the Sieder-Tate parameter are obtained by varying the water velocity and holding the other parameters, such as water temperatures, steam vapor temperatures and condenser tube wall temperature, nearly constant. When $1/U_n$ is plotted versus $Re^{-0.8} Pr^{-1/3} (\mu/\mu w)^{-0.14}$ a linear regression subroutine [17] fits these points to a straight line and then solves for the slope, M, and the intercept, B. Knowing the slope, M, the Sieder Tate constant, C_i, can be found from equation (12c). The inside heat transfer coefficient, h_i, is then found from equation (8).

Once the inside heat transfer coefficient, h_i, is known, then the Nusselt number can be solved for in equation (8), to find the Stanton number,

$$St = \frac{Nu}{RePr} = \frac{h}{c_p G} \tag{13}$$

The cooling water properties (ρ, μ, k, c_p, Pr) are obtained as shown in Appendix C. Appendix C also demonstrates the procedure for arriving at the water viscosity evaluated at the condenser tube wall, μ_w.

c. Outside Heat Transfer Coefficient

The outside heat transfer coefficient, h_o, can now be found from equation (9). Figure 14 schematically illustrates the various steps outlined above.

d. Friction Factor

The friction factor for the test tube is found from:

$$f_{ts} = \frac{(\rho_b)(\Delta P_{ts})(2g_c)}{4(L_{ts}/D_i)\ G^2} \tag{14}$$

ΔP_{ts} is the pressure drop in the enhanced section of the test tube. The measured pressure drop, ΔP_m is taken over the entire tube length. Since the enhanced section is only 0.972m long, the pressure drop over each of the smooth ends must be subtracted off of the measured pressure drop. This is done by calculating the friction factor in the smooth ends using:

$$f_s = \frac{0.079}{Re^{0.25}} \quad \text{for } Re = 30{,}000 \tag{15}$$

or

$$f_s = \frac{0.046}{Re^{0.2}} \quad \text{for } Re = 30{,}000 \tag{16}$$

The smooth-end-section pressure drops can then be calculated from,

$$\Delta P_s = \frac{(f_s)(4)(L_s/D_i)(G^2)}{(\rho_b)(2g_c)} \qquad (17)$$

The cross sectional flow area of the enhanced section of the test tube is different from the cross sectional flow area of the smooth end of the tube. Therefore, the water undergoes an expansion and a contraction at the exit and entrance to the enhanced section of the tube. Associated with the expansion and contraction processes are certain irreversible losses which cause additional pressure drops to occur. These pressure drops also should be subtracted off of the measured pressure drop and are estimated following the calculational procedure as shown in reference [18]:

$$\Delta P_{e/cn} = \rho V_{ts}^2 (K_e + K_{cn}) \qquad (18)$$

Since the variations in the contraction and expansion coefficients K_c and K_e are small over the range of Reynolds numbers used, an average of these values was used in equation (18).

Therefore, ΔP_{ts} is found using equations (17) and (18):

$$\Delta P_{ts} = \Delta P_m - \Delta P_s - \Delta P_{e/cn} \qquad (19)$$

and the friction factor for the test section is determined according to equation (14).

e. Performance Criteria

To compare the enhanced, or augmented tubes with the smooth tube, it was necessary to use some meaningful performance criteria. The following procedures are similar to those outlined by Reilly [11] and Fenner [12].

(1) Colburn Analogy. Use of the Colburn Analogy, as found in Reference [19], provided one such criterion. Using this analogy, the heat transfer performance is compared to the friction factor performance as seen by the reaction:

$$j = StPr^{2/3} = \frac{f}{2} \tag{20}$$

(2) Surface Area Ratios. Bergles [3] outlines several performance criteria based on the inside heat transfer coefficients by solving for the ratio of augmented to smooth tube surface areas while holding various parameters constant.

(a) External Resistance Equal To Zero. If the external thermal resistance is set equal to zero, and the pumping power is allowed to increase, one such ratio is defined by

$$\frac{A_a}{A_s} = \frac{h_s}{h_a} = \frac{Nu_s/Pr^{1/3}(\mu/\mu_w)^{0.14}}{Nu_a/Pr^{1/3}(\mu/\mu_w)^{0.14}} \tag{21}$$

which assumes that Q, $\dot{m}$, D_i, T_b and LMTD* are constant, and $R_{ext} = Rw + 1/h_o = 0$. In equation (21) the augmented heat transfer coefficient h_a is the value h_i referred to earlier.

---

* During these tests, the LMDT was not really kept constant, but was allowed to vary between 37 and 48°C.

In this situation, the flow velocities for the smooth and augmented tubes are the same.

The area ratio defined by equation (21) does not, however, take into account the increase in pressure drop and hence the increase in friction factor caused by enhancement techniques. The increase in pressure drop can be included when evaluating the performance of an enhanced tube compared to that of a smooth tube. Bergles [3] shows this by defining an area ratio for constant pumping power as well as for the conditions defined earlier.

The pumping power is given by:

$$Wp = \left(\rho v \frac{\pi D^2}{4}\right) 4f \left(\frac{L}{D}\right) \left(\frac{v^2}{2g_c}\right) \tag{22}$$

$$Wp = \left(\frac{\rho}{2g_c}\right) (\pi DL) f v^3$$

where πDL is the inside surface area for the tube in question. By setting the pumping power of a smooth tube equal to the pumping power of an enhanced tube, it is found that:

$$\frac{A_a}{A_s} = \frac{v_s^3 f_s}{v_a^3 f_a} = \frac{Re_s^3 f_s}{Re_a^3 f_a} \tag{23}$$

Notice, that in this situation of constant pumping power, the flow velocities and hence Reynolds numbers are different for the smooth and the augmented tube. In equation (23) the augmented Reynolds number Re_a and friction factor f_a are the values Re and f_{ts} referred to earlier.

The heat flow rate is given by:

$$Q = h_i A_i LMTD_i \tag{24}$$

Since the heat flow is also assumed to be constant in both the enhanced and smooth tubes, the area ratio can be found

$$\frac{A_a}{A_s} = \frac{h_s}{h_a} = \frac{Nu_s/Pr^{1/3}(\mu/\mu_w)^{0.14}}{Nu_a/Pr^{1/3}(\mu/\mu_w)^{0.14}} \tag{25}$$

Equation (23) can now be set equal to equation (25) to show:

$$\frac{A_a}{A_s} = \frac{Nu_s/Pr^{1/3}(\mu/\mu_w)^{0.14}}{Nu_a/Pr^{1/3}(\mu/\mu_w)^{0.14}} = \frac{Re_s^3 f_s}{Re_a^3 f_a} \tag{26}$$

If Nu_s is replaced in the above equation by the Sieder-Tate relationship as found in Holman [14]:

$$Nu_s = 0.027 Re_s^{0.8} Pr^{1/3}(\mu/\mu_w)^{0.14} , \tag{27}$$

and f_s is replaced by equation (16)

$$f_s = \frac{0.046}{Re_s^{0.2}} , \tag{16}$$

equation (26) can be solved for the smooth tube Reynolds number in terms of the augmented conditions:

$$Re_s = \left[\frac{0.027 f_a Re_a^3}{0.046 Nu_a/Pr^{1/3}(\mu/\mu_w)^{0.14}} \right]^{0.5} \tag{28}$$

In this expression,

$$Re_s = \frac{G_s D_i}{\mu} = \frac{\rho D_i v_s}{\mu} \quad , \text{ and} \tag{29}$$

$$Re_a = \frac{G_a D_i}{\mu} = \frac{\rho D_i v_a}{\mu} \quad . \tag{30}$$

To find the area ratio, the procedure begins by choosing a value of Re_a. The related quantities f_a and $Nu_a/Pr^{1/3}(\mu/\mu_w)^{0.14}$ are then found from experimental data. Equation (28) is solved for Re_s, and knowing Re_s and f_s from equation (16), equation (26) can be solved for the resulting ratio.

(b) External Resistance Not Equal To Zero. Since a sizeable portion of the overall resistance in a naval condenser could be caused by the wall resistance and the outside thermal resistance, the area ratios as defined by Bergles [3] should be expanded to include these external resistances. If the heat flow is given by equation (3):

$$Q = U_n A_n \text{ LMTD} \tag{3}$$

and thin tube-wall is assumed, then the external resistance effects on the area ratio can be included in the analysis. The wall thickness must be assumed to be small since the nominal area is based on an outside diameter of the tube.

Invoking all of the assumptions made earlier, then the results of the constant pumping power case are again:

$$\frac{A_a}{A_s} = \frac{v_s^3 f_s}{v_a^3 f_a} \tag{23}$$

In addition, constant heat flow results in:

$$\frac{A_a}{A_s} = \frac{U_s}{U_a} \tag{31}$$

As before, these two area ratios can be set equal, and it is found that:

$$\frac{A_a}{A_s} = \frac{U_s}{U_a} = \frac{v_s^3 f_s}{v_a^3 f_a} \tag{32}$$

As mentioned by Search [1], for smooth tubes, it is found in general that the overall heat transfer coefficient can be correlated by:

$$U_s = C\sqrt{v_s} = F_1 F_2 F_3 C'\sqrt{v_s} \tag{33}$$

where

C' = empirically determined coefficient

F_1 = cleanliness correction factor

F_2 = material correction factor

F_3 = inlet water correction factor .

Therefore, C is a coefficient which varies with tube size, material and water inlet temperature. Also, from equation (16), it is known that

$$f_s = \frac{0.046}{Re_s^{0.2}} \tag{16}$$

When equation (16) and (33) are substituted into equation (32), together with the use of equation (29), the smooth tube velocity can be found:

$$v_s = \left[\frac{f_a v_a^3 C}{(U_a)(0.046)} \left(\frac{\rho D_i}{\mu} \right)^{1/5} \right]^{1/2.3} . \qquad (34)$$

As done in the earlier case, the procedure here is to select a velocity in the augmented tube, v_a. Values of f_a and U_a are determined from experimental data, and v_s can be found from equation (34). Knowing v_s, then equation (33) is solved for U_s and equation (32) is solved for the area ratio.

In selecting the values of the constants to substitute into equations (34), the following procedures were utilized:

(1) U_a was corrected to 21.1°C coolant inlet temperature using the procedure defined in Reference [20].

(2) The dynamic viscosities used were obtained in the data reduction program at each flow point.

(3) C was determined by using the values of U_n and v_s for smooth stainless steel tube in Run 9, and solving C' in equation (33) with application of correction factors defined in Reference [20]. For run 9, the average value of C=2016 was computed. The value for C' was not a constant over the range of flows observed; therefore, an average value of C'=2922 was computed and used.

2. Reduction Based On The Hydraulic Diameter, D_h

The reduction procedures for this method were similar to the procedures used for the reduction based on D_i. The major obstacle in obtaining meaningful results was in

determining the enhanced section's geometry and, once determined, how best to apply it to the available equations.

For General Atomic tubes, the cross-sectional area and wetted perimeter information provided by General Atomic Company was used. For Turbotec tubes, the volumes of the enhanced sections were measured and, by using the length of the enhanced section, the cross-sectional area was obtained. The wetted perimeter was found by using a thin wire from an enlarged view of the tube, Figure 15. The hydraulic diameter was then found from:

$$D_h = \frac{4Ac}{Pw} \tag{35}$$

Similar problems were encountered in determining the wall thickness and subsequent wall resistance.

To introduce this geometry into the equations used to solve for the heat transfer coefficients, it is first necessary to recall that the resistance to heat flow across a tube is equal to the sum of the individual resistances as shown earlier. Therefore,

$$\frac{1}{A_o U_o} = \frac{1}{A_o h_o} + \frac{Rw}{A_{met}} + \frac{1}{h_i A_i} \tag{36}$$

where:

$$A_o = Pw_o L_{ts} \tag{37}$$

$$A_i = Pw_i L_{ts} \tag{38}$$

$$A_{met} = P_{bar} L_{ts} \tag{39}$$

$$P_{bar} = (Pw_o + Pw_i)/2 \tag{40}$$

By setting $1/A_oU_o=1/A_nU_n$, and multiplying through by A_o allows us to obtain the overall heat transfer coefficient based on the same nominal geometry that was used in the plain-end reduction. The equation takes the form:

$$\frac{A_o}{A_nU_n} = \frac{1}{R_o} + \frac{A_oRw}{A_{met}} + \frac{A_o}{A_ih_i} \qquad (41)$$

Equation (41) is solved exactly as was equation (10) in the first section to obtain the Wilson plot. The inside and outside heat transfer coefficients are then obtained as they were in the plain-end reduction except as modified by the different goemetry.

Other reductions used are identical to the smooth end reduction scheme except as modified by different geometry.

3. Data Reduction Computer Program

An existing computer program of Reilly [11] for reduction of data was modified to include heat transfer rate equations (1) and (2). Details of the program may be found in Reilly [11].

IV. RESULTS AND DISCUSSION

A. INTRODUCTION

Figure 16 is the definition of helix angle, groove depth, pitch, tube inside diameter, tube outside diameter and tube wall thickness. Table 3 lists special characteristics of the General Atomic, Turbotec and Yorkshire tubes. Table 4 lists the various runs made and the corresponding tubes used during these tests. Tables 5 through 13 contain all the raw data used to evaluate the performance of the enhanced and smooth tubes.

Three runs were made for practice. For the stainless steel smooth tube, six runs were made with different tube bundle layouts as shown in Figure 17. The corrected overall heat transfer coefficient versus cooling water velocity for the smooth tube with different bundle configurations is shown in Figure 18. It was found that the corrected overall heat transfer coefficient was different for every bundle configuration. The highest corrected overall heat transfer coefficient was found for configuration F. This configuration gives good steam flow around the test tube when comparing with the other configurations, and it was therefore used for testing the enhanced tubes.

During these tests, good filmwise condensation was obtained except for the Turbotec tube (T-1). Run 14 and Run 15 were made with the same tube and the tube was cleaned three different times. Filmwise condensation could not be obtained for the Turbotec tube (T-1). The tube was then heated at 260^{o}C for one hour, and was tested again. Mixed condensation was obtained

as seen from Figure 19. (For the conditions shown, the cooling water velocity is 6.94 m/sec.) Notice that most of the grooves are covered with condensate but there are some spots on the grooves in the right side of the photographs. These spots correspond to tiny drops on the surface.

Since a linear regression subroutine was used to obtain the slope for the Wilson Plot, the heat transfer information obtained was very much dependent on how well the linear regression program could fit the data.

Table 14 through 22 contain all the results obtained, based on the plain-end inside-diameter.

B. RESULTS BASED ON SMOOTH END DIAMETER, D_i

1. Heat Transfer Coefficients

The corrected overall heat transfer coefficients versus cooling water velocity are shown in Figures 20 and 21. Tube Y-1 shows an increase of about 56 percent, and tube Y-2 shows an increase of about 51 percent over the smooth tube (S-1) value at a cooling water velocity of 5 m/sec. Tube GA-1 shows an increase of about 56 percent while tube GA-2 shows an increase of about 24 percent at the same cooling water velocity.

As seen from Figure 21, tube T-2 shows an increase of about 54 percent while the tube T-1 shows an increase of about 87 percent. The special tube G-1 shows an increase of about 18 percent while tube H-1 shows a decrease of about 40 percent.

Reilly [11] reported experimental results of 15.88 mm nominal outside diameter 45° HA and 30° HA General Atomic tubes.

Figure 22 shows comparisons of the corrected overall heat transfer coefficients versus cooling water velocity for the 20.5 mm and 15.88 mm nominal outside diameter General Atomic tubes. As shown in Figure 22, larger diameter tubes have lower overall heat transfer coefficients. From Nusselt Theory, $h_o \propto 1/D^{1/4}$. Therefore as D increases, h_o should decrease as shown (+ vs. # symbols). Notice that Run 20 data, for HA=30° is lower than other tubes. This was an unexpected result.

2. Overall Heat Balance

Figures 23 and 24 demonstrate how close the heat transfer rates compared. In these figures TRAN1 represents the heat transfer rate as measured by the collected condensate whereas TRAN2 represents the heat trahsfer rate as measured by the cooling water flow. In general TRAN1 is below TRAN2. The mass flow rate used in the calculation of TRAN1 was based on measurements of condensate in the hotwell. The drainage of the condensate was not steady-state during the tests. A lower measured mass flow of condensate than the actual mass flow of condensate should be expected due to that unsteady condition. Further, since the calculation at TRAN1 is based on the measured vice actual mass flow rate, it should be no surprise that TRAN1 will be somewhat lower than the actual heat transfer rate. Since no equivalent unsteady condition is involved in the measurement leading to the calculation of TRAN2, we would expect TRAN1 to be lower than TRAN2.

3. Pressure Drop

Figures 25 and 26 show comparisons of the corrected pressure drop versus cooling water velocity for all tubes. Tube Y-1 shows an increase of about 138 percent, and tube Y-2 shows an increase of about 86 percent over the smooth tube value (S-1) at 5 m/sec cooling water velocity. Tube GA-1 shows an increase of about 32 percent while tube GA-1 shows an increase of about 6 percent at the same cooling water velocity.

As seen from Figure 26, tube T-1 shows an increase of about 295 percent while the tube T-2 shows an increase of about 250 percent over the smooth tube (S-1) value at 5 m/sec cooling water velocity. Tube G-1 shows an increase of about 130 percent while tube H-1 shows an increase of about 55 percent at the same cooling water velocity.

4. Sieder-Tate Parameters

The Wilson plots for all tubes are shown in Figures 27 and 28. These figures show that the generated lines fit the data very well within the uncertainty bands around the data points. As seen in Table 14, the Sieder-Tate constant for the smooth tube was about 0.024, which is in agreement with the range of values of 0.023 to 0.027 found in the literature.

Figure 29 shows that tubes GA-1 and Y-1, with an average C_i of 0.040, reflect a factor of about 1.67 increase over that for a smooth tube. Tube GA-2 with a C_i of about 0.032, shows a factor of about 1.33 increase over the smooth tube value, which is slightly better than that for tube Y-2.

Figure 30 shows also that tubes T-1 and T-2 with a C_i of about 0.040, gives an improvement factor of about 1.67, and tube G-1 with a C_i of about 0.037, shows a factor of about 1.54 increase over the smooth tube value. These increases presumably are due to increased surface area, turbulence and swirl effects.

The Sieder-Tate constant was found to be about 0.019 for tube H-1, which is below the smooth tube value. As seen from Table 21, the corrected overall heat transfer coefficients for this tube are less than the smooth tube, and increase very slowly with increasing cooling water velocity. This tube had a special outside surface structure as shown in Figure 9. Because of this structure, it tended to hold the condensate on the outside surface. Also, the outside heat transfer coefficients were found to be about 100 percent less than the smooth tube value. Therefore, this tube's data is not meaningful for comparison purpose.

5. Friction Factor

The friction factor results are given in Figures 31 and 32. Here, as expected, the friction factor for the enhanced tubes are greater than for smooth tube except the H-1 and GA-2 tubes. The friction factors for these tubes are near

the smooth tube value. The reason is seen in the following friction factor equation:

$$f_{ts} = \frac{(\rho_b)(\Delta P_{ts})(2g_c)}{4(L_{ts}/D_i)G^2}$$

As seen from Figures 24 and 25, tubes GA-2 and H-1 have pressure drops near the smooth tube value; also GA-2 and H-1 have diameters which are less than the smooth tube diameter so that their friction factors will decrease.

Tube T-1 shows the largest friction factor overall, and tubes T-2 and Y-1 also show large friction factors for the other tube types, which have the most severe corrugations and groove depths.

In examining the tube characteristics given in Table 3 and Figures 31 and 32 together, Tubes T-1 and T-2 have the largest groove depth and they have the highest friction factor. Tube Y-1 has a 0.94 mm groove depth and a 80^{o} HA; therefore it has a larger friction factor than the other tube types. Tubes GA-1 and GA-2 have 1.10 mm groove depth but they have a larger number of groove starts so that the distance between ribs is very small. Therefore, these tubes have the lowest friction factor compared with the other tubes. It is apparent that as tube groove depth increases and pitch decreases (or helix angle increases), the friction factor increases .

6. Tube Performance Criteria

a. Colburn Analogy

The Colburn Analogy can be used to define a performance factor that directly relates heat transfer to pressure

drop. Comparisons of this tube performance factor (2j/f) versus Reynolds number are shown in Figures 33 and 34. As given by this ratio the effect of friction factor is seen to be relatively more important than heat transfer for the tubes T-1, T-2, Y-1 and Y-2 which have high friction factors. Tubes GA-1 and GA-2 have friction factors near the smooth tube results, and these lower friction factors give higher results for 2j/f.

b. Surface Area Ratios

Use of surface area ratios as defined by equation (26) provides an additional performance parameter more useful perhaps for the design engineer than the Colburn Analogy. Neglecting the external thermal resistance ($R_{ext} = 0$), Figure 35 shows that this area ratio makes tubes GA-1, GA-2, and Y-1 appear very good for condenser use. Tubes Y-2 and G-1 appear to perform like the smooth tube. Tube GA-1 shows the greatest reduction in required surface area. It is also seen that tubes GA-2 and Y-1 appear to perform well.

The area ratio for the smooth tube (S-1) is found to be about 1.14. Actually this ratio should be very close to unity. The reason for the higher area ratio is seen in the following equation:

$$\frac{A_a}{A_s} = \frac{Nu_s/Pr^{1/3}(\mu/\mu_w)^{0.14}}{Nu_a/Pr^{1/3}(\mu/\mu_w)^{0.14}} = \frac{Re_s^{\,3} f_s}{Re_a^{\,3} f_a} \qquad (26)$$

where;

$$Nu_s = 0.027 Re_s^{0.8} Pr^{1/3} (\mu/\mu_w)^{0.14} \quad (27)$$

$$Re_s = \left[\frac{0.027 f_a Re_a^3}{0.046\ Nu_a/Pr^{1/3} (\mu/\mu_w)^{0.14}} \right]^{0.5} \quad (28)$$

As seen from equations (27) and (28), the Sieder-Tate constant for the smooth tube is 0.027, but the actual Sieder-Tate constant found from experimental data is 0.024, leading to the apparent discrepancy in area ratio.

Area ratios for a non-zero external resistance can also be found, and are shown in Figure 36. Again, tube GA-1 is seen to have the best overall performance. Tube T-1 has the misleading data due to mixed condensation and therefore the curve is dashed.

When comparing Figures 35 and 36, the taking into account of R_{ext} has a significant effect on the results. The area ratio, as expected, will increase when the wall resistance is taken into account.

c. Internal And External Performance

Table 23 gives ratios of the average Sieder-Tate coefficients for the augmented tube data ($\bar{C}_{ia}$) to that of smooth tube data ($\bar{C}_{is}$), and average outside heat transfer coefficients for the augmented tube data ($\bar{h}_{oa}$) to that of smooth tube data ($\bar{h}_{os}$) for each tube type.

The study of Table 3 and 23 indicates that the inside and outside heat transfer coefficients are related to change in pitch (for approximately constant groove depth).

This is shown in Figures 37 and 38. In Figure 37, the value of ratios of $\bar{C}_{ia}/\bar{C}_{is}$ is plotted versus varying pitch (for constant groove depth). The trends of the data in the $\bar{C}_{ia}/\bar{C}_{is}$ curve reveal that there is perhaps an optimum pitch (at a constant groove depth) to increase the inside heat transfer coefficient. This could be due to the fact that as pitch changes from being very large to very small, the nature of the internal flow changes from predominately swirling motion to a flow dominated by large scale turbulent mixing. The optimum pitch could therefore be one that produces a combination of these mechanisms.

In Figure 38, the value of ratios of $\bar{h}_{oa}/\bar{h}_{os}$ is plotted versus varying pitch (for constant groove depth). As seen in Figure 38, the outside heat transfer improves with decreased pitch. With reduced pitch, condensate drainage improves, and more channels are provided, presenting more tube surface area to the steam flow.

The maximum $\bar{h}_{oa}/\bar{h}_{os}$ ratio was obtained for tube Y-2 which has a helix angle of 85^{o} from the tube axis. The maximum $\bar{C}_{ia}/\bar{C}_{is}$ ratio was obtained for tube GA-1 which has a helix angle of 45^{o} from the tube axis.

The $\bar{h}_{oa}/\bar{h}_{os}$ ratios for tubes T-1 and T-2 were about 1.84 and 1.39 respectively. Tubes T-1 and T-2 have the same pitch/diameter ratio and therefore they should have about the same $\bar{h}_{oa}/\bar{h}_{os}$ ratio. The value of 1.84 obtained for tube T-1 is misleading due to mixed condensation of both filmwise and dropwise modes.

C. RESULTS BASED ON THE HYDRAULIC DIAMETER, D_h

1. Heat Transfer Results

Tables 24 through 27 contain all the results obtained, for General Atomic and Turbotec tubes based on the hydraulic diameter. The inside and outside heat transfer coefficients are both smaller in value for the results based on the hydraulic diameter in comparison to the smooth end results. The major reason for this is that the actual surface areas of the enhanced sections are larger than the surface area at the smooth ends. As shown earlier, the heat transfer rate can be computed as:

$$Q = U_n A_n LMTD = U_o A_o LMTD \qquad (3)$$

For a measured value of Q and LMTD, the UA product must remain constant. Using equation (41), it is easily seen that if A_i and A_o both increase when using the hydraulic diameter reduction scheme, it follows that the calculated inside and outside heat transfer coefficients must decrease. In addition, as would be expected, the Nusselt number and Stanton number also decrease as seen in the tabular results.

2. Friction Factor

The friction factor found using the hydraulic diameter is less than the corresponding friction factor using the smooth end diameter, as seen when comparing Figures 31, 32 and 39. The reason for the smaller friction factor is seen in the following friction factor equation:

$$f_{ts} = \frac{(\rho)(\Delta P_{ts})(2g_c)}{4(l_{ts}/D_i)G^2} \qquad (14)$$

Since G, the mass rate of flow per unit area, is inversely proportional to diameter squared, then the friction factor is proportional to D^5. Since D_h is less than D_i for all tubes for which a hydraulic diameter was calculated, then the friction factor will decrease accordingly.

3. Performance Criteria

As seen in Figure 40, the tube performance factor 2j/f, when using the hydraulic diameter, increases significantly for Turbotec tubes and decreases for General Atomic tubes when compared to the results based on the smooth end diameter. However, as seen in Figure 40, tubes GA-1 and GA-2 are still better in this respect than any other tubes.

V. CONCLUSIONS

As a result of the above-mentioned tests, the following conclusions are reached:

1. The maximum corrected overall heat transfer coefficient was obtained with the tube T-1, and was about 1.9 times that of the corresponding smooth tube. As mentioned earlier for this tube mixed condensation was obtained. For filmwise condensation, the best result was obtained for tubes Y-1 and GA-1. The minimum corrected overall heat transfer coefficient was obtained with tube H-1 which was manufactured for use with refrigerants.

2. For constant heat load and constant pumping power, tube GA-1 would allow for approximately a 42 percent reduction in the required surface area at the Reynolds number of 40,000.

3. The maximum inside heat transfer coefficient ($\overline{C}_{ia}/\overline{C}_{is}$ = 1.66) was obtained with tube Y-1.

4. For inside heat transfer, an optimum pitch/diameter may be near one. (i.e., Helix angle near 45^{o}).

5. The maximum outside heat transfer coefficient ($\overline{h}_{oa}/\overline{h}_{os}$ = 1.94) was obtained with tube Y-2.

6. Outside heat transfer increases as pitch/diameter decreases; this also agrees with Reference [21].

7. The tests of tube T-1 re-affirmed the well-known fact that to get a higher overall heat transfer coefficient, it may be appropriate to promote dropwise condensation on the outside tube surface.

8. The largest pressure drop measured for all the enhanced tubes was for tube T-1. The minimum pressure drop measured was for tube GA-2.

9. Pressure drop increases as groove depth increases and pitch/diameter decreases.

10. The larger diameter tubes have less overall heat transfer coefficient and, less pressure drop when compared with the small diameter tubes.

11. It is found that, for constant groove depth/diameter [e/D] ratio, as pitch/diameter [P/D] ratio increases for tubes GA-1 and GA-2, C_i decreases. This result agrees with Reference [21]

12. Yorkshire Imperial Metals tubes are better than General Atomic tubes on outside heat transfer since they have larger helix angle (i.e., HA near 80°).

13. The optimum shape may be 45° to 60° helix angle on the inside surface and 90° helix angle on the outside surface of the tube.

14. For tube Y-1, $\bar{h}_{oa}/\bar{h}_{os}$ was found to be about 1.4; this result agrees with Reference [22].

VI. RECOMMENDATIONS

The following recommendations are made for further experiments.

1. Tests should be performed using various steam velocities and various test condenser pressures.

2. Testing of enhanced tubes should be done in a vertical orientation. This would determine the effect of condensation drainage vertically rather than horizontally off a tube's surface.

3. To evaluate the effects of tube-to-tube interactions, tests should be performed using several active tubes instead of one active tube.

4. To increase the condenser vacuum, it is recommended that a higher capacity vacuum pump be connected to the system.

5. To prevent moisture in the cold trap, it is recommended that a larger secondary condenser be connected to the system.

6. To get continuous condensation flow from the test condenser to the test condenser hotwell, a vacuum regulator line should be put between the test condenser and the test condenser hotwell.

VII. TABLES

Channel Number	Location	Channel	Location
40	Tc_i	48	Tv
41	Tc_o	49	Tv
42	Tc_o	50	Tv
43	Tc_o	51	Tw
44	Tc_o	52	Test Condenser Hotwell
45	Tv	53	Tc_i
46	Tv	54	Secondary Condenser Hotwell
47	Tv		

Table 1. Location of Stainless Steel Sheathed Copper Constantan Thermocouples

Channel Number	Location	Channel Number	Location
1	Hotwell	6	Condensate Header
2	Feedwater Tank	7	Tc into Cooling Tower
3	Condenser Window	8	Tc out of Cooling Tower
4	Tc_i	9	Cooling Tower Ambient
5	Tc_o		

Table 2. Location of Teflon Coated Copper Constantan Thermocouples

Table 3. Summary of Test Tubes

TUBE TYPE	HELIX ANGLE (Deg.)	No. OF GROOVE STARTS n	GROOVE DEPTH(mm) e	PITCH(mm) p	p/D_o	e/D_o
GA-1 General Atomic AISI 409	45 (L)	19	1.10	76.20	3.754	0.054
GA-2 General Atomic AISI 304	30 (L)	24	1.10	139.70	6.663	0.052
T-1 Turbotec Cu (122)	45 (L)	3	2.90	63.50	2.851	0.130
T-2 Turbotec with Micro Grooves , Cu (122)	45 (R)	3	2.15	63.50	2.853	0.097
Y-1 Yorkshire Roped 90-10 CuNi	80 (R)	3	0.94	15.88	0.628	0.037
Y-2 Yorkshire Roped with Enhanced Profile ,90-10 CuNi	85 (R)	3	0.33	6.35	0.251	0.013

L - Left handed spiral
R - Right handed spiral

Table 4. Enhanced Tubing Characteristics

Run No.	Tube Type	Material	Filmwise Performance	A_n ($\times 10^4$ m^2)	A_c ($\times 10^4$ m^2)	D_o (mm)	D_i, D_h (mm)	t_w (mm)	k_w (W/m°C)	R_w ($\times 10^6$ m^2C/W)	Ke+Kc
9	Smooth (S-1)	AISI304	Excellent	729.66	4.12	25.40	22.91, —	1.245	19.18	68.32	0.0
10	General Atomic (GA-1)	AISI409	Excellent	619.60	3.31	20.30	19.25, 16.28	0.525	22.00	24.50	0.07
11 16	Yorkshire Roped (Y-1)	90-10 CuNi	Poor Excellent	772.16	4.07	25.30	23.54, —	0.880	44.67	20.42	0.03
12	Yorkshire Roped with En.Pro.(Y-2)	90-10 CuNi	Excellent	771.10	4.23	25.26	23.55, —	0.859	44.67	19.90	0.02
13	Turbotec with Micro Grooves (T-2)	Cu(122)	Excellent	679.42	2.86	22.26	20.02, 19.05	1.122	339.2	3.49	0.13
14 15	Turbotec (T-1)	Cu(122)	Mixed Film +Dropwise	679.90	2.65	22.28	20.55, 16.33	0.864	339.2	2.65	0.08
17 18	Hitachi (H-1)	Titanium	Excellent Excellent	579.80	1.68	19.00	14.62, —	2.19	17.00	146.45	0.64
19	German* (G-1)	Cu(122)	Excellent	772.63	4.42	25.31	24.89, —	0.213	339.2	0.63	0.05
20	General Atomic (GA-2)	AISI304	Excellent	639.90	3.41	20.97	19.81, 15.44	0.577	15.30	38.76	0.05

* Manufactured at the Hochschule der Bundeswehr , Hamburg, West Germany.

% FLOW	T_v (°C)	T_w (°C)	Tc_i (°C)	Tc_o (°C)	P (KPa)
15	66.35	24.60	18.80	23.78	0.53
20	66.10	24.10	19.00	23.20	0.91
30	65.25	23.90	19.20	22.55	1.88
40	65.87	23.80	19.70	22.48	3.20
50	66.32	23.60	20.10	22.50	4.65
60	66.37	24.20	20.40	22.58	6.50
70	66.50	24.30	20.60	22.55	8.51
80	66.93	25.00	21.00	22.80	10.86
90	66.77	25.50	21.30	23.00	13.31
100	67.23	24.90	21.70	23.20	16.32

Table 5. Raw Data for Stainless Steel Smooth Tube , Run 9 .

% FLOW	T_v (°C)	T_w (°C)	Tc_i (°C)	Tc_o (°C)	P (KPa)
15	66.47	37.30	20.80	29.23	1.48
20	66.67	37.10	20.60	27.85	2.35
30	66.90	34.10	20.65	26.38	4.90
40	67.02	31.20	20.80	25.58	8.16
45	67.68	29.90	20.35	24.78	10.11
50	67.53	31.60	20.60	24.80	12.05
60	67.58	30.60	20.70	24.40	16.76
65	67.83	30.50	20.45	23.88	19.37
70	67.65	28.60	20.90	24.23	21.91
80	67.62	27.90	20.90	23.90	27.62
90	67.80	26.80	20.70	23.45	33.78
100	67.82	27.50	20.70	23.23	41.28

Table 6. Raw Data for 45° HA General Atomic Tube , Run 10 .

% FLOW	Tv (°C)	Tw (°C)	Tc_i (°C)	Tc_o (°C)	P (KPa)
15	70.73	39.30	20.40	27.75	1.10
20	70.87	37.50	20.30	26.53	1.79
30	70.65	34.70	20.40	25.13	3.83
40	70.17	32.80	20.40	24.25	6.25
50	70.27	31.50	20.40	23.75	9.17
60	69.72	30.80	20.45	23.45	12.53
70	69.38	30.00	20.50	23.20	16.32
80	69.75	28.70	20.60	23.03	20.97
90	69.95	28.50	20.25	22.50	25.62
100	69.50	28.20	20.05	22.15	31.14

Table 7. Raw Data for 30°HA General Atomic Tube , Run 20

% FLOW	Tv (°C)	Tw (°C)	Tc_i (°C)	Tc_o (°C)	P (KPa)
15	68.05	45.00	23.30	32.48	2.35
20	68.27	42.80	23.05	31.15	3.96
30	68.47	40.50	23.20	29.73	8.57
40	68.27	38.80	23.65	29.28	14.79
50	68.53	37.90	23.60	28.60	22.76
60	69.32	37.10	23.90	28.30	31.92
70	68.97	36.40	24.10	28.00	42.75
80	69.28	36.10	24.30	27.90	55.03
90	69.28	35.10	24.40	27.80	68.90
100	69.42	35.60	24.60	27.70	85.20

Table 8. Raw Data for Turbotec Tube with Micro Grooves , Run 13

% FLOW	Tv (°C)	Tw (°C)	Tc_i (°C)	Tc_o (°C)	P (KPa)
10	68.97	50.80	22.20	34.73	0.97
15	68.98	46.80	22.00	32.00	2.01
20	68.73	45.00	22.00	30.90	3.39
.30	69.00	41.90	22.20	29.58	7.09
40	69.82	39.30	22.60	29.00	12.46
50	69.48	37.40	22.90	28.73	19.90
60	70.12	36.00	23.10	28.43	29.19
70	69.85	35.00	23.40	28.30	40.59
80	69.32	34.30	23.65	28.15	53.33
90	70.03	33.80	23.95	28.10	66.83
100	69.45	33.30	24.10	27.93	83.72

Table 9. Raw Data for Turbotec Tube , Run 15

% FLOW	Tv (°C)	Tw (°C)	Tc_i (°C)	Tc_o (°C)	P (KPa)
15	66.73	47.50	25.45	33.15	0.85
20	66.87	47.30	25.70	32.60	1.54
30	66.85	44.00	26.05	31.70	3.23
40	67.02	41.20	26.65	31.35	5.59
50	67.60	41.50	26.75	30.85	8.44
60	67.75	41.70	27.20	30.85	11.65
70	67.75	41.00	27.50	30.73	15.19
80	67.73	38.40	27.60	30.65	19.27
90	67.78	39.10	27.80	30.50	23.67
100	67.83	39.70	27.85	30.38	28.44

Table 10. Raw Data for Yorkshire Roped Tube , Run 16

% FLOW	Tv (°C)	Tw (°C)	Tc_i (°C)	Tc_o (°C)	P (KPa)
15	69.10	41.20	21.65	28.95	0.66
20	68.92	39.70	21.30	28.23	1.16
30	68.97	37.50	21.45	27.35	2.45
40	68.63	35.90	21.35	26.50	4.27
50	69.23	35.30	21.50	25.98	6.44
60	69.13	34.80	21.60	25.65	9.04
70	69.15	34.50	21.80	25.50	11.99
80	69.17	34.10	22.00	25.35	15.29
90	69.15	33.90	22.10	25.23	18.99
100	68.80	33.60	22.20	25.15	23.10

Table 11. Raw Data for Yorkshire Roped Tube with Enhanced Profile , Run 12

% FLOW	Tv (°C)	Tw (°C)	Tc_i (°C)	Tc_o (°C)	P (KPa)
5	69.80	48.90	20.65	27.85	0.82
10	69.55	44.30	20.60	25.30	2.83
20	69.13	41.10	20.25	23.03	9.73
30	68.80	39.90	20.10	22.20	20.84
40	68.38	39.40	20.10	21.73	35.47
50	68.32	38.90	19.95	21.33	53.33
60	68.15	38.50	19.90	21.10	75.94
70	68.47	38.50	19.80	20.90	101.17
80	68.47	37.60	19.80	20.80	130.87
90	68.28	37.50	19.70	20.60	163.11
100	68.02	37.70	19.50	20.40	202.97

Table 12. Raw Data for Hitachi Tube , Run 18

% FLOW	Tv (^{o}C)	Tw (^{o}C)	Tc_i (^{o}C)	Tc_o (^{o}C)	P (KPa)
10	69.42	42.10	22.55	31.73	0.47
15	69.45	39.30	23.00	30.43	0.85
20	69.67	37.40	23.10	29.35	1.70
25	69.18	36.40	23.30	29.00	2.42
30	69.12	35.80	23.40	28.63	3.04
40	69.03	34.50	23.20	27.65	4.90
50	69.15	33.40	23.10	27.03	7.13
60	69.55	32.70	23.10	26.63	9.73
70	69.53	32.40	23.30	26.45	12.65
80	69.65	32.20	23.50	26.45	15.92
90	69.55	32.20	23.90	26.55	19.31
100	69.35	32.20	24.25	26.75	23.17

Table 13. Raw Data for German Tube , Run 19

VELOCITY (m/sec)	U_n ($W/m^{2o}C$)	U_c ($W/m^{2o}C$)	h_i ($W/m^{2o}C$)	h_o ($W/m^{2o}C$)
0.83	2047.180	2461.184	3437.871	11705.643
1.13	2333.983	2887.804	4391.793	10515.131
1.71	2893.610	3796.205	6118.981	12028.078
2.26	3131.900	4217.153	7645.188	10771.876
2.80	3345.176	4613.189	9094.997	10473.552
3.38	3671.884	5258.409	10608.392	11603.105
3.93	3820.028	5567.618	11969.515	11435.457
4.44	3972.607	5897.766	13248.465	11588.826
5.02	4100.290	6183.639	14661.106	11564.137
5.53	4197.820	6408.173	15842.207	11571.722

REYNOLDS NO	PLAIN END REYN NO	FLOW RATE PER AREA (Kg/m^2 sec)	FRICTION FACTOR	SIEDER-TATE CONSTANT
20018.92	20018.92	823.80	0.00641541	0.02436817
27166.67	27166.67	1122.61	0.00587090	0.02437996
41021.53	41021.52	1708.65	0.00528805	0.02439414
54354.95	54354.94	2246.73	0.00524483	0.02438074
67811.56	67811.55	2789.75	0.00490050	0.02436788
82231.19	82231.17	3368.92	0.00469295	0.02435562
95707.91	95707.89	3913.46	0.00455308	0.02435015
108873.54	108873.51	4419.91	0.00460942	0.02432987
123717.77	123717.75	4998.83	0.h0438288	0.02431653
137256.37	137256.34	5505.06	0.00445187	0.02429575

Table 14. Smooth Stainless Steel Tube Results, Run 9

NUSSELT NO	$Nu/Pr^{1/3}(\mu/\mu_w)^{0.14}$	STANTON NO	J FACTOR	PERFORM. FACTOR
125.47302	67.29880	0.00099678	0.0033958	1.0586312
130.36613	85.85315	0.00093439	0.0031032	1.0878084
223.56438	119.58996	0.00085782	0.0029426	1.1129106
279.17274	149.70556	0.00081274	0.0027780	1.0592471
331.93218	178.58770	0.00077870	0.0026523	1.0824550
386.97844	208.27072	0.00075215	0.006529	1.0883933
436.52300	235.10377	0.00073058	0.0024771	1.0880785
482.77329	260.42177	0.00071603	0.0024147	1.0477115
533.95706	288.30159	0.00070064	0.0023544	1.0743642
578.47960	313.00842	0.00068750	0.0022975	1.0229683

X_{in}	PRESSURE DROP(Kpa)	PRANDTL NO	μ/μ_w	DOTMS (Kg/sec)
0.1954043D-03	0.36891	6.28799	1.01019	0.3430170
0.1524633D-03	0.62688	6.31753	1.00926	0.4674353
0.1097892D-03	1.30032	6.35322	1.00935	0.7093705
0.8787045D-04	2.24314	6.31950	1.00865	0.9355025
0.7386198D-04	3.28163	6.28603	1.00710	1.1616042
0.6332379D-04	4.51341	6.25670	1.00835	1.4027630
0.5612247D-04	5.90901	6.24308	1.00838	1.6294969
0.5070328D-04	7.63144	6.19284	1.00949	1.8403754
0.4581704D-04	9.29238	6.16000	1.01034	2.0814293
0.4240004D-04	11.53882	6.10910	1.00748	2.2922154

Table 14. Page 2.

Re_s (R_{ext}=o)	AREA RATIO (R_{ext}=0)	Re_s ($R_{ext} \neq 0$)	AREA RATIO ($R_{ext} \neq 0$)
21187.93	1.1595	19174.48	0.8767
28351.70	1.1459	25975.13	0.8968
42327.37	1.1349	38738.58	0.8856
57465.65	1.1579	53782.10	0.9618
70868.45	1.1478	67645.36	1.0076
85758.42	1.1464	81903.13	1.0080
99826.88	1.1468	96807.58	1.0523
115789.92	1.1658	113025.80	1.0895
129989.16	1.1552	128721.77	1.1239
147583.28	1.1777	147228.20	1.1698

Table 14. Page 3.

VELOCITY M/SEC	UN W/(C*M**2)	UC W/(C*M**2)	HI W/(C*M**2)	HO W/(C*M**2)
1.18	4718.240	5334.813	8573.471	15515.852
1.61	5400.457	6223.781	10924.821	15588.686
2.45	6326.178	7486.271	15063.593	15729.834
3.23	6886.786	8284.309	18609.038	15614.469
3.62	6949.453	8375.158	20236.572	14860.777
4.01	7353.365	8968.876	22089.314	15684.338
4.84	7787.772	9623.624	25592.924	15947.064
5.23	7683.665	9465.149	27163.757	14963.344
5.62	8119.173	10134.815	28689.150	16151.669
6.35	8250.756	10340.670	31530.114	15807.589
7.18	8460.126	10671.667	34614.568	15812.399
7.91	8531.463	10785.426	37446.494	15490.174

REYNOLDS NO	PLAIN END REYN NO	FLOW RATE PER AREA KG/(SEC*M**2)	FRICTION FACTOR	SIEDER TATE CONSTANT
25941.26	25941.26	1177.13	0.00747931	0.04114205
34763.31	34763.30	1604.42	0.00624092	0.04122253
51955.86	51955.85	2435.23	0.00556047	0.04129610
68046.56	68046.54	3212.08	0.00534067	0.04132991
75251.58	75251.57	3601.10	0.00527151	0.04139534
83615.49	83615.47	3989.30	0.00509878	0.04138090
100653.90	100653.88	4818.03	0.00482741	0.04139665
107880.41	107880.39	5208.13	0.00477660	0.04143752
116957.82	116957.80	5596.92	0.00466388	0.04139534
131843.54	131643.51	6322.21	0.00462788	0.04141245
147850.39	147850.36	7151.53	0.00436989	0.04144677
162442.88	162442.84	7876.89	0.00445333	0.04145869

Table 15. 45°HA General Atomic Tube Results Based on D_i ,Run 10

NUSSELT NO	NU/PR(1/3)(U/UW)(0.14	STANTON NO	J FACTOR	PERFORM FACTOR
259.16280	139.79077	0.00174076	0.0055800	1.4921158
330.38648	177.02362	0.00162723	0.0052827	1.6929200
457.05424	244.57745	0.00147805	0.0046542	1.7459708
565.69106	303.74493	0.00138425	0.0045703	1.7115136
615.48648	329.73395	0.00134255	0.0044783	1.6990536
671.60238	358.61542	0.00132290	0.0044028	1.7269884
778.42230	416.13039	0.00126905	0.0042340	1.7541444
827.01984	440.23878	0.00124597	0.0041836	1.7517057
872.56794	469.21789	0.00122461	0.0040849	1.7517113
959.37090	516.00060	0.00119144	0.0039849	1.7221206
1054.09501	566.69371	0.00115625	0.0038880	1.7794345
1140.66175	611.18941	0.00113564	0.0038258	1.7181573

XIN	PRESSURE DROP(KPA)	PRANDTL NO	U/UW	DOT(MS(KG/SEC)
0.15967710-03	1.05159	5.63907	1.03549	0.3426032
0.12531770-03	1.62949	5.84937	1.03740	0.4669657
0.90891520-04	3.34435	5.95174	1.03119	0.7087733
0.73576570-04	5.53783	5.99426	1.02387	0.9346760
0.67862610-04	6.93996	6.03216	1.02203	1.0481012
0.61986710-04	8.22747	6.07155	1.02656	1.1610965
0.53501940-04	11.36159	6.09404	1.02412	1.4022884
0.50409240-04	13.13453	6.15267	1.02505	1.5158275
0.47727490-04	14.81264	6.09216	1.01820	1.6289841
0.43427620-04	18.75366	6.11664	1.01664	1.8400818
0.39556900-04	22.65628	6.16602	1.01437	2.0814554
0.38567560-04	28.00910	6.18324	1.01682	2.2925723

RES	ARAT	RESR	ARATR
23414.31	0.6046	23212.44	0.5901
29484.47	0.5741	29746.70	0.5885
43261.58	0.5647	44753.66	0.6210
57033.73	0.5672	60345.18	0.6647
63235.69	0.5675	68357.22	0.7050
69847.62	0.5650	75378.37	0.6994
83324.06	0.5607	91505.09	0.7288
89413.36	0.5607	100474.91	0.7773
96612.44	0.5598	107667.60	0.7582
109589.35	0.5630	124429.48	0.8035
120947.69	0.5547	139892.64	0.8338
135336.77	0.5630	156975.82	0.8825

Table 15. Page 2.

VELOCITY M/SEC	UN W/(C*M**2)	UC W/(C*M**2)	HI W/(C*M**2)	HO W/(C*M**2)
1.12	3537.785	4099.811	6374.750	12834.610
1.52	4013.141	4752.120	8094.403	12547.126
2.31	4579.181	5566.978	11171.178	11777.961
3.05	4925.376	6087.124	13830.547	11393.538
3.78	5283.174	6643.143	16361.565	11647.556
4.57	5764.537	7422.501	18975.619	12664.810
5.31	6056.346	7913.454	21330.734	13028.011
6.00	6092.041	7974.506	23420.530	12466.210
6.78	6310.453	8352.946	25762.024	12715.836
7.47	6511.110	8708.173	27760.421	13035.182

REYNOLDS NO	PLAIN END REYN NO	FLOW RATE PER AREA KG/(SEC*M**2)	FRICTION FACTOR	SIEDER TATE CONSTANT
24709.53	24709.52	1111.68	0.00617615	0.03229805
33196.58	33196.58	1515.14	0.00530249	0.03235173
49675.32	49675.31	2299.68	0.00492912	0.03240487
64898.07	64898.05	3033.39	0.00458588	0.03244091
80152.63	80152.61	3767.08	0.00433841	0.03246160
96536.01	96535.99	4549.61	0.00399773	0.03247197
111898.78	111898.76	5285.30	0.00384357	0.03248029
126289.81	126289.78	5969.97	0.00392930	0.03248341
141483.41	141483.38	6753.32	0.00370017	0.03251992
154892.28	154892.25	7438.67	0.00374426	0.03254299

Table 16. 30^{O}HA General Atomic Tube Results Based on D_i ,Run 20

NUSSELT NO	NU/PR1/3(U/UW)0.14	STANTON NO	J FACTOR	PERFORM FACTOR
198.78313	105.55228	0.00137033	0.0044595	1.4440988
252.82635	133.89733	0.00127651	0.0041991	1.5838365
349.50168	185.14949	0.00116059	0.0038506	1.5656408
433.18397	229.55044	0.00108924	0.0036475	1.5907755
512.78440	271.95926	0.00103756	0.0034888	1.6083540
594.90094	315.68929	0.00099633	0.0033572	1.6795337
668.90687	355.36922	0.00096408	0.0032538	1.6931403
734.51098	391.52174	0.00093712	0.0031648	1.6106945
808.85276	429.25325	0.00091117	0.0030996	1.6753971
872.21485	461.82871	0.00089135	0.0030461	1.6270783

XIN	PRESSURE DROP(KPA)	PRANDTL NO	U/UW	DOTMS(KG/SEC)
0.16344030-03	0.75230	5.87071	1.04395	0.3427095
0.12872440-03	1.19952	5.96630	1.04107	0.4670899
0.93275960-04	2.56820	6.06222	1.03526	0.7089456
0.75343360-04	4.15666	6.12799	1.03123	0.9351357
0.63689580-04	6.06418	6.16602	1.02824	1.1613190
0.54916370-04	8.15034	6.18516	1.02660	1.4025573
0.48853480-04	10.57483	6.20053	1.02457	1.6293543
0.44494460-04	13.79286	6.20631	1.02086	1.8404266
0.40451860-04	16.61847	6.27427	1.02165	2.0819174
0.37540700-04	20.40111	6.31753	1.02163	2.2931973

RES	ARAT	RESR	ARATR
22762.75	0.7828	21433.51	0.6615
29160.65	0.7524	27995.04	0.6712
43766.05	0.7529	43453.25	0.7380
56613.85	0.7461	57935.96	0.7960
69437.31	0.7415	72332.68	0.8314
81773.67	0.7281	85711.28	0.8306
94312.28	0.7250	100034.38	0.8550
108926.87	0.7384	117982.23	0.9235
119705.83	0.7263	131545.21	0.9459
132981.21	0.7344	146981.40	0.9719

Table 16. Page 2.

VELOCITY M/SEC	UN W/(C*M**2)	UC W/(C*M**2)	HI W/(C*M**2)	HO W/(C*M**2)
0.79	3105.080	3309.575	4389.927	17316.497
1.08	3981.543	4324.144	5583.375	25577.983
1.64	5097.844	5673.370	7732.788	26657.758
2.16	5849.403	6619.959	9580.850	25593.552
2.68	6201.064	7073.968	11361.750	21308.036
3.23	6775.186	7830.966	13186.276	21583.508
3.76	7190.773	8391.527	14855.725	21301.479
4.24	7354.403	8615.216	16360.547	19804.363
4.80	7759.871	9176.934	18043.196	20200.049
5.29	8132.477	9702.663	19477.678	20842.087

REYNOLDS NO	PLAIN END REYN NO	FLOW RATE PER AREA KG/(SEC*M**2)	FRICTION FACTOR	SIEDER TATE CONSTANT
21337.24	21337.24	786.70	0.00982643	0.02989258
28746.81	28746.80	1072.18	0.00937563	0.02993229
43288.45	43288.44	1627.20	0.00862207	0.02995924
56517.15	56517.14	2146.39	0.00877154	0.02999476
69900.94	69900.92	2665.50	0.00861448	0.03000885
84215.03	84215.02	3219.19	0.00829233	0.03001732
97882.09	97882.07	3739.59	0.00817471	0.03001543
110619.88	110619.86	4223.94	0.00821624	0.03001355
125084.05	125084.02	4777.54	0.00796568	0.03001449
137802.93	137802.90	5261.91	0.00803168	0.03001355

Table 17, Yorkshire Roped With Enhanced Profile Tube Results Based on D_i, Run 12.

162.20021	86.87079	0.00133375	0.0042557	0.8661659
206.57009	110.41078	0.00124457	0.0040055	0.8544517
286.35029	153.33037	0.00113569	0.0036765	0.8528153
355.20586	190.01564	0.00106606	0.0034797	0.7934060
421.42977	225.33852	0.00101855	0.0033329	0.7737906
489.24307	261.62742	0.00097878	0.0032086	0.7738767
551.14913	295.05767	0.00094925	0.0031106	0.7610182
606.94014	325.37459	0.00092553	0.0030316	0.7379537
669.38368	358.99817	0.00090244	0.0029566	0.7423283
722.57880	387.90361	0.00088452	0.0028973	0.7214568

XIN	PRESSURE DROP(KPA)	PRANDTL NO	U/UW	DOTMS(KG/SEC)
0.18536660-03	0.50455	5.69953	1.04528	0.3425703
0.14575070-03	0.89403	5.77377	1.04288	0.4668827
0.10524080-03	1.89346	5.82460	1.03796	0.7085670
0.84944020-04	3.35111	5.89217	1.03498	0.9346512
0.71630540-04	5.07520	5.91914	1.03388	1.1606959
0.61719910-04	7.12559	5.93541	1.03282	1.4018005
0.54783870-04	9.47927	5.93179	1.03189	1.6284106
0.49744920-04	12.15535	5.92817	1.03068	1.8393231
0.45105830-04	15.07608	5.92998	1.03015	2.0803896
0.41783850-04	18.43958	5.92817	1.02925	2.2913069

RES	ARAT	RESR	ARATR
25396.35	1.0383	23379.43	0.8235
34409.79	1.0416	30404.68	0.7366
51743.15	1.0395	44985.00	0.7025
69938.56	1.0675	60583.55	0.7141
87543.59	1.0772	77391.35	0.7628
105410.53	1.0764	93440.16	0.7681
123492.48	1.0834	110087.06	0.7853
141643.81	1.0963	126142.76	0.8282
159650.81	1.0935	144993.72	0.8350
176333.05	1.1057	161764.22	0.8415

Table 17. Page 2.

VELOCITY M/SEC	UN W/(C*M**2)	UC W/(C*M**2)	HI W/(C*M**2)	HO W/(C*M**2)
0.79	3824.192	4148.037	6217.618	14658.287
1.08	4631.401	5115.034	7953.339	16564.777
1.64	5711.018	6464.756	10995.529	17562.416
2.16	6254.782	7170.390	13632.622	16494.810
2.68	6637.053	7677.306	16205.378	15641.403
3.24	7147.370	8368.456	18879.738	15982.163
3.76	7351.211	8649.265	21256.426	15371.574
4.25	7858.247	9359.826	23274.419	16484.814
4.80	7862.107	9365.302	25735.455	15380.993
5.29	8079.406	9675.275	27840.522	15443.514

REYNOLDS NO	PLAIN END REYN NO	FLOW RATE PER AREA KG/(SEC*M**2)	FRICTION FACTOR	SIEDER TATE CONSTANT
23182.87	23182.86	786.14	0.01347031	0.04031401
31493.92	31493.91	1071.28	0.01336367	0.04032824
47524.90	47524.89	1625.79	0.01215883	0.04035441
62838.49	62838.48	2144.10	0.01219203	0.04034250
77714.37	77714.36	2662.68	0.01199197	0.04036157
94284.51	94284.49	3215.41	0.01129450	0.04034012
109721.87	109721.85	3735.12	0.01090538	0.04033190
123965.56	123965.53	4218.91	0.01087906	0.04033061
140283.39	140283.36	4771.78	0.01040437	0.04032824
154388.91	154388.88	5255.66	0.01032199	0.04033190

Table 18. Yorkshire Roped Tube Results Based on D_i ,Run 16

227.45432	125.19570	0.00184147	0.0058878	0.6412582
291.05361	160.02591	0.00177547	0.0053326	0.7980678
402.64412	222.55006	0.00161734	0.0048783	0.8024270
499.06423	278.19102	0.00152052	0.0045774	0.7508811
593.52824	329.68972	0.00145541	0.0043950	0.7329845
691.11035	384.84795	0.00140417	0.0042255	0.7482396
777.95073	434.39206	0.00136097	0.0040900	0.7500868
851.78090	478.93365	0.00131930	0.0039640	0.7287371
941.79272	528.70563	0.00128978	0.0038738	0.7446509
1018.91797	570.87390	0.00126682	0.0038070	0.7376553

XIN	PRESSURE DROP(KPA)	PRANDTL NO	U/UW	DOTMS(KG/SEC)
0.1782152D-03	0.69184	5.18712	.04953	0.3420987
0.1393235D-03	1.27450	5.20514	1.04947	0.4661812
0.1007783D-03	2.67048	5.23839	1.04174	0.7074661
0.8128295D-04	4.65753	5.22324	1.03395	0.9330384
0.6837957D-04	7.06456	5.24752	1.03535	1.1587035
0.5869242D-04	9.70355	5.22022	1.03521	1.3992319
0.5212965D-04	12.64311	5.20965	1.03308	1.6253898
0.4760974D-04	16.09155	5.20815	1.02603	1.8359179
0.4305682D-04	19.68738	5.20514	1.02785	2.0765113
0.3980134D-04	23.69311	5.20965	1.02959	2.2870751

RES	ARAT	RESR	ARATR
28050.96	0.7801	27970.97	0.7739
39130.08	0.7965	38272.58	0.7486
58670.11	0.7919	57423.36	0.7457
79892.86	0.8110	79508.50	0.8001
100072.77	0.8189	101585.48	0.8541
120157.89	0.8126	123192.20	0.8714
139515.47	0.8113	146009.39	0.9215
159372.22	0.8185	166129.58	0.9194
178571.93	0.8121	191395.76	0.9861
197623.55	0.8156	213613.59	1.0142

Table 18. Page 2.

VELOCITY M/SEC	UN W/(C*M**2)	UC W/(C*M**2)	HI W/(C*M**2)	HO W/(C*M**2)
1.09	4834.155	4917.010	8007.135	15506.755
1.49	5669.294	5783.587	10153.462	15779.159
2.26	6785.824	6950.221	14039.228	15463.805
2.99	7748.169	7963.239	17440.844	16177.727
3.71	8424.133	8678.985	20646.760	16297.775
4.48	8787.950	9065.652	23959.839	15651.503
5.20	9110.459	9409.264	26952.802	15380.469
5.87	9439.067	9760.196	29694.874	15383.120
6.64	10082.355	10449.598	32681.426	16215.549
7.32	10104.115	10472.974	35364.849	15615.823

REYNOLDS NO	PLAIN END REYN NO	FLOW RATE PER AREA KG/(SEC*M**2)	FRICTION FACTOR	SIEDER TATE CONSTANT
26488.17	26488.17	1087.70	0.01684705	0.03946382
35512.48	35512.47	1482.55	0.01513609	0.03953851
53180.74	53180.72	2250.22	0.01423592	0.03959958
70138.28	70138.26	2967.73	0.01421812	0.03959958
86439.68	86439.66	3685.71	0.01427416	0.03963455
104391.46	104391.44	4451.15	0.01369523	0.03963455
121141.33	121141.30	5170.84	0.01362831	0.03963938
136959.91	136959.88	5840.53	0.01381988	0.03963508
154927.59	154927.55	6605.97	0.01351525	0.03963455
170813.73	170813.70	7275.61	0.01386309	0.03962971

Table 19. Turbotec With Micro Grooves Tube Results Based On D_i, Run 13.

317.51274	172.71294	0.00163738	0.0050773	0.6708920
439.70405	238.94269	0.00149150	0.0046717	0.6563304
546.24157	298.16341	0.00140490	0.0044005	0.6189982
647.22078	352.73139	0.00133909	0.0042185	0.5910749
751.07696	410.20935	0.00128674	0.0040536	0.5919757
845.00148	462.12603	0.00124600	0.0039284	0.5765066
930.86761	509.74646	0.00121537	0.0038291	0.5541465
1024.47542	562.57000	0.00118262	0.0037256	0.5513184
1108.45840	608.18937	0.00116194	0.0036576	0.5276706

XIN	PRESSURE DROP(KPA)	PRANOTL NO	U/UW	OOTMS(KG/SEC)
0.1587913D-03	1.94698	5.36034	1.04737	0.3422682
0.1252324D-03	3.24885	5.46048	1.04298	0.4665144
0.9057520D-04	7.03783	5.54350	1.03977	0.7080773
0.7290965D-04	12.22635	5.54350	1.03515	0.9338593
0.6159041D-04	18.92966	5.59150	1.03379	1.1597839
0.5307392D-04	26.48898	5.59150	1.03158	1.4006476
0.4718053D-04	35.57197	5.59817	1.02979	1.6271121
0.4282366D-04	46.02131	5.59224	1.02882	1.8378438
0.3891025D-04	57.57681	5.59150	1.02600	2.0787041
0.3595767D-04	71.64021	5.58485	1.02725	2.2894211

RES	ARAT	RESR	ARATR
36713.24	0.8883	35036.34	0.7793
47997.54	0.8690	45900.83	0.7668
72523.77	0.8739	70193.25	0.7975
98271.94	0.8930	95016.88	0.8126
123858.53	0.9084	120737.90	0.8457
149307.74	0.9070	148914.08	0.9004
175421.29	0.9159	177664.49	0.9491
202193.99	0.9303	206529.05	0.9872
228991.75	0.9312	233421.53	0.9825
258224.65	0.9483	267750.31	1.0495

Table 19. Page 2.

VELOCITY M/SEC	UN W/(C*M**2)	UC W/(C*M**2)	HI W/(C*M**2)	HO W/(C*M**2)
0.66	4181.836	4228.694	5531.717	24685.970
1.04	5040.851	5109.094	7789.965	17677.530
1.42	6065.179	6164.247	9902.086	18957.930
2.15	7472.624	7623.577	13670.910	19276.905
2.83	8371.456	8561.368	16935.629	18941.743
3.52	9533.678	9780.760	20039.019	20770.876
4.25	10360.505	10652.961	23209.880	21202.611
4.93	11161.659	11501.836	26108.117	22016.305
5.57	11731.896	12108.305	28733.265	22291.713
6.30	12070.267	12469.071	31687.545	21744.956
6.94	12412.856	12835.016	34182.738	21645.799

REYNOLDS NO	PLAIN END REYN NO	FLOW RATE PER AREA KG/(SEC*M**2)	FRICTION FACTOR	SIEDER TATE CONSTANT
16640.06	16640.06	657.68	0.02011333	0.04022090
25333.95	25333.95	1032.40	0.01657484	0.04036200
34128.86	34128.85	1407.05	0.01499509	0.04041581
51184.81	51184.80	2135.56	0.01353177	0.04047127
67382.29	67382.28	2816.60	0.01380927	0.04047994
83695.44	83695.42	3497.57	0.01448530	0.04047870
100971.41	100971.39	4224.01	0.01465572	0.04048366
117510.33	117510.31	4906.75	0.01523371	0.04047498
132870.47	132870.44	5542.22	0.01580883	0.04047003
150677.82	150677.79	6268.31	0.01548002	0.04045767
165911.37	165911.34	6903.87	0.01609783	0.04045891

Table 20. Turbotec Tube Results Based on D_i ,Run 15

NUSSELT NO	NU/PR1/3(U/UW)0.14	STANTON NO	J FACTOR	PERFORM FACTOR
177.00659	95.80219	0.00201128	0.0061054	0.6071000
250.14155	134.56582	0.00180396	0.0056027	0.6760488
318.38722	171.02059	0.00168237	0.0052706	0.7029812
440.17152	236.84240	0.00153021	0.0048369	0.7149015
545.40465	295.17269	0.00143726	0.0045495	0.6589006
645.32823	351.06511	0.00136953	0.0043342	0.5984280
747.53283	407.97933	0.00131342	0.0041600	0.5676915
840.69777	460.51865	0.00127188	0.0040228	0.5281393
925.11602	508.01442	0.00123927	0.0039165	0.4954859
1019.92245	561.61675	0.00120841	0.0038114	0.4924262
1100.26846	606.61727	0.00118355	0.0037337	0.4638814

XIN	PRESSURE DROP(KPA)	PRANDTL NO	U/UW	DOTMS(KG/SEC)
0.2284933D-03	0.82797	5.28885	1.06046	0.2181052
0.1622735D-03	1.68046	5.47339	1.05479	0.3423731
0.1276660D-03	2.82338	5.54515	1.05181	0.4666180
0.9247491D-04	5.86813	5.61992	1.04533	0.7082153
0.7464884D-04	10.41670	5.63167	1.03856	0.9340688
0.6308811D-04	16.84883	5.62999	1.03329	1.1598966
0.5446943D-04	24.86338	5.63672	1.02956	1.4008073
0.4842249D-04	34.87453	5.62495	1.02649	1.6272221
0.4399831D-04	46.17323	5.61824	1.02436	1.8379646
0.3989588D-04	57.83805	5.60151	1.02257	2.0787568
0.3698369D-04	72.96120	5.60318	1.02119	2.2895276

RES	ARAT	RESR	ARATR
23828.11	0.8947	21521.47	0.6727
34285.83	0.8522	31769.09	0.6884
45230.98	0.8369	41499.90	0.6576
67059.80	0.8281	61652.91	0.6544
91657.68	0.8531	84773.10	0.6856
119158.66	0.8849	108523.23	0.6811
147327.94	0.9023	134408.16	0.6978
177499.16	0.9278	161220.14	0.7088
206993.88	0.9512	188147.95	0.7281
235257.10	0.9531	216850.01	0.7587
266712.59	0.9756	247084.57	0.7876

Table 20. Page 2.

VELOCITY M/SEC	UN W/(C*M**2)	UC W/(C*M**2)	HI W/(C*M**2)	HO W/(C*M**2)
0.65	1248.469	1527.745	2623.211	6284.561
1.31	1592.268	2076.355	4481.105	5219.583
2.80	1972.165	2772.884	8098.466	4996.119
4.24	2257.694	3372.589	11237.168	5529.369
5.60	2312.914	3497.319	13983.598	5181.539
6.95	2419.895	3747.853	16578.697	5307.091
8.40	2552.203	4075.035	19243.603	5622.338
9.75	2691.558	4442.266	21674.632	6055.142
11.02	2760.992	4634.630	23828.470	6202.497
12.46	2812.697	4782.195	26264.400	6264.644
13.72	2928.621	5127.261	28349.811	6702.734

REYNOLDS NO	PLAIN END REYN NO	FLOW RATE PER AREA KG/(SEC*M**2)	FRICTION FACTOR	SIEDER TATE CONSTANT
10713.44	10713.43	650.86	0.00891790	0.01870521
20838.74	20838.73	1302.28	0.00744522	0.01876636
43301.81	43301.80	2785.35	0.00482088	0.01882922
65012.44	65012.43	4227.35	0.00433368	0.01885286
85296.92	85296.90	5575.72	0.00424879	0.01886443
105280.44	105280.42	6924.38	0.00411290	0.01887788
126760.21	126760.18	8362.79	0.00398035	0.01888463
146766.16	146766.13	9715.22	0.00392739	0.01889200
165593.66	165593.63	10973.80	0.00407908	0.01889446
186675.60	186675.56	12412.58	0.00390821	0.01890185
204579.65	204579.61	13672.02	0.00414216	0.01891297

Table 21. Hitachi Tube Results Based on D_i ,Run 18

103.38078	53.51516	0.00082213	0.0037260	0.7320004
187.46051	96.39109	0.00069451	0.0023523	0.9758873
260.44067	133.59005	0.00063490	0.0021679	1.0007328
324.29290	166.10785	0.00059899	0.0020534	0.9665849
384.74982	196.71214	0.00057181	0.0019693	0.9576013
446.75514	228.29400	0.00054954	0.0018970	0.9531638
503.38979	256.79017	0.00053279	0.0018438	0.9389214
553.48440	282.85846	0.00051855	0.0017960	0.8805866
610.30455	311.43981	0.00050529	0.0017545	0.8978538
659.15057	335.31222	0.00049515	0.0017258	0.8332915

XIN	PRESSURE DROP(KPA)	PRANDTL NO	U/UW	OOTMS(KG/SEC)
0.3119235D-03	0.50474	5.84582	1.06893	0.1092088
0.1826174D-03	1.68628	6.03433	1.06109	0.2185103
0.1010582D-03	4.99284	6.23337	1.05673	0.4673561
0.7283415D-04	10.93442	6.30963	1.05503	0.7093094
0.5853041D-04	17.62907	6.34725	1.05443	0.9355539
0.4936966D-04	26.31686	6.39120	1.05395	1.1618453
0.4253330D-04	37.14743	6.41334	1.05329	1.4031972
0.3776324D-04	49.46465	6.43761	1.05378	1.6301224
0.3434999D-04	65.54732	6.44573	1.05143	1.8413001
0.3116454D-04	80.34536	6.47016	1.05164	2.0827140
0.2887263D-04	103.30476	6.50706	1.05295	2.2940357

RES	ARAT	RESR	ARATR
14334.24	1.8220	13145.72	1.4299
27183.81	1.7797	26198.92	1.6049
48821.02	1.5784	51618.76	1.8449
72325.04	1.5596	79127.41	2.0060
96525.18	1.5801	110763.18	2.3227
119669.40	1.5846	141100.05	2.5133
144374.54	1.5866	173281.57	2.6448
166463.14	1.5958	203943.66	2.7252
196049.22	1.6356	240066.67	2.8840
218895.28	1.6225	273492.28	3.0266
249164.06	1.6715	310919.21	3.1071

Table 21. Page 2.

VELOCITY M/SEC	UN W/(C*M**2)	UC W/(C*M**2)	HI W/(C*M**2)	HO W/(C*M**2)
0.45	2573.613	2577.821	3439.590	10845.137
0.71	3228.771	3235.397	4884.009	9918.614
0.96	3641.346	3649.776	6206.779	9081.603
1.21	4218.854	4230.174	7438.015	10035.404
1.46	4653.755	4667.533	8616.943	10394.397
1.93	5166.512	5183.499	10677.861	10239.357
2.40	5597.066	5617.007	12632.118	10255.348
2.90	5988.831	6011.667	14644.702	10321.163
3.36	6220.287	6244.926	16497.288	10154.900
3.80	6576.788	6604.339	18186.193	10472.738
4.30	6733.744	6762.628	20098.605	10281.329
4.73	7071.311	7103.170	21747.846	10636.915

REYNOLDS NO	PLAIN END REYN NO	FLOW RATE PER AREA KG/(SEC*M**2)	FRICTION FACTOR	SIEDER TATE CONSTANT
13370.16	13370.15	448.57	0.02623366	0.03645944
20793.30	20793.30	703.90	0.01855570	0.03649691
28047.56	28047.56	959.32	0.02043652	0.03654017
35249.25	35249.24	1207.56	0.01827779	0.03654685
42372.87	42372.86	1455.84	0.01555300	0.03655911
55199.74	55199.72	1920.44	0.01429128	0.03661178
68023.96	68023.95	2385.04	0.01342794	0.03664450
81804.75	81804.73	2880.56	0.01248852	0.03666262
95054.91	95054.89	3346.24	0.01200183	0.03666148
107594.52	107594.50	3779.55	0.01185085	0.03665242
122339.31	122339.28	4274.53	0.01116623	0.03662981
135525.20	135525.17	4707.48	0.01106118	0.03660504

Table 22. German Tube Results Based on D_i ,Run 19

190.07197	103.89498	0.00165877	0.0051752	0.5577988
241.83678	132.15582	0.00154665	0.0048627	0.4758883
289.86280	158.69728	0.00147242	0.0046349	0.5071603
335.91887	183.93554	0.00141486	0.0044634	0.5739632
416.86042	227.59891	0.00132898	0.0042320	0.5922437
493.59470	269.23903	0.00126587	0.0040545	0.6038875
572.51853	312.20941	0.00121506	0.0039043	0.6252585
644.92340	352.03788	0.00117829	0.0037854	0.6307962
710.77145	388.62834	0.00115002	0.0036886	0.6225042
785.02980	430.41480	0.00112382	0.0035902	0.6430377
848.87277	466.82763	0.00110425	0.0035121	0.6350375

XIN	PRESSURE DROP(KPA)	PRANDTL NO	U/UW	DOTMS(KG/SEC)
0.2741978D-03	0.41461	5.45566	1.04300	0.2182055
0.1931117D-03	0.72202	5.51074	1.03575	0.3424068
0.1519622D-03	1.47677	5.57489	1.03203	0.4666537
0.1268082D-03	2.09272	5.58485	1.02948	0.5874090
0.1094601D-03	2.58818	5.60318	1.02823	0.7081854
0.8833753D-04	4.13750	5.68246	1.02638	0.9341866
0.7467340D-04	5.93534	5.73217	1.02438	1.1601882
0.6441226D-04	8.13295	5.75985	1.02239	1.4012292
0.5717894D-04	10.54740	5.75812	1.02210	1.6277535
0.5186846D-04	13.28704	5.74426	1.02122	1.8385347
0.4693216D-04	16.01469	5.70981	1.02045	2.0793160
0.4337212D-04	19.24217	5.67225	1.01961	2.2899229

RES	ARAT	RESR	ARATR
22468.69	1.1218	22828.36	1.1728
30699.37	1.0104	31714.41	1.1067
44751.33	1.0738	46480.11	1.1940
54413.27	1.0456	55975.93	1.1318
61448.19	0.9943	63610.92	1.0954
78733.38	0.9798	82944.30	1.1336
95991.24	0.9705	102556.77	1.1681
113371.31	0.9561	122855.20	1.1973
131097.35	0.9525	144457.81	1.2499
149312.35	0.9574	164748.71	1.2811
166978.90	0.9454	187666.01	1.3111
186061.03	0.9505	208834.21	1.3132

Table 22. Page 2.

Table 23 . Summary Of Heat Transfer Capabilities Of Enhanced Condenser Tubing

Tube No.	Tube Type	$\bar{C}_{ia}/\bar{C}_{io}$	$\bar{h}_{oa}/\bar{h}_{os}$
GA-1	General Atomic (45^{o}HA)	1.70	1.38
GA-2	General Atomic (30^{o}HA)	1.33	1.10
T-1	Turbotec (Normal)	1.66	1.84
T-2	Turbotec with Micro Grooves	1.63	1.39
Y-1	Yorkshire Roped	1.66	1.41
Y-2	Yorkshire Roped with Enhanced Profile	1.23	1.94
G-1	Special German	1.50	0.90

Inside Heat Transfer Coefficient (Sieder-Tate)

$$Nu_i = h_i D_i / k_b = C_i Re^{0.8} Pr^{1/3} \quad (\mu/\mu_w)^{0.14}$$

Outside Heat Transfer Coefficient Nusselt)

$$h_o = 0.725 \left[\frac{\rho_f \ (\rho_f - \rho_v) g h_{fg} k_f^{\ 3}}{\mu_f D_o (T_s - T_w)} \right]^{0.25}$$

VELOCITY M/SEC	UN W/(C*M**2)	UC W/(C*M**2)	HI W/(C*M**2)	HO W/(C*M**2)
1.04	4718.240	5334.813	6379.140	10791.411
1.42	5400.457	6223.781	8128.675	10837.981
2.15	6326.178	7486.271	11708.152	10928.132
2.84	6886.786	8284.309	13846.160	10854.459
3.18	6949.453	8375.158	15057.136	10370.976
3.52	7353.365	8968.876	16435.679	10899.089
4.26	7787.772	9623.624	19042.560	11066.618
4.60	7683.665	9465.149	20211.348	10436.994
4.94	8119.173	10134.815	21346.325	11196.771
5.58	8250.756	10340.670	23460.160	10977.737
6.32	8460.126	10671.667	25755.166	10980.805
6.96	8531.463	10785.426	27862.276	10774.986

REYNOLOS NO	PLAIN END REYN NO	FLOW RATE PER AREA KG/(SEC*M**2)	FRICTION FACTOR	SIEDER TATE CONSTANT
19294.23	25941.26	1035.16	0.0081 7990	0.03280915
25835.77	34763.30	1410.91	0.00682550	0.03287333
38643.01	51955.85	2141.52	0.00608132	0.03293200
50610.72	68046.54	2824.68	0.00584093	0.03295896
55965.57	75251.57	3166.78	0.00576539	0.03301114
62190.36	83615.47	3508.16	0.00557638	0.03299962
74862.96	100653.88	4236.94	0.00527959	0.03301219
80237.79	107880.39	4580.00	0.00523402	0.03304478
86989.26	116957.80	4921.89	0.00510074	0.03301114
97912.00	131643.51	5559.71	0.00506137	0.03302478
109966.10	147850.36	6289.01	0.00477921	0.03305216
120819.50	162442.84	6926.89	0.00487047	0.03306166

Table 24. 45^{O}HA General Atomic Tube Results Based on D_h ,Run 10

NUSSELT NO	NU/PR1/3(U/UW)0.14	STANTON NO	J FACTOR	PERFORM FACTOR
163.09134	87.97044	0.00147286	0.0047212	1.1543522
208.22711	111.40109	0.00137680	0.0044697	1.3097012
287.62457	158.91277	0.00125058	0.0041071	1.3507431
355.61222	191.14691	0.00117121	0.0038669	1.3240859
387.32609	207.50182	0.00113593	0.0037891	1.3144463
422.63987	225.87695	0.00111930	0.0037252	1.3360577
489.86173	261.87116	0.00107375	0.0035824	1.3570665
520.44149	277.08035	0.00105421	0.0035397	1.3551798
549.10785	295.27916	0.00103614	0.0034562	1.3551841
603.73282	324.71956	0.00100808	0.0033716	1.3322917
663.34277	356.62077	0.00097830	0.0032896	1.3766318
717.81928	384.62195	0.00096086	0.0032370	1.3292256

XIN	PRESSURE DROP(KPA)	PRANDTL NO	U/UW	DOTMS(KG/SEC)
0.20234550-03	1.05159	5.73907	1.03549	0.3426032
0.15880470-03	1.62969	5.84937	1.03740	0.4669657
0.11517930-03	3.34435	5.95174	1.03119	0.7087733
0.93237470-04	5.58784	5.99926	1.02387	0.9348760
0.85743200-04	6.93097	6.09216	1.02203	1.0481012
0.76550600-04	8.22748	6.07155	1.02656	1.1610865
0.67798040-04	11.36159	6.09404	1.02412	1.4022884
0.63879440-04	13.13454	6.15267	1.02505	1.5158275
0.60481000-04	14.81265	6.09216	1.01820	1.6289841
0.55032200-04	18.75366	6.11664	1.01664	1.8400818
0.50129710-04	22.65629	6.16602	1.01437	2.0814554
0.46339030-04	28.00911	6.18324	1.01682	2.2925723

Table 24. Page 2

VELOCITY M/SEC	UN W/(C*M**2)	UC W/(C*M**2)	HI W/(C*M**2)	HO W/(C*M**2)
1.01	3537.785	4099.811	4488.781	8293.163
1.38	4013.141	4752.120	5699.675	8128.413
2.09	4579.181	5566.978	7866.187	7683.395
2.75	4925.376	6087.124	9738.782	7458.641
3.42	5283.174	6643.143	11520.999	7607.330
4.13	5764.537	7422.501	13361.685	8195.960
4.79	6056.346	7913.454	15020.040	8403.520
5.42	6092.041	7974.506	16491.570	8081.890
6.13	6310.453	8352.946	18140.333	8225.202
6.75	6511.110	8708.173	19547.505	8407.605

REYNOLDS NO	PLAIN END REYN NO	FLOW RATE PER AREA KG/(SEC*M**2)	FRICTION FACTOR	SIEDER TATE CONSTANT
17397.97	24709.52	1004.16	0.00590035	0.02347165
23373.70	33196.58	1368.61	0.00506571	0.02351065
34976.37	49675.31	2077.26	0.00470901	0.02354927
45694.70	64898.05	2740.02	0.00488109	0.02357546
56435.43	80152.61	3402.75	0.00414467	0.02359050
67970.95	96535.99	4109.59	0.00381921	0.02359804
78787.88	111898.76	4774.13	0.00367193	0.02360408
88920.59	126289.78	5392.58	0.00375383	0.02360635
99618.40	141483.38	6100.17	0.00353494	0.02363288
109059.58	154892.25	6719.23	0.00357706	0.02364965

Table 25. 30°HA General Atomic Tube Results Based on D_h ,Run 20

NUSSELT NO	NU/PRI/3(U/UW)0.14	STANTON NO	J FACTOR	PERFORM FACTOR
109.10736	57.93515	0.00106823	0.0034764	1.1783582
138.77041	73.49308	0.00099509	0.0032734	1.2923816
191.83322	101.62418	0.00090473	0.0030080	1.2775342
237.76445	125.99481	0.00084911	0.0028434	1.2980436
281.45524	149.27201	0.00080882	0.0027197	1.3123874
326.52708	173.27440	0.00077668	0.0026171	1.3704686
367.14718	195.05377	0.00075154	0.0025365	1.3815714
403.15573	214.89703	0.00073053	0.0024671	1.3144604
443.96018	235.60697	0.00071030	0.0024163	1.3670932
478.73813	253.48687	0.00069484	0.0023746	1.3276661

XIN	PRESSURE DROP(KPA)	PRANDTL NO	U/UW	DOTMS(KG/SEC)
0.2163973D-03	0.75230	5.87071	1.04395	0.3427095
0.1704329D-03	1.19952	5.96630	1.04107	0.4670899
0.1234987D-03	2.56820	6.06222	1.03526	0.7089456
0.9975570D-04	4.15667	6.12799	1.03123	0.9351357
0.8432594D-04	6.06418	6.16602	1.02824	1.1613190
0.7271007D-04	8.15034	6.18516	1.02660	1.4025573
0.6468272D-04	10.57483	6.20053	1.02457	1.6293548
0.5891132D-04	13.79287	6.20631	1.02086	1.8404266
0.5355885D-04	16.61847	6.27427	1.02165	2.0819174
0.4970443D-04	20.40112	6.31753	1.02163	2.2931973

Table 25. Page 2

VELOCITY M/SEC	UN W/(C*M**2)	UC W/(C*M**2)	HI W/(C*M**2)	HO W/(C*M**2)
1.21	4834.155	4917.010	8400.502	16278.051
1.64	5669.294	5783.587	10652.272	16565.618
2.49	6785.824	6950.221	14728.934	16232.718
3.29	7748.169	7963.239	18297.662	16986.471
4.09	8424.133	8678.985	21661.075	17113.256
4.93	8787.950	9065.652	25136.916	16430.853
5.73	9110.459	9409.264	28276.915	16144.759
6.47	9439.067	9760.196	31153.697	16147.557
7.32	10082.355	10449.598	34286.969	17026.416
8.06	10104.115	10472.974	37102.222	16393.187

REYNOLDS NO	PLAIN END REYN NO	FLOW RATE PER AREA KG/(SEC*M**2)	FRICTION FACTOR	SIEDER TATE CONSTANT
27789.47	26488.17	1198.72	0.01320474	0.03793022
37257.12	35512.47	1633.86	0.01186369	0.03800200
55793.37	53180.72	2479.89	0.01115813	0.03806070
73584.00	70138.26	3270.64	0.01114418	0.03806070
90686.25	86439.66	4061.89	0.01116810	0.03809431
109519.95	104391.44	4905.46	0.01073434	0.03809431
127092.70	121141.30	5898.61	0.01068189	0.03809895
143688.41	136959.88	6436.65	0.01083204	0.03809482
162538.79	154927.55	7280.21	0.01056327	0.03809431
179205.39	170813.70	8018.20	0.01086590	0.03808966

Table 26. Turbotec with Micro Grooves Tube Results Based on D_h, Run 13

NUSSELT NO	NU/PRL/3(U/UW)0.14	STANTON NO	J FACTOR	PERFORM FACTOR
249.80418	136.17249	0.00167564	0.0051322	0.7773338
317.11006	172.49390	0.00155873	0.0048334	0.8148304
439.14840	238.03965	0.00141985	0.0044473	0.7971446
545.54881	297.78527	0.00133741	0.0041891	0.7518028
646.39995	352.28404	0.00127477	0.0040159	0.7178887
750.12442	409.68911	0.00122493	0.0038589	0.7189828
843.92982	461.53995	0.00118615	0.0037397	0.7001947
929.68705	509.09998	0.00115699	0.0036452	0.6730374
1023.17615	581.85653	0.00112581	0.0035466	0.6696025
1107.05262	607.41805	0.00110613	0.0034819	0.6408811

XIN	PRESSURE DROP(KPA)	PRANDTL NO	U/UW	DOTMS(KG/SEC)
0.1528143D-03	1.94898	5.36034	1.04737	0.3422682
0.1205186D-03	3.24885	5.46048	1.04398	0.4665144
0.8716592D-04	7.03783	5.54350	1.03977	0.7080773
0.7018530D-04	12.22635	5.54350	1.03515	0.9338593
0.5927213D-04	18.92966	5.59150	1.03379	1.1597839
0.5107619D-04	26.48899	5.59150	1.03158	1.4006476
0.4540484D-04	35.57198	5.59317	1.02979	1.6271121
0.4121176D-04	46.02132	5.59224	1.02862	1.8378438
0.3744565D-04	57.57682	5.59150	1.02660	2.0787041
0.3460420D-04	71.64021	5.58485	1.02725	2.2894211

Table 26. Page 2

VELOCITY M/SEC	UN W/(C*M**2)	UC W/(C*M**2)	HI W/(C*M**2)	HO W/(C*M**2)
0.83	4181.836	4228.694	5500.757	24614.374
1.30	5040.851	5109.094	7746.366	17614.877
1.77	6085.179	6164.247	9846.665	18892.970
2.69	7472.624	7623.577	13594.396	19211.419
3.54	8371.456	8561.368	16840.843	18876.813
4.40	9533.678	9780.760	19926.863	20703.169
5.31	10360.505	10652.961	23079.977	21134.339
6.17	11161.659	11501.836	25961.993	21947.061
6.97	11731.896	12108.305	28572.448	22222.167
7.89	12070.267	12469.071	31510.193	21676.023
8.69	12412.856	12835.016	33991.421	21576.983

REYNOLDS NO	PLAIN END REYN NO	FLOW RATE PER AREA KG/(SEC*M**2)	FRICTION FACTOR	SIEDER TATE CONSTANT
16546.92	16640.06	822.79	0.01021452	0.03193379
25192.15	25333.95	1291.58	0.00841750	0.03204582
33937.83	34128.85	1760.29	0.00761523	0.03208854
50898.32	51184.80	2671.70	0.00687209	0.03213257
67005.14	67382.28	3523.72	0.00701301	0.03213946
83226.97	83695.42	4375.64	0.00735634	0.03213847
100406.25	100971.39	5284.47	0.00744288	0.03214241
116852.59	117510.31	6138.60	0.00773641	0.03213552
132126.76	132870.44	6933.62	0.00802849	0.03213159
149834.43	150677.79	7841.99	0.00786150	0.03212178
164982.72	165911.34	8637.11	0.00817526	0.03212276

Table 27. Turbotec Tube Results Based on D_h ,Run 15

NUSSELT NO	NL/PRI/3(U/UW)0.14	STANTON NO	J FACTOR	PERFORM FACTOR
139.90654	75.72234	0.00159867	0.0048529	0.9501945
197.71283	106.36123	0.00143388	0.0044533	1.0581087
251.65422	135.17519	0.00133723	0.0041894	1.1002616
347.91290	187.20095	0.00121629	0.0038447	1.1189186
431.08948	233.30539	0.00114241	0.0036162	1.0312695
510.08938	277.48292	0.00108857	0.0034451	0.9366217
590.85221	322.46809	0.00104398	0.0033066	0.8885148
664.49005	363.99533	0.00101095	0.0031975	0.8266103
731.21450	401.53613	0.00098504	0.0031131	0.7755032
806.14978	443.90358	0.00096050	0.0030295	0.7707144
869.65551	479.47212	0.00094075	0.0029678	0.7260378

XIN	PRESSURE DROP(KPA)	PRANDTL NO	U/UW	DOTMS(KG/SEC)
0.2295217D-03	0.82797	5.28885	1.06046	0.2181052
0.1630038D-03	1.68046	5.47339	1.05479	0.3423731
0.1282408D-03	2.62338	5.54515	1.05181	0.4666180
0.9289110D-04	5.86813	5.61992	1.04533	0.7082153
0.7498480D-04	10.41670	5.63167	1.03856	0.9340688
0.6337204D-04	16.84883	5.62999	1.03329	1.1598966
0.5471457D-04	24.86338	5.63672	1.02956	1.4008073
0.4864042D-04	34.87453	5.62495	1.02649	1.6272221
0.4419632D-04	46.17323	5.61824	1.02436	1.8379646
0.4007543D-04	57.83806	5.60151	1.02257	2.0787568
0.3715013D-04	72.96121	5.60318	1.02119	2.2895276

Table 27. Page 2

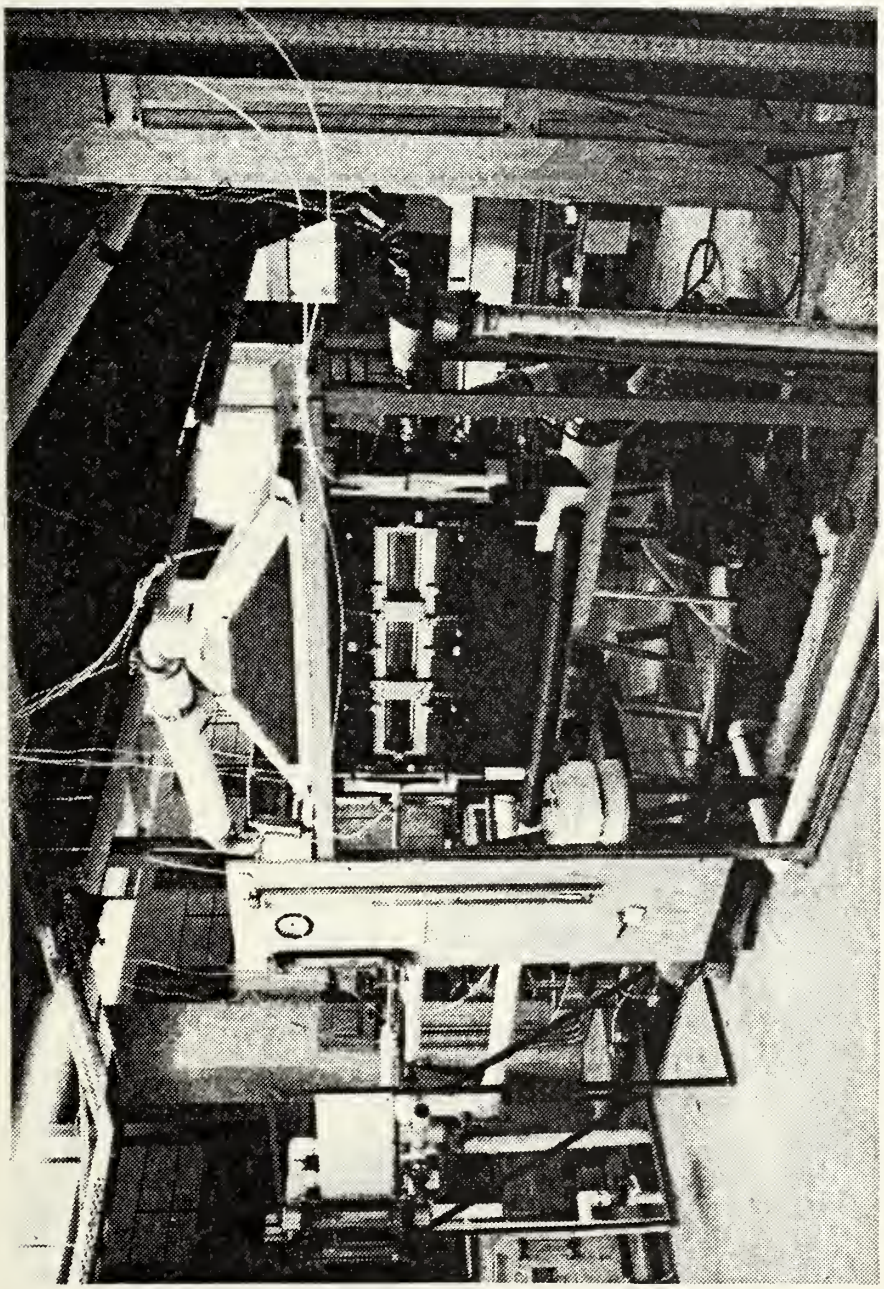

Figure 1. Photograph Of Test Facility.

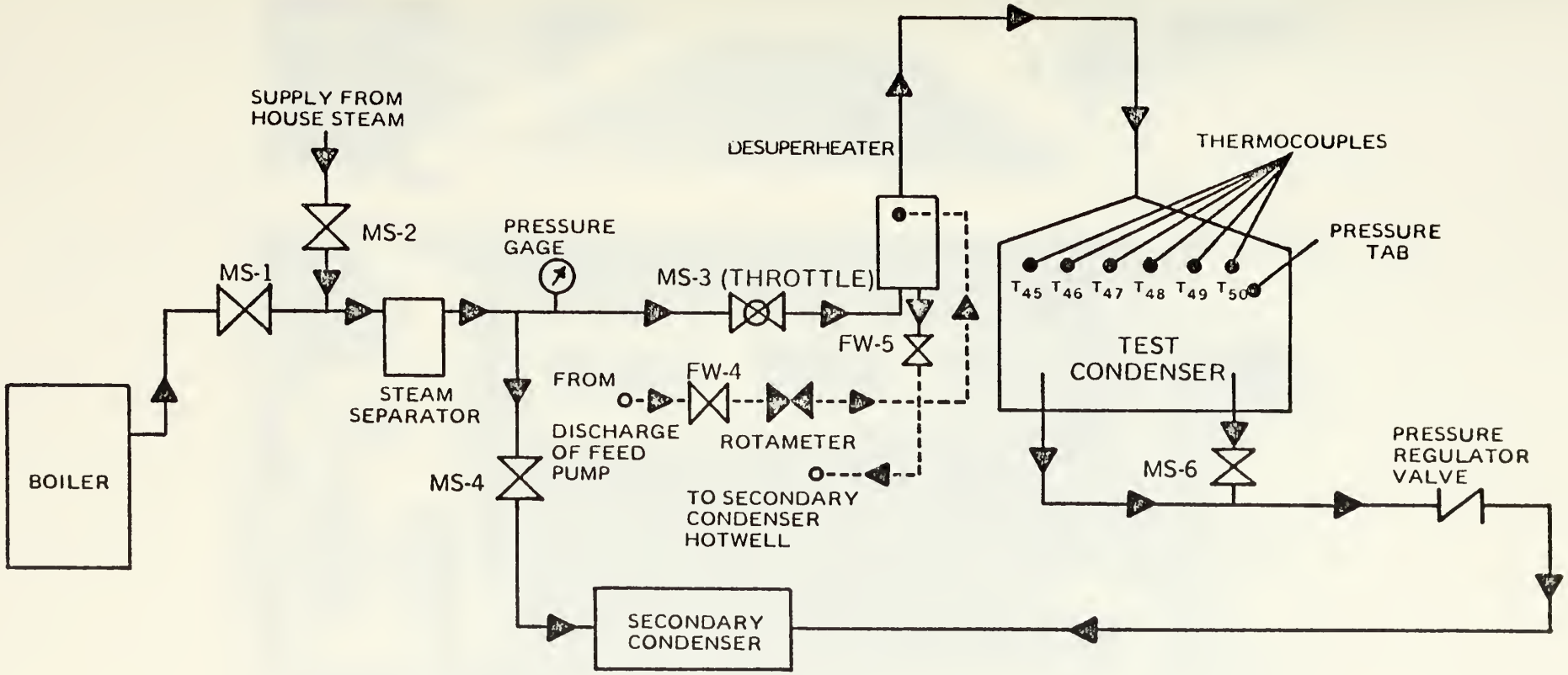

Figure 2. Schematic Diagram of Steam System

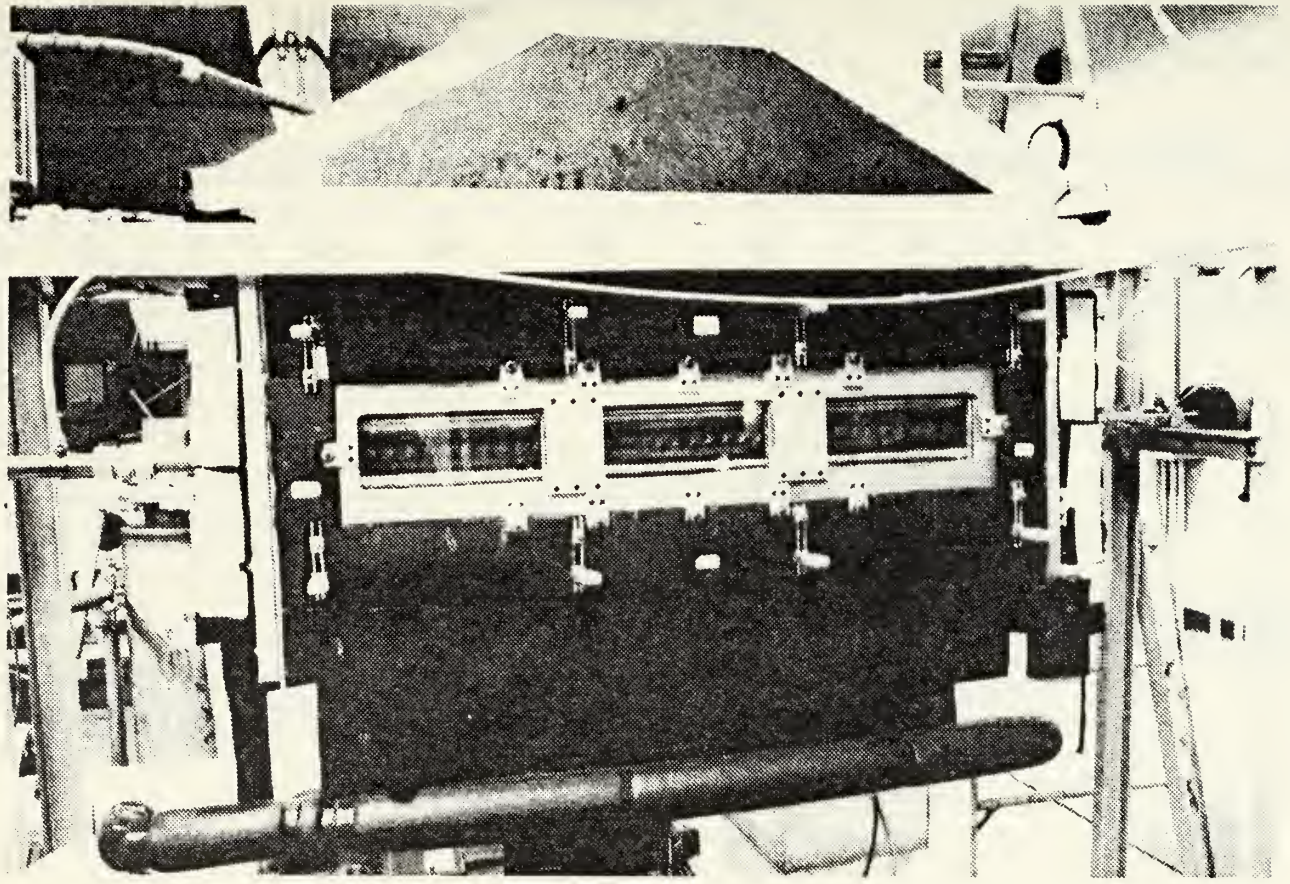

Figure 3. Photograph Of Test Condenser.

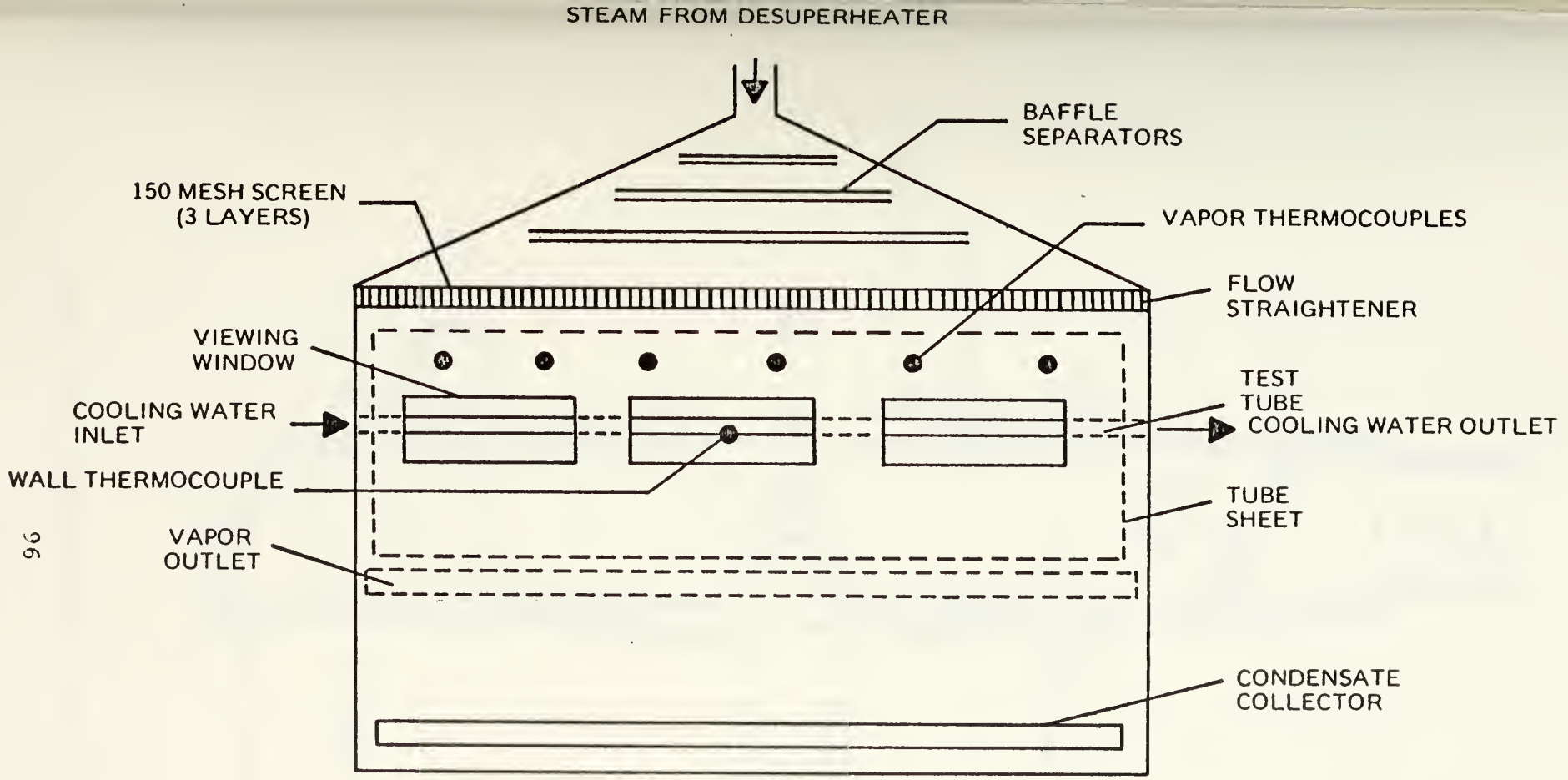

Figure 4. Test Condenser Schematic, Front View

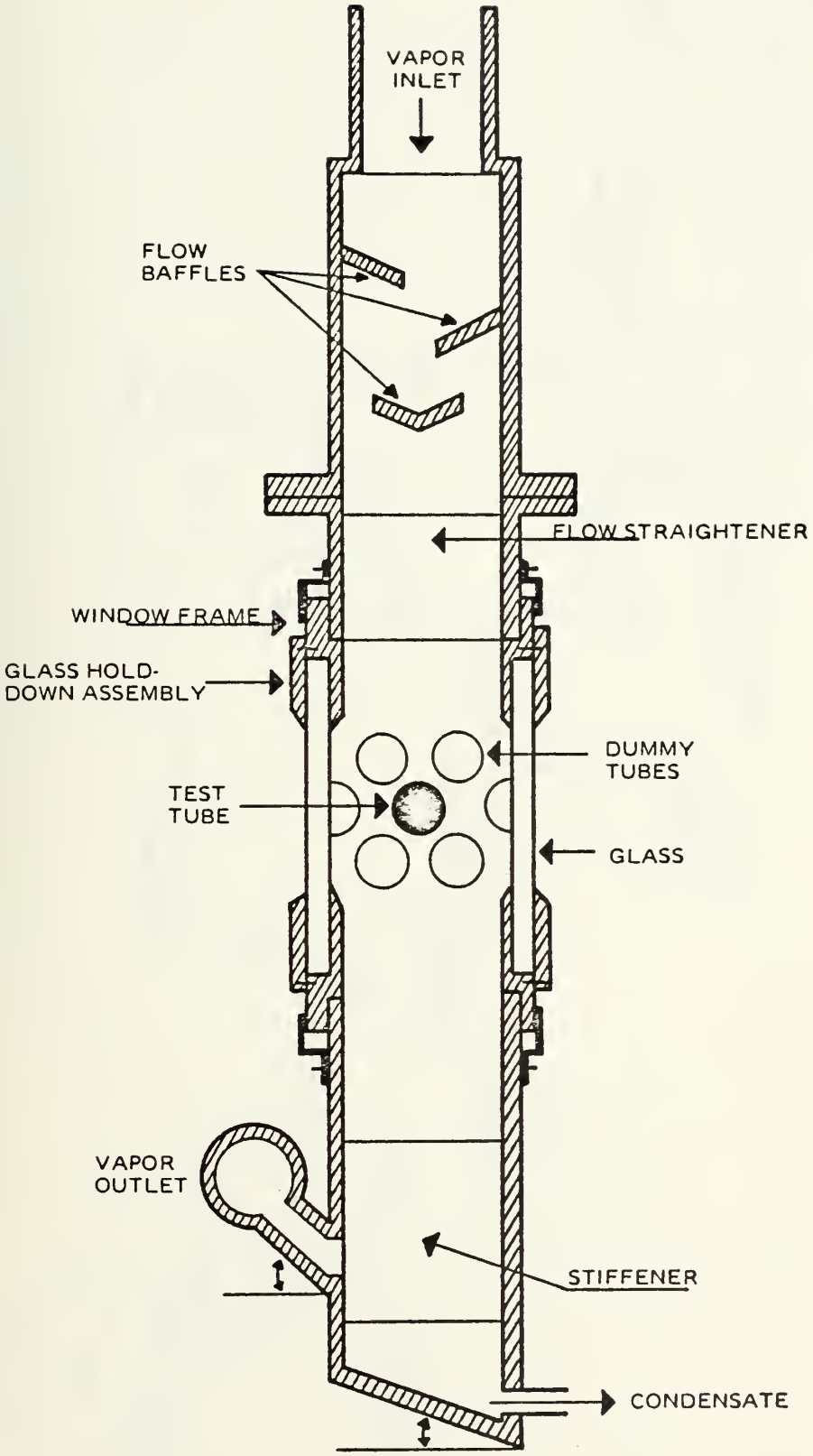

Figure 5. Test Condenser Schematic, Side View

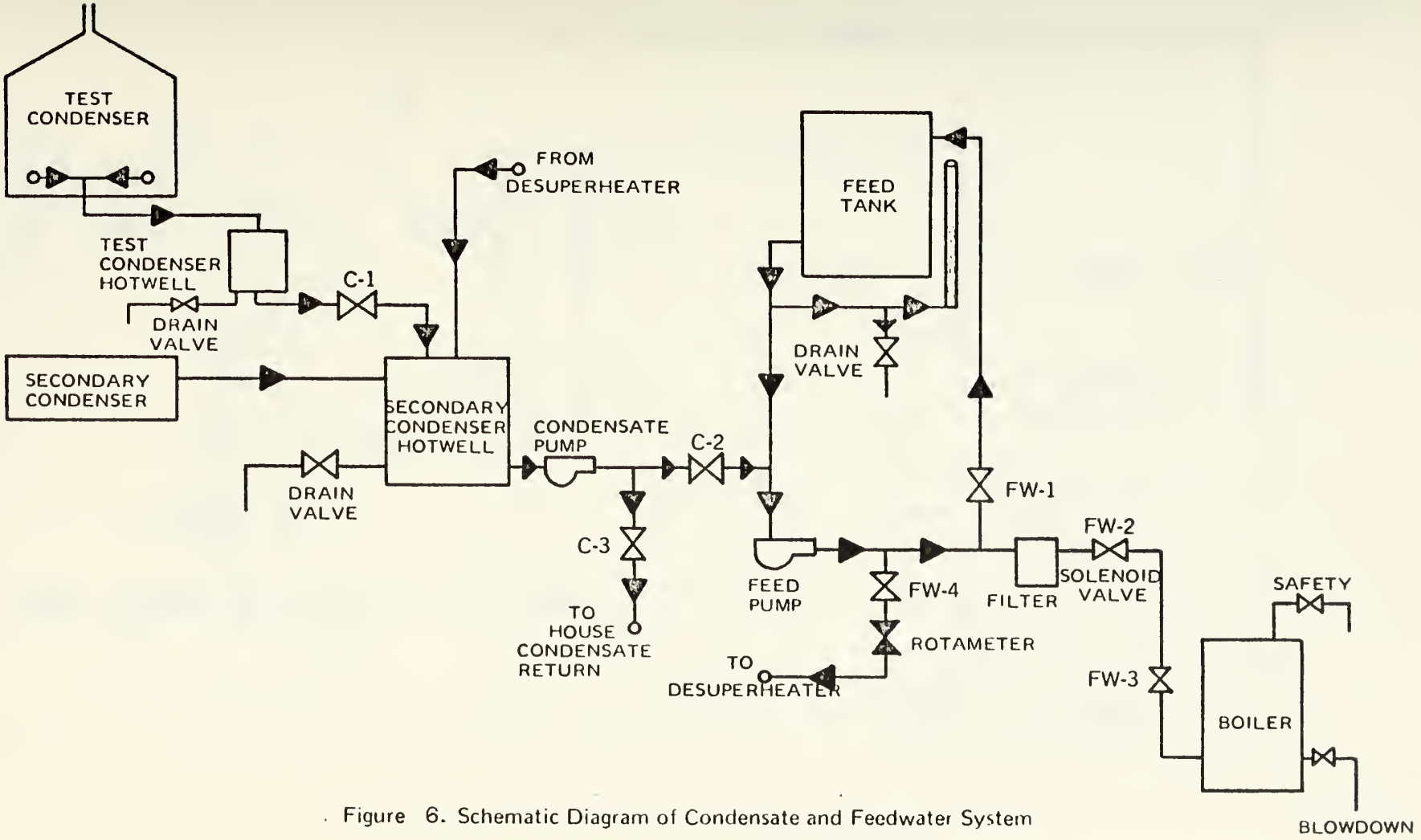

Figure 6. Schematic Diagram of Condensate and Feedwater System

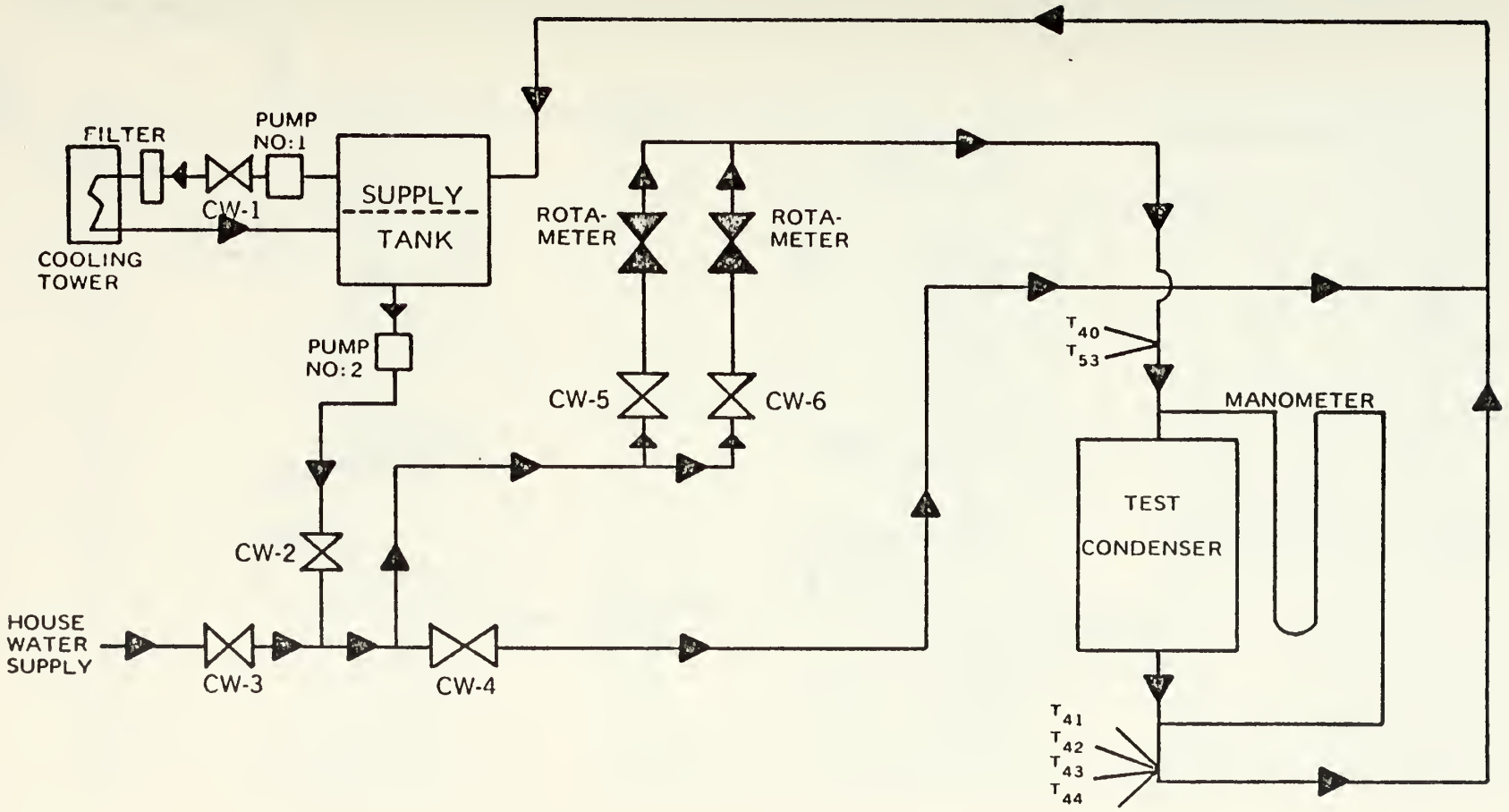

Figure 7. Schematic Diagram of Cooling Water System

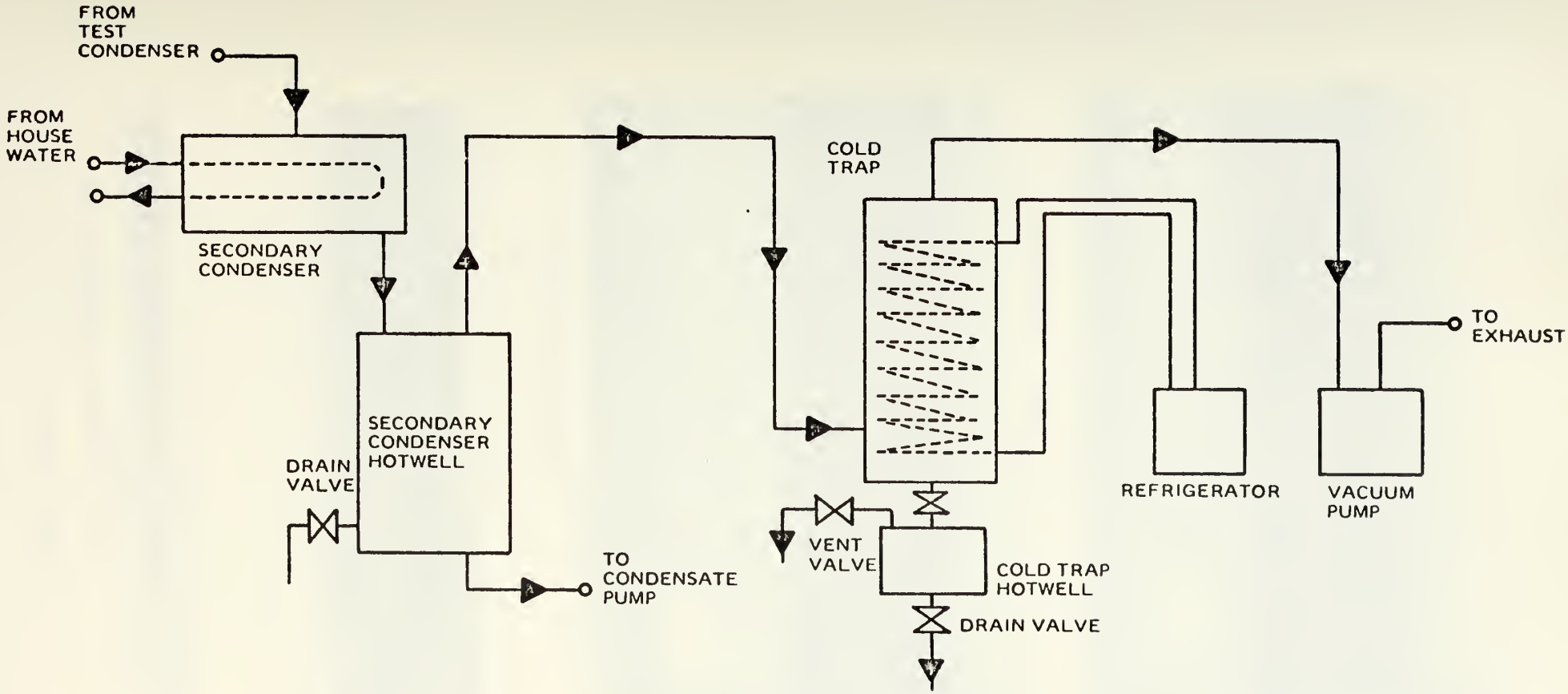

Figure 8. Schematic Diagram of Vacuum System

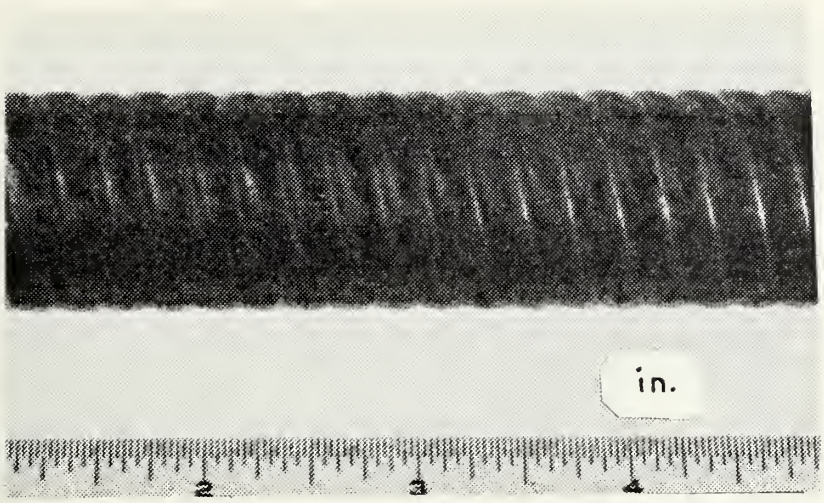

(a) Yorkshire Roped Tube,Run 16

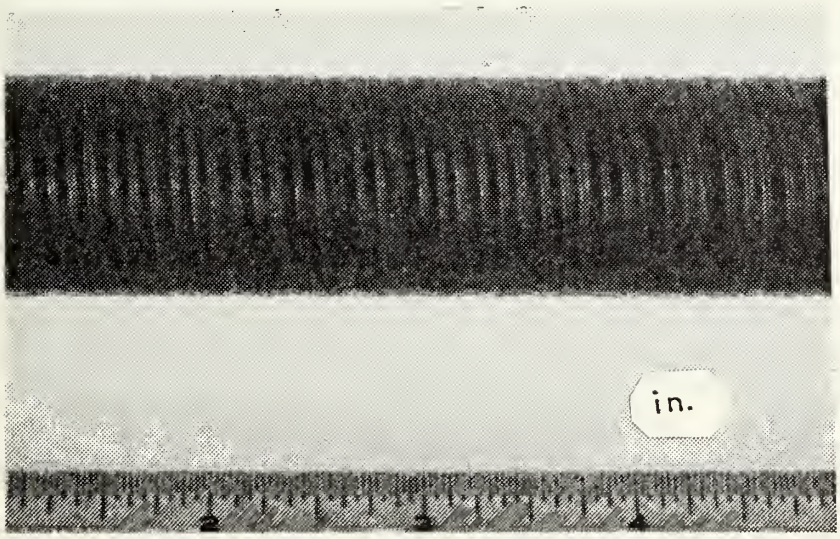

(b) Yorkshire Roped with Enhanced Profile Tube,Run 12

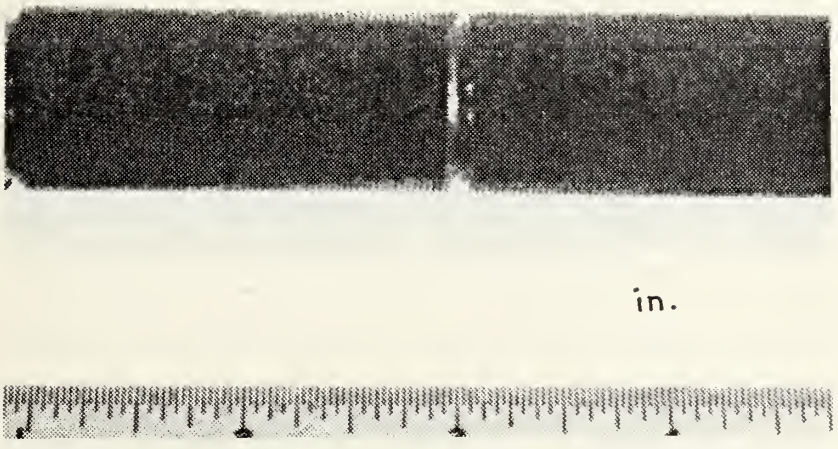

(c) Hitachi Tube,Run 18

Figure 9. Photograph of Test Tubes

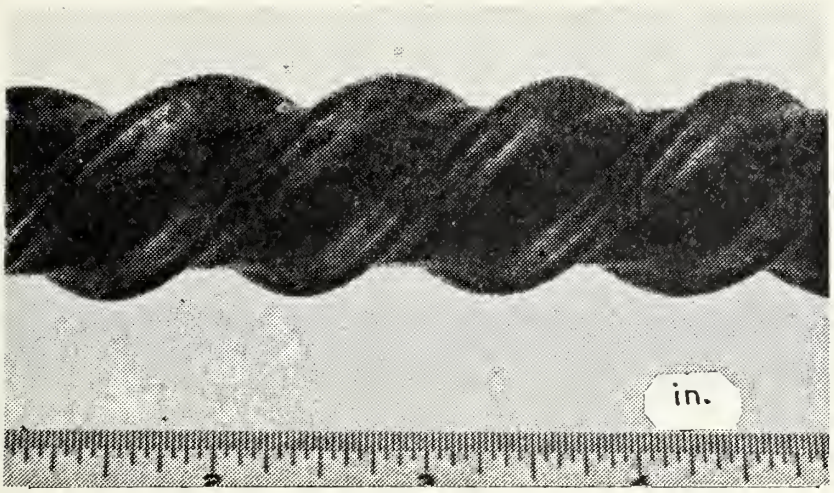

(a) Turbotec Tube,Run15

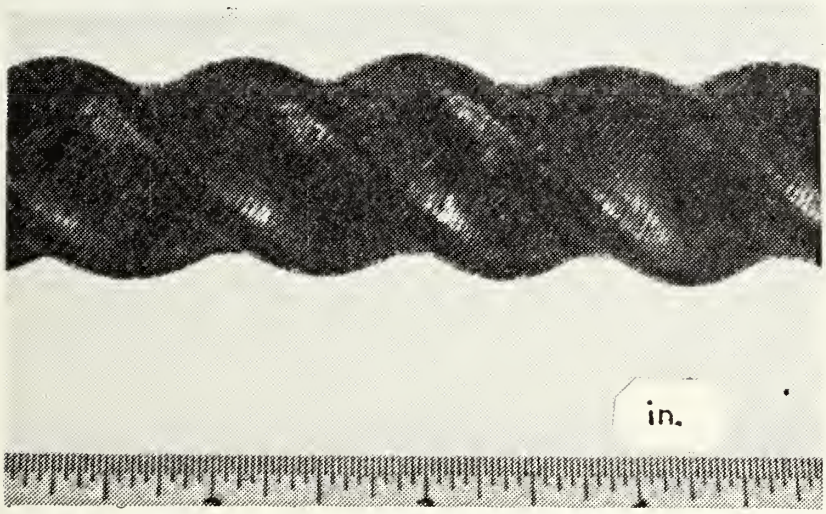

(b) Turbotec Tube with Micro Grooves,Run 13

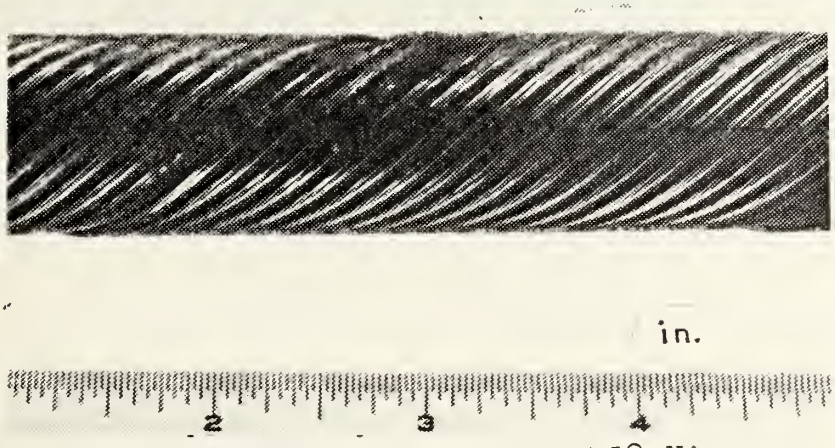

(c) General Atomic Tube,45° HA, Run 10

Figure 10. Photograph of Test Tubes

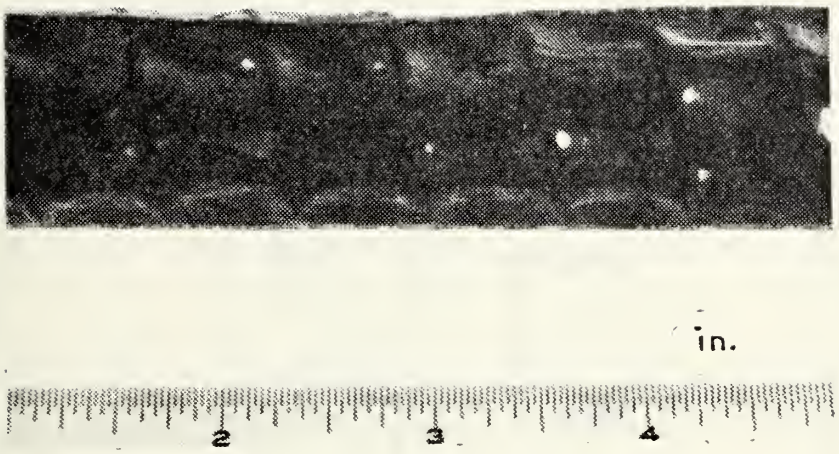

German Tube, Run 19

Figure 11. Photograph of Test Tube

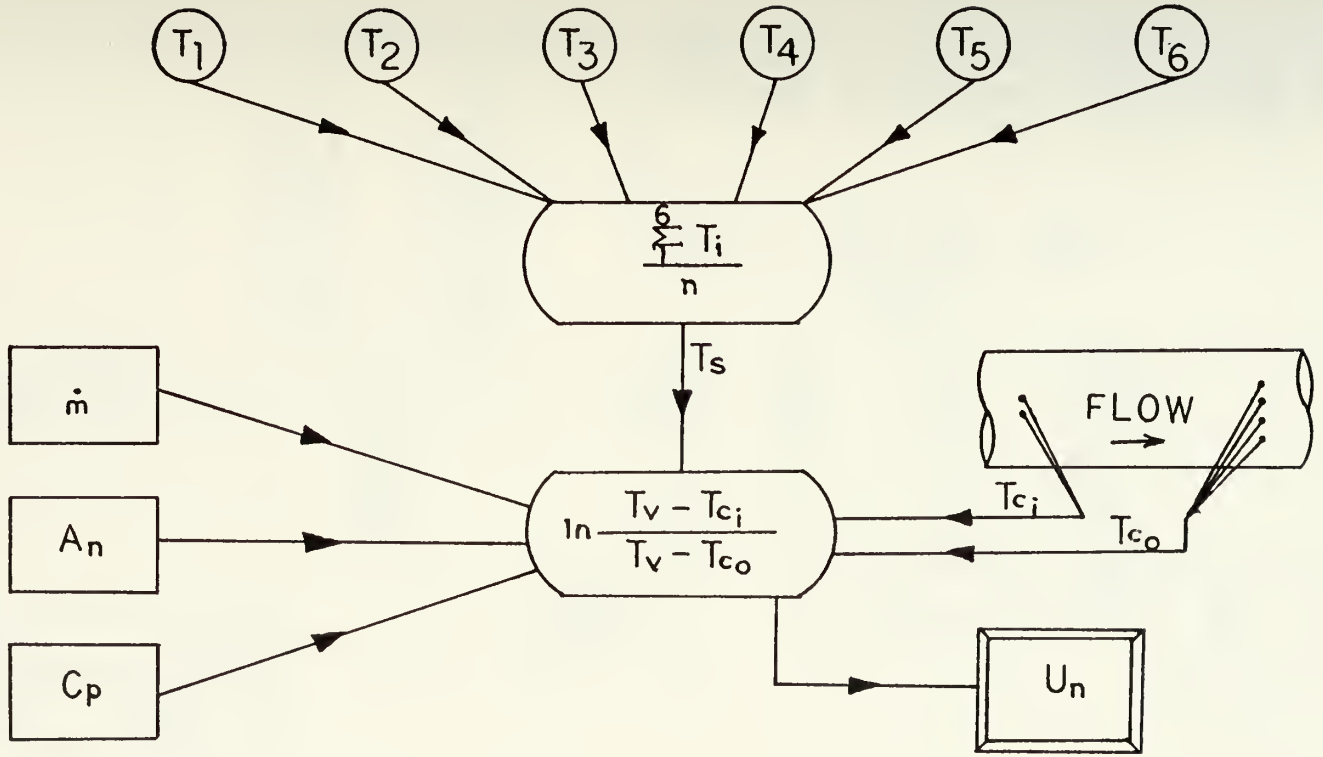

Figure 12. Schematic Representation of Procedure Used to Find Un

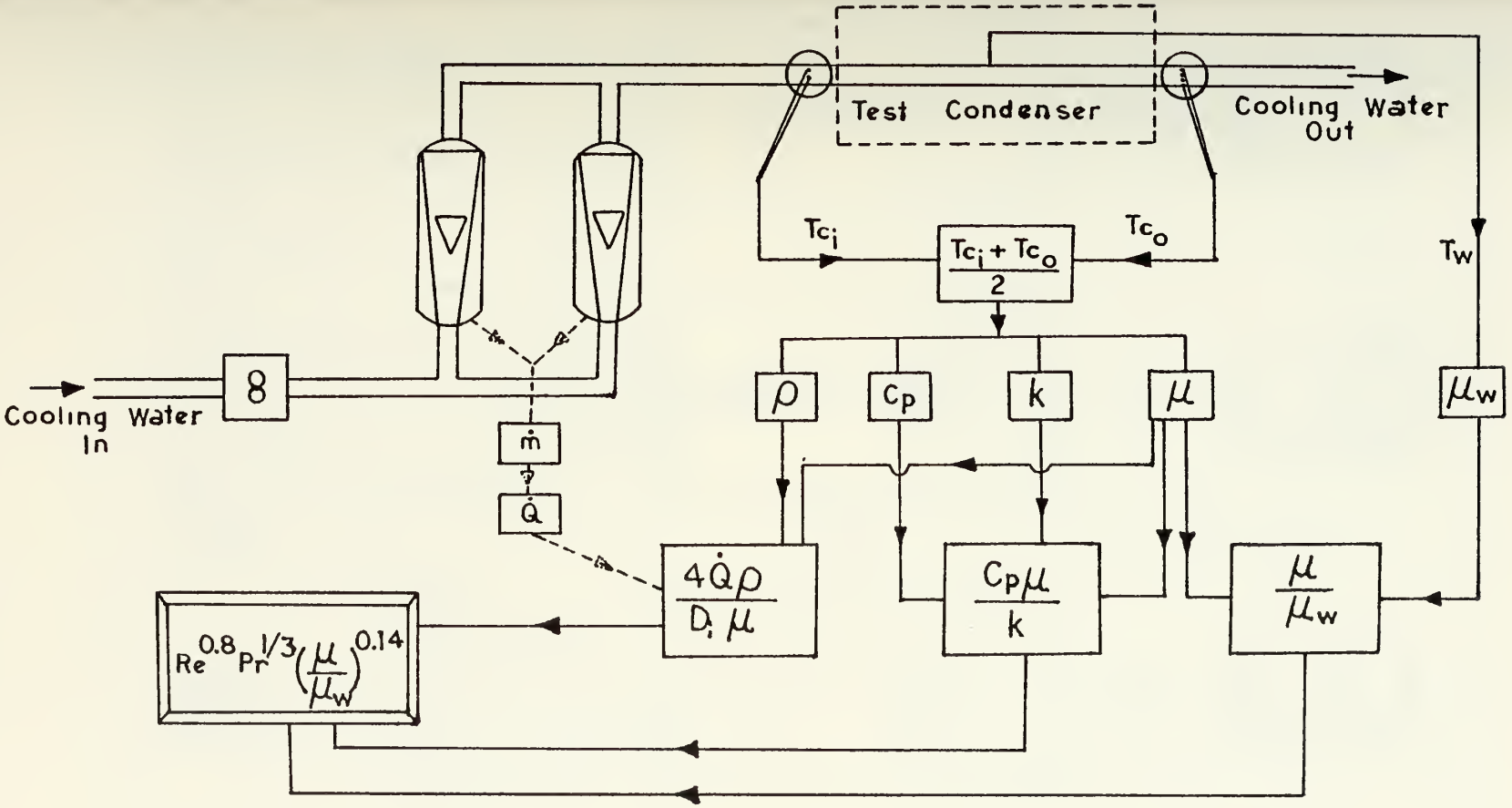

Figure 13. Schematic Representation of Procedure Used to Find Sieder-Tate Parameter

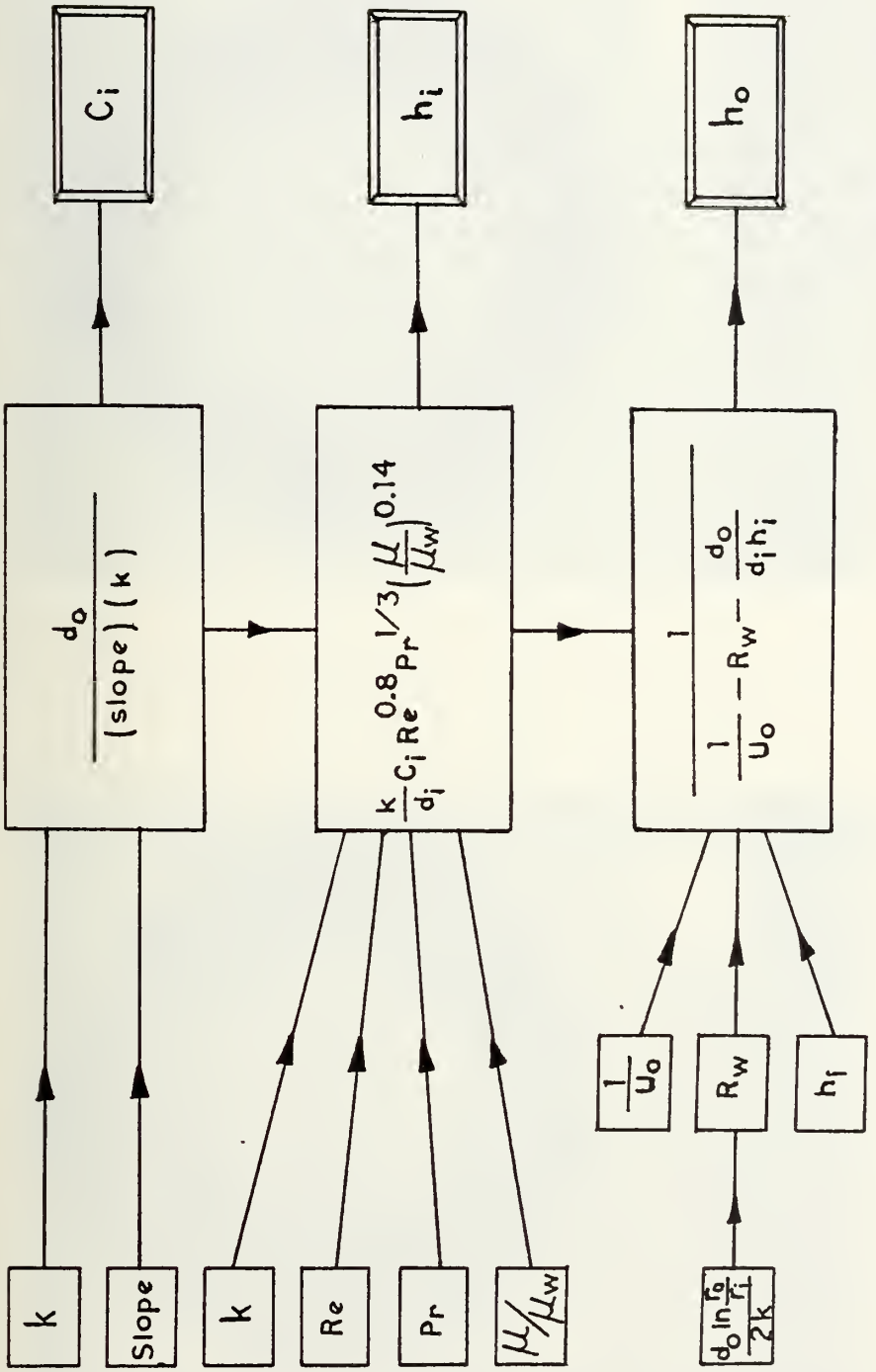

Figure 14. Schematic Representation of Procedure Used to Find Sieder-Tate Coefficient Ci, hi and ho

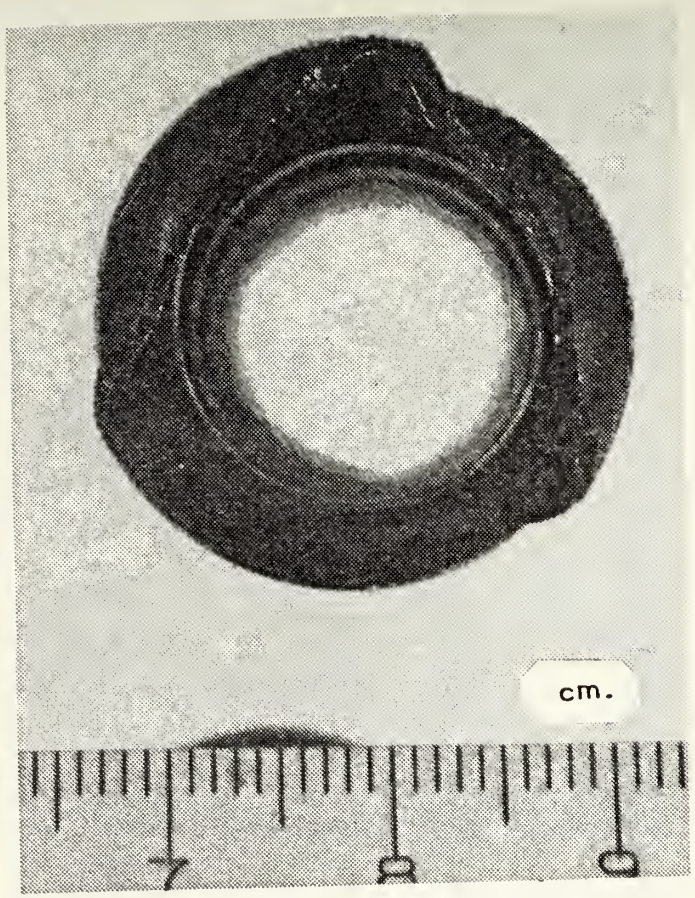

(a) Turbotec Tube, Run 15.

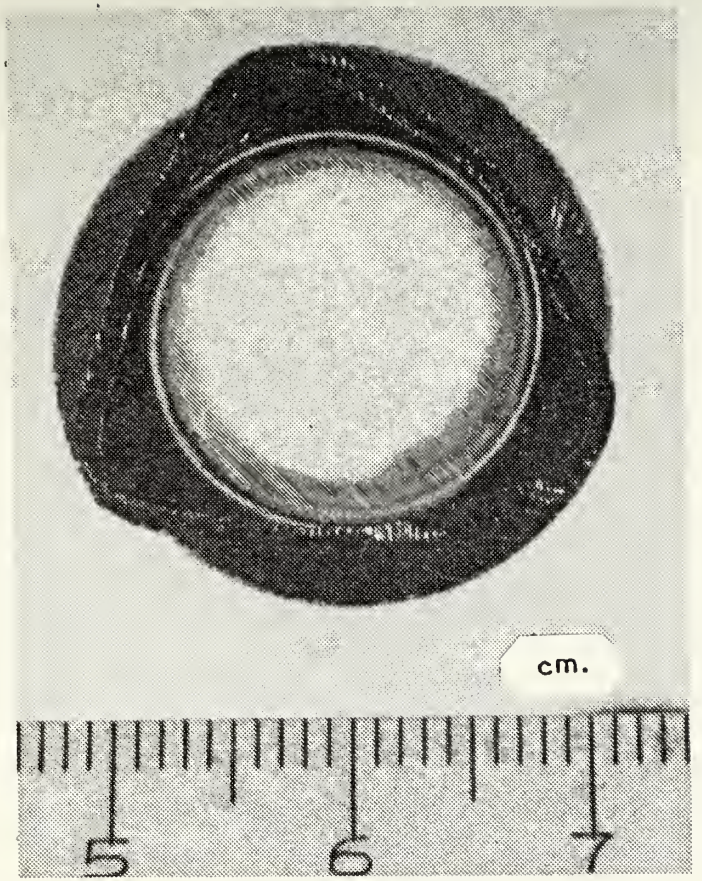

(b) Turbotec Tube with Micro Grooves, Run 13.

Figure 15. Cross Sectional View Of Turbotec Tubes.

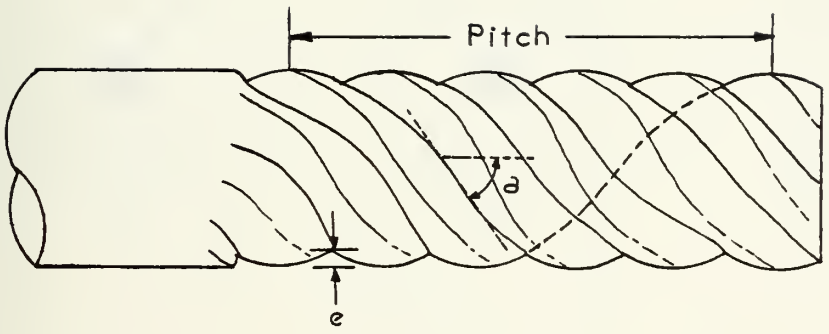

a = Helix Angle
e = Groove Depth

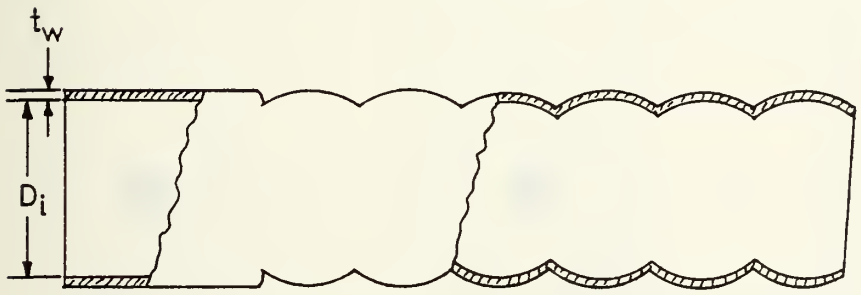

$D_o = D_i + 2t_w$ = Outside Diameter
D_i = Inside Diameter
t_w = Wall Thickness

Figure 16. Definition of Helix Angle, Groove Depth, Pitch, D_i, D_o, and t_w .

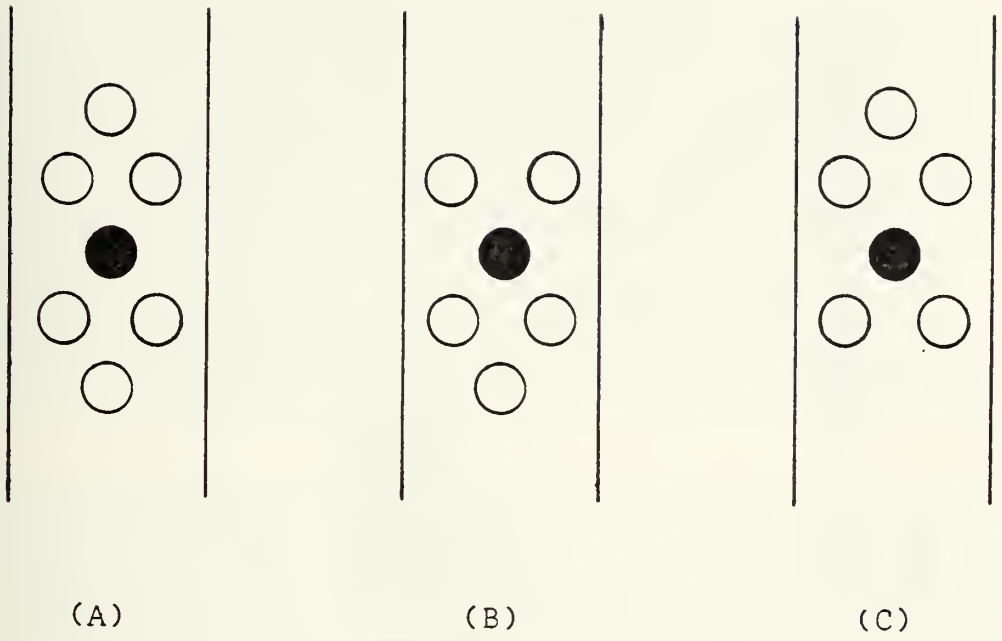

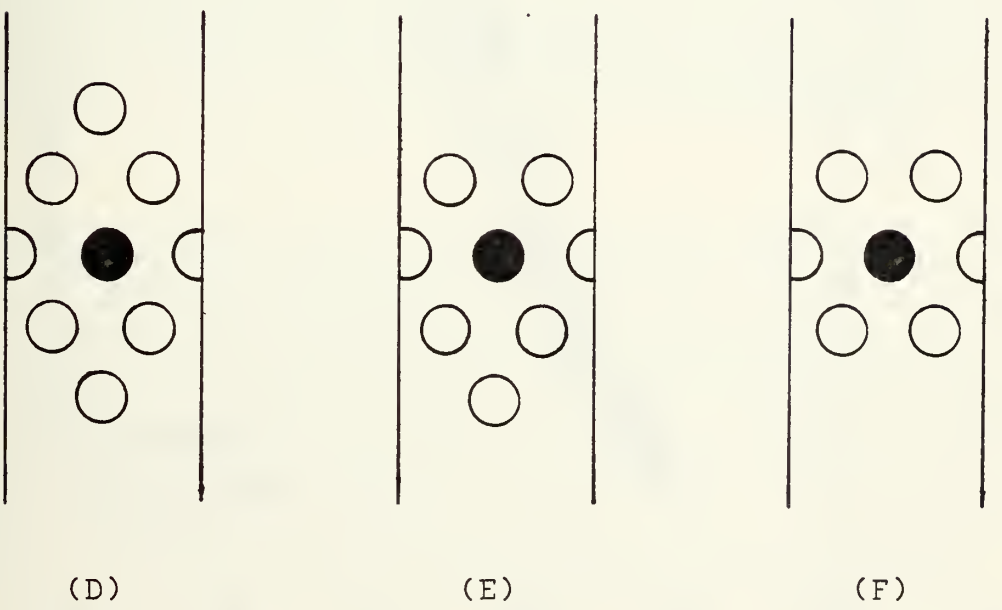

Figure 17. Condenser Tube Configuration

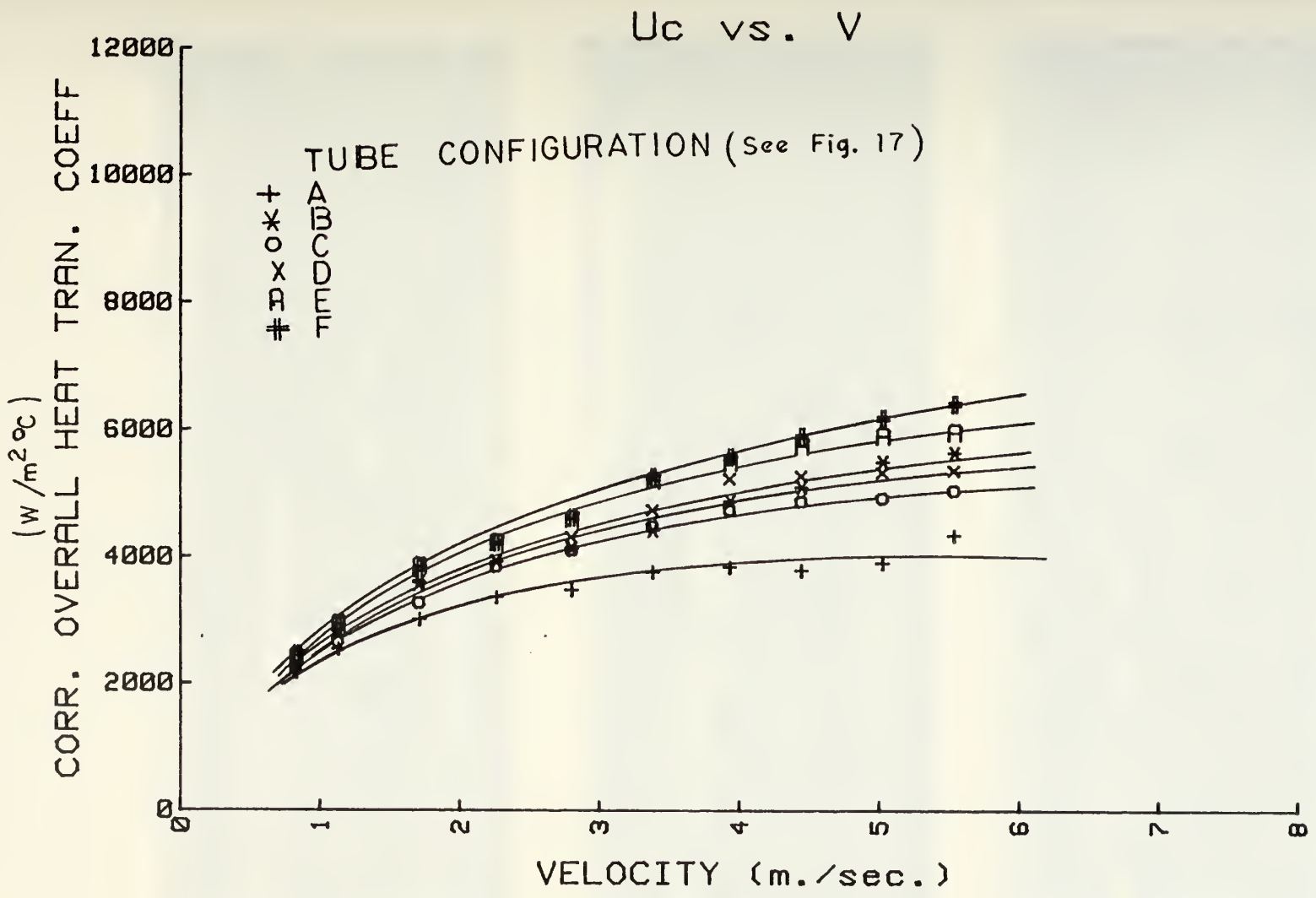

Figure 18. Smooth Tube Uc vs. V of Cooling Water

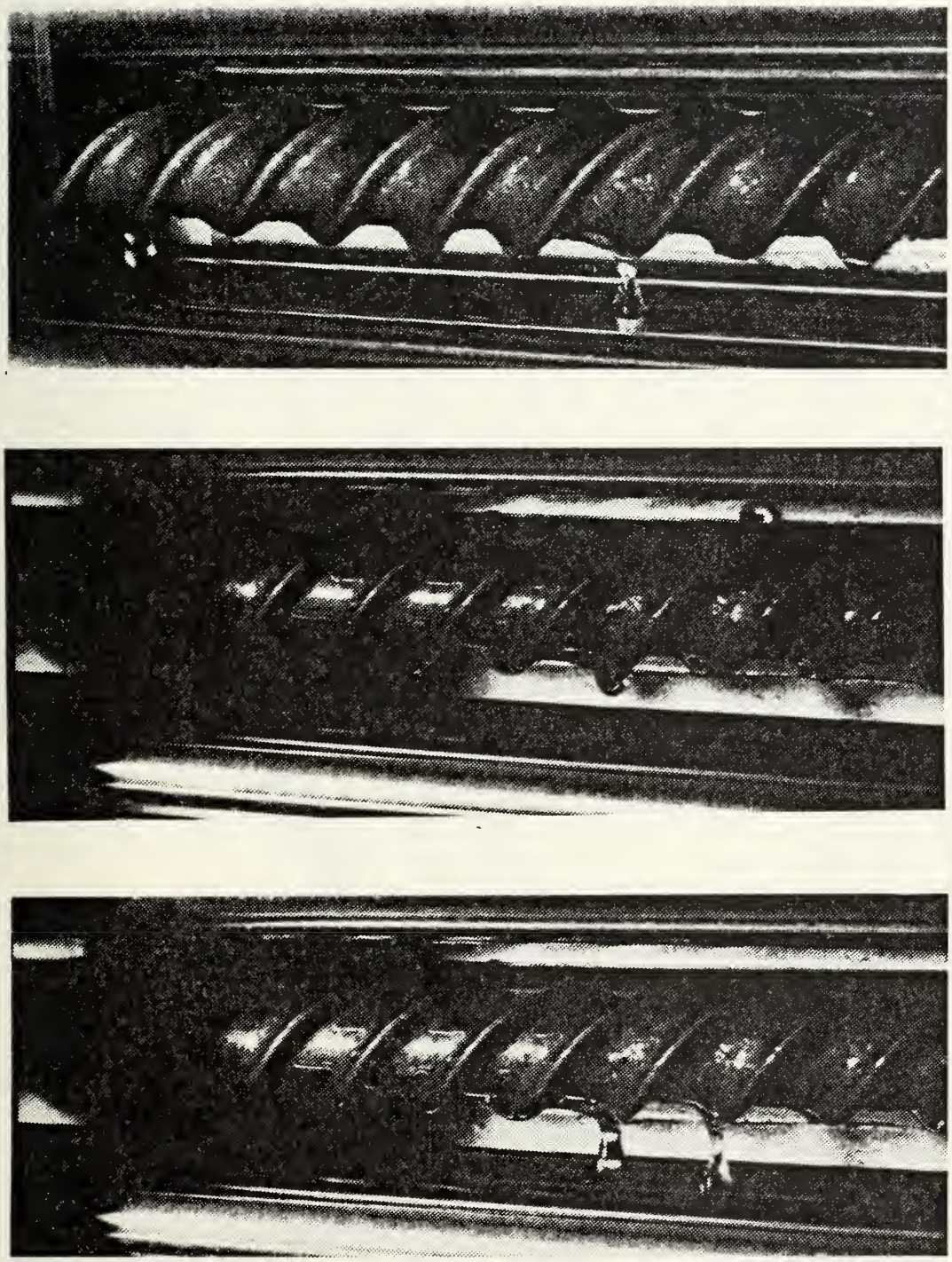

Figure 19. Photographs Of Mixed Condensation On Turbotec Tube.

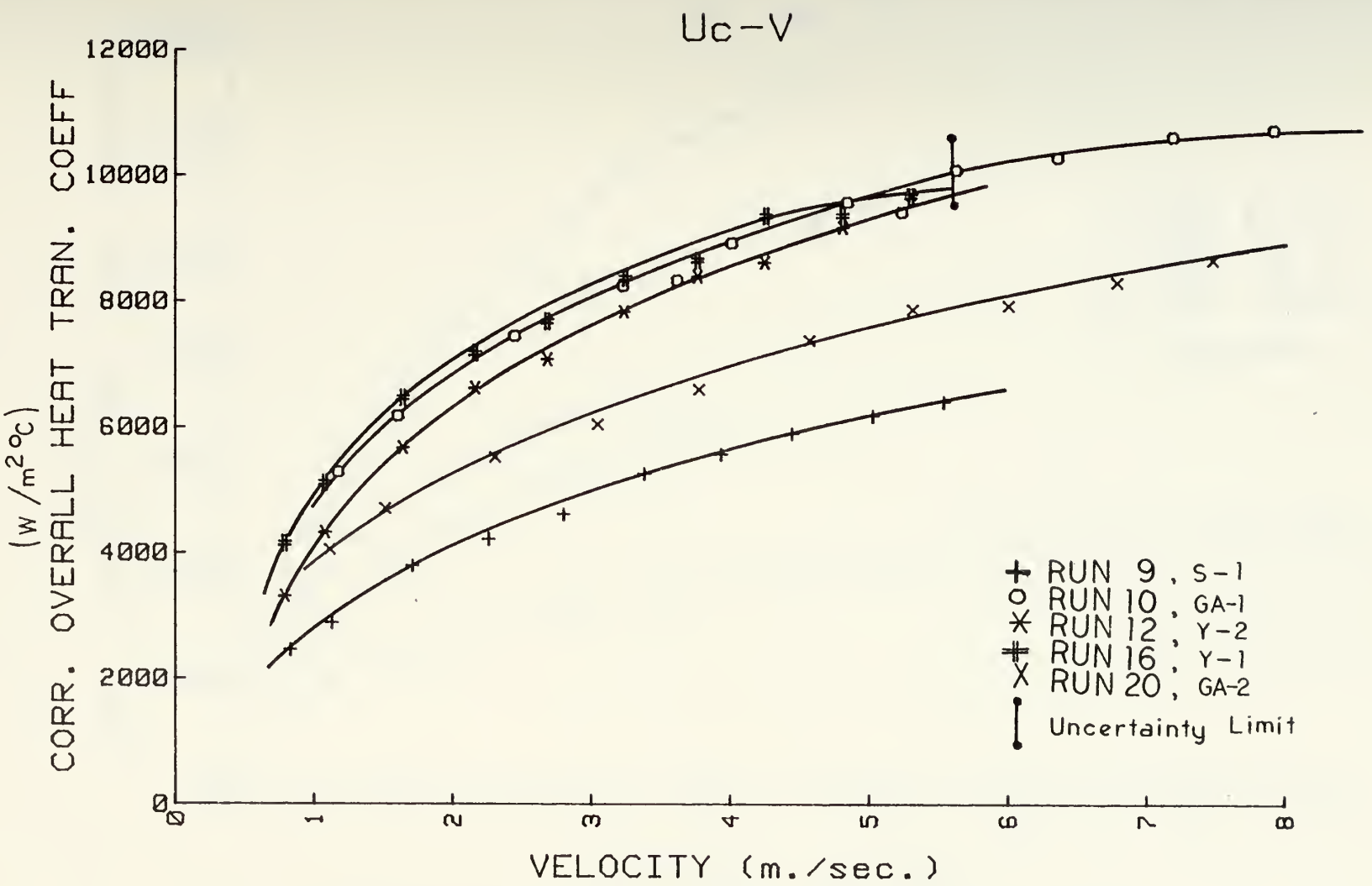

Figure 20. Corrected Overall Heat Transfer Coofficient Versus Cooling Water Velocity.

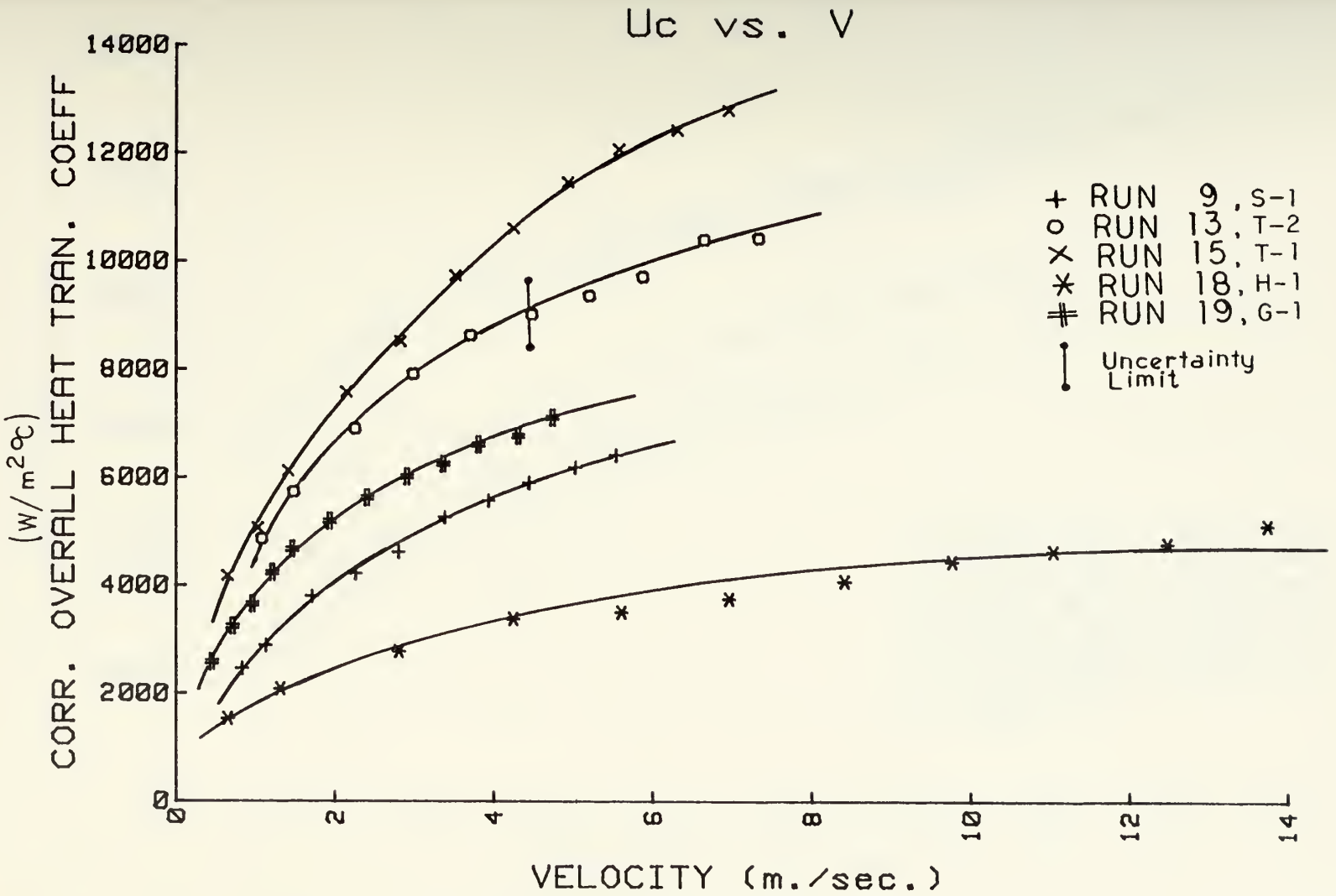

Figure 21. Corrected Overall Heat Transfer Coefficient Versus Cooling Water Velocity.

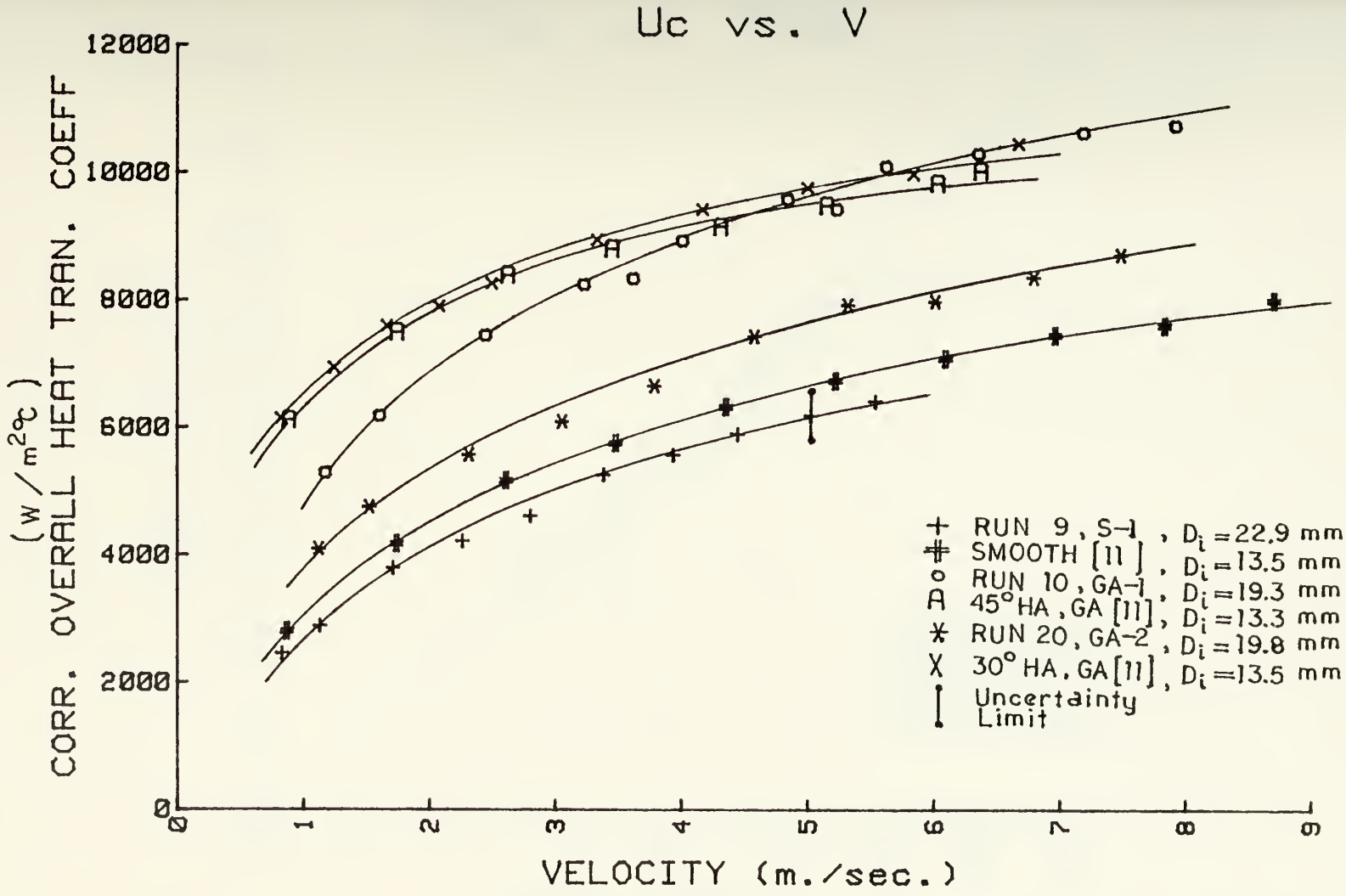

Figure 22. Corrected Overall Heat Transfer Coefficient Versus Cooling Water Velocity.

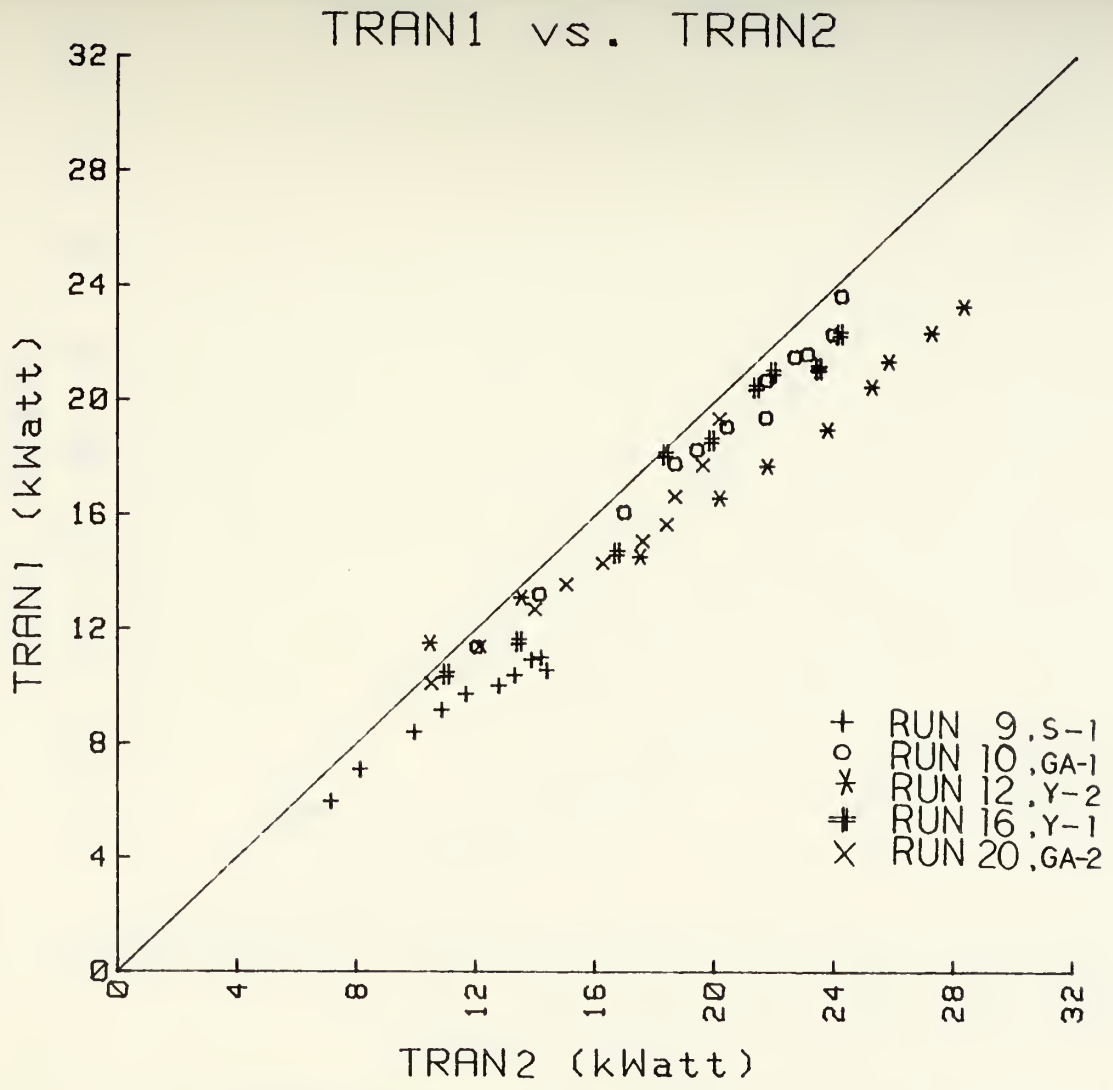

Figure 23. Overall Heat Balance

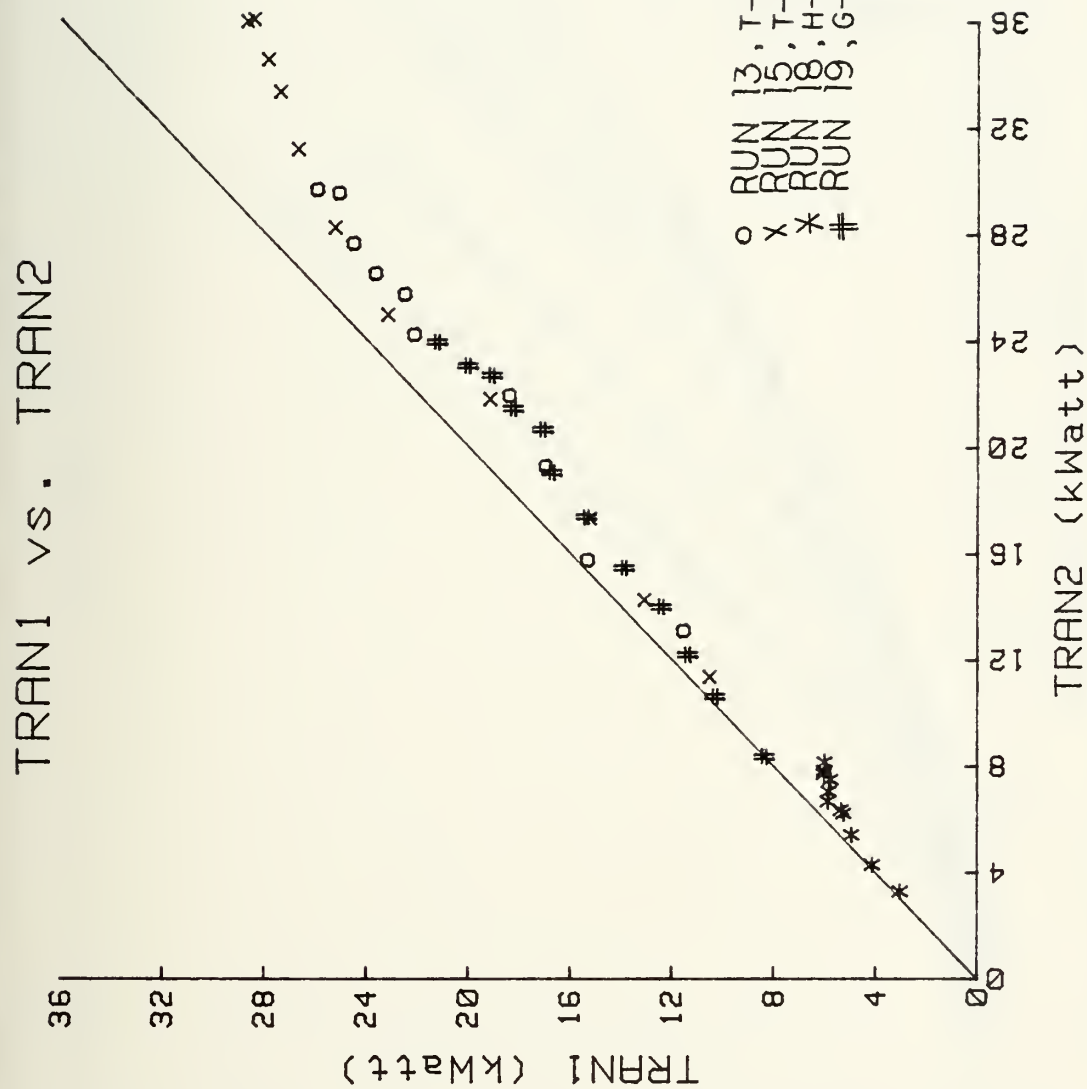

Figure 24. Overall Heat Balance.

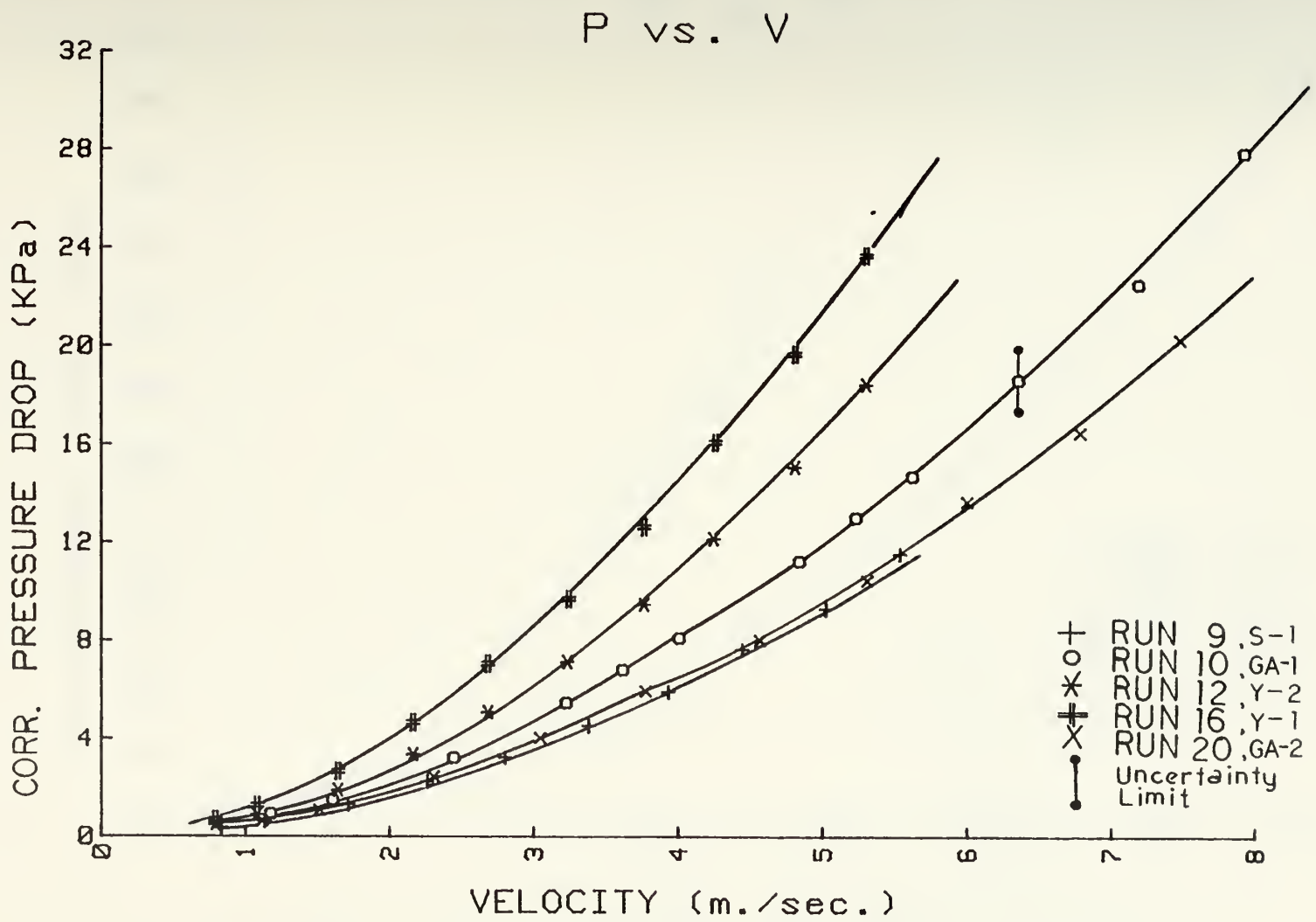

Figure 25. Corrected Pressure Drop Versus Cooling Water Velocity.

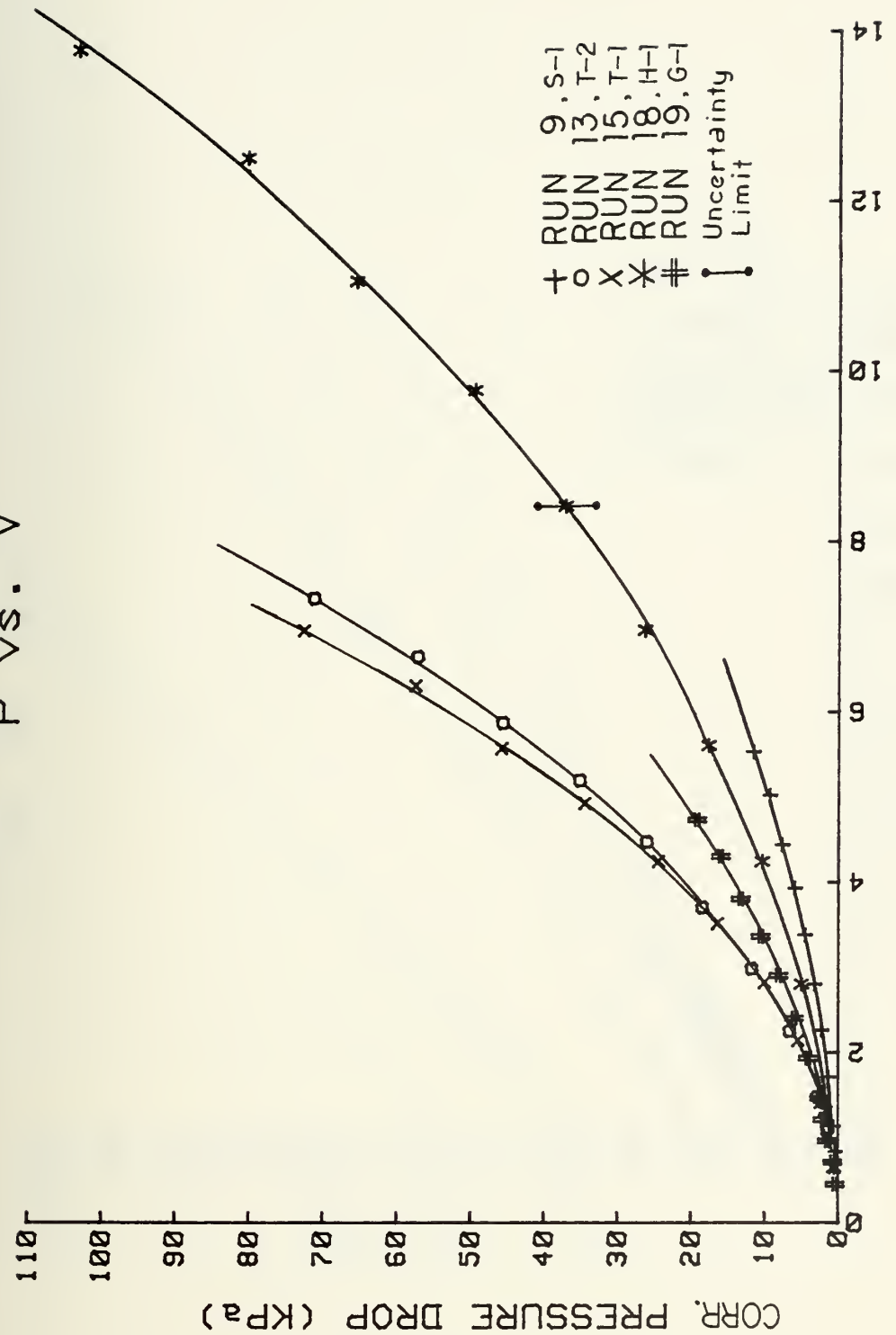

Figure 26. Corrected Pressure Drop Versus Cooling Water Velocity.

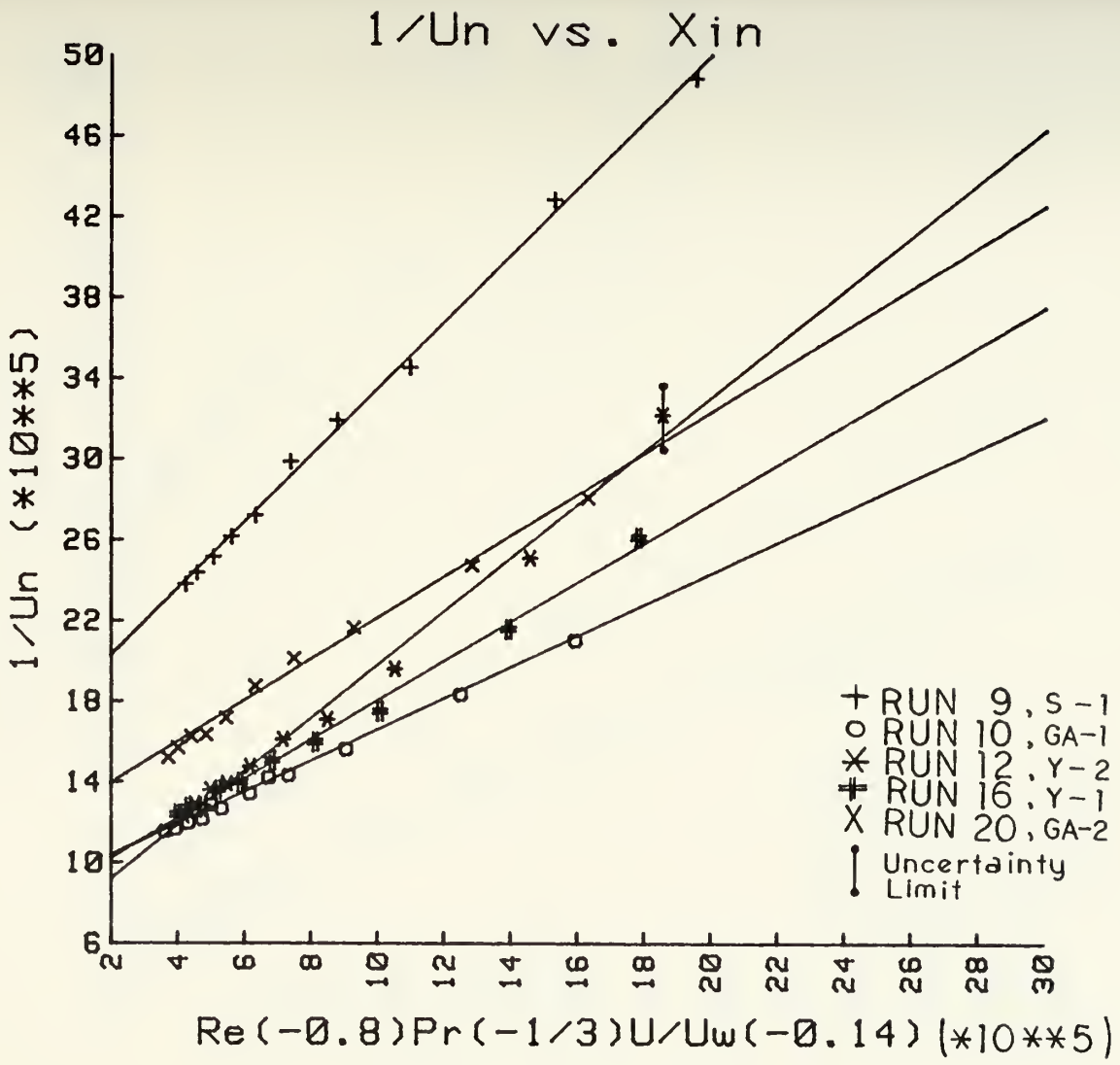

Figure 27. Wilson Plot

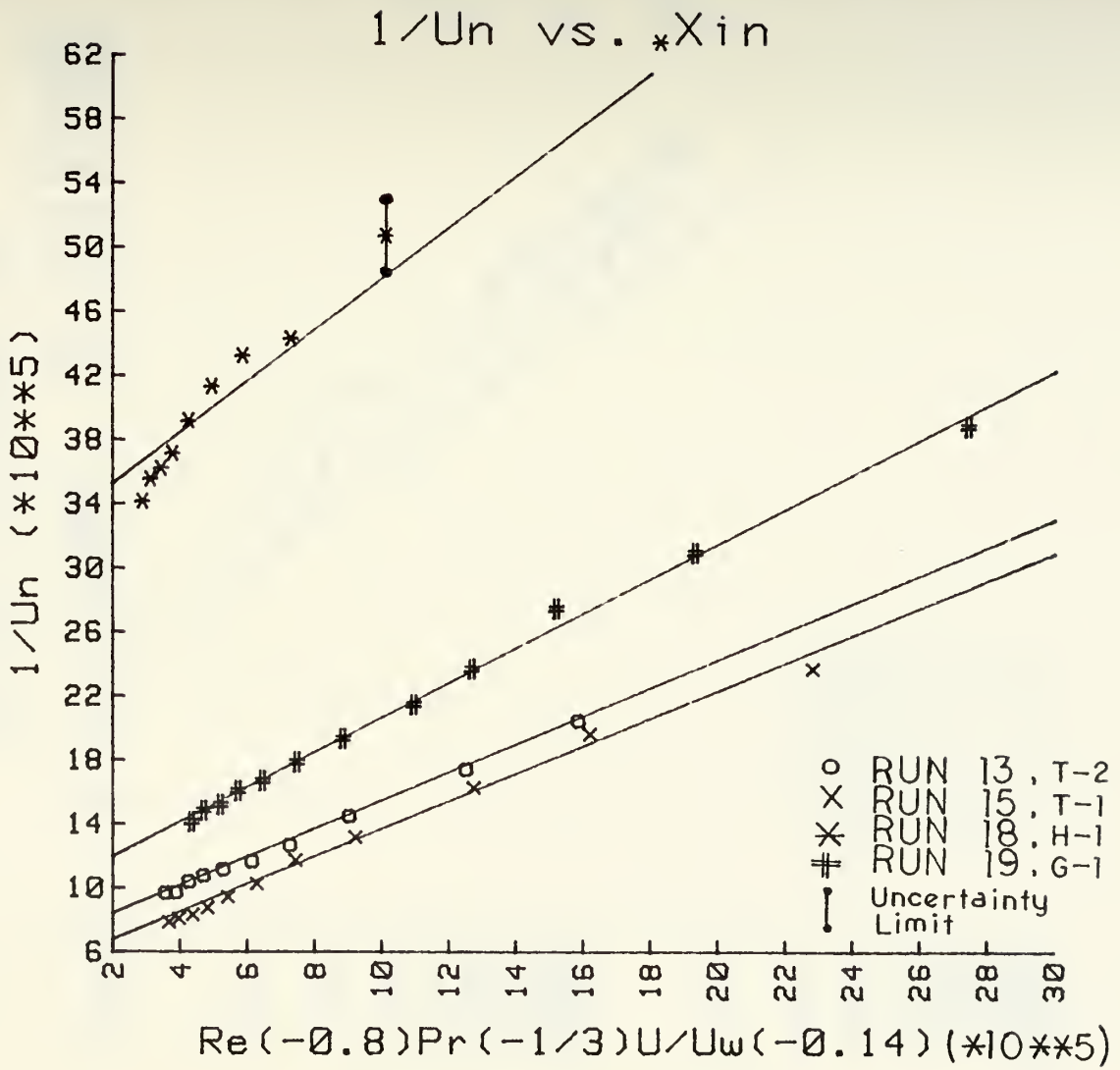

Figure 28. Wilson Plot.

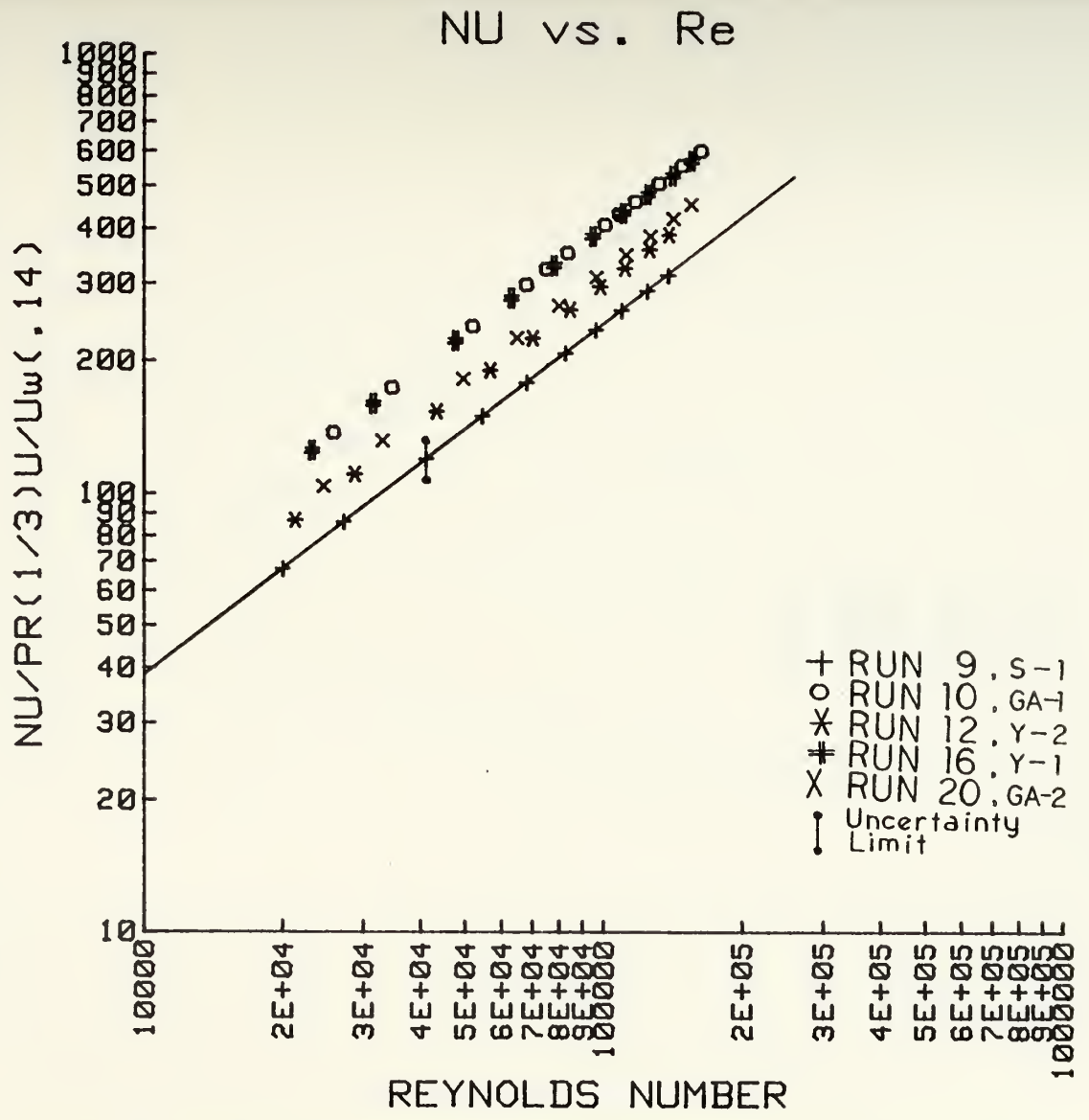

Figure 29. Inside Nusselt Number Correlation Versus Reynolds Number.

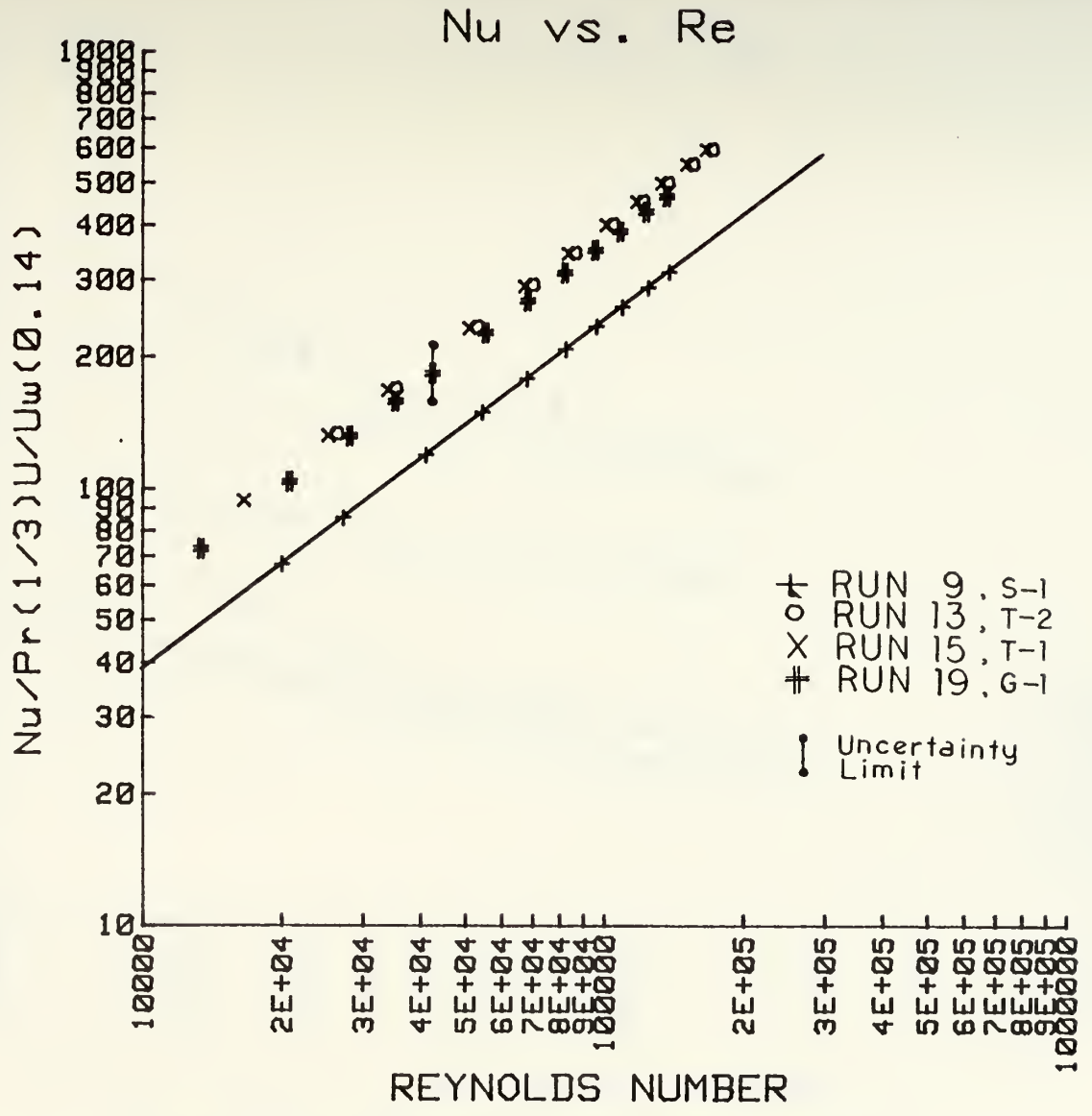

Figure 30. Inside Nusselt Number Correlation Versus Reynolds Number.

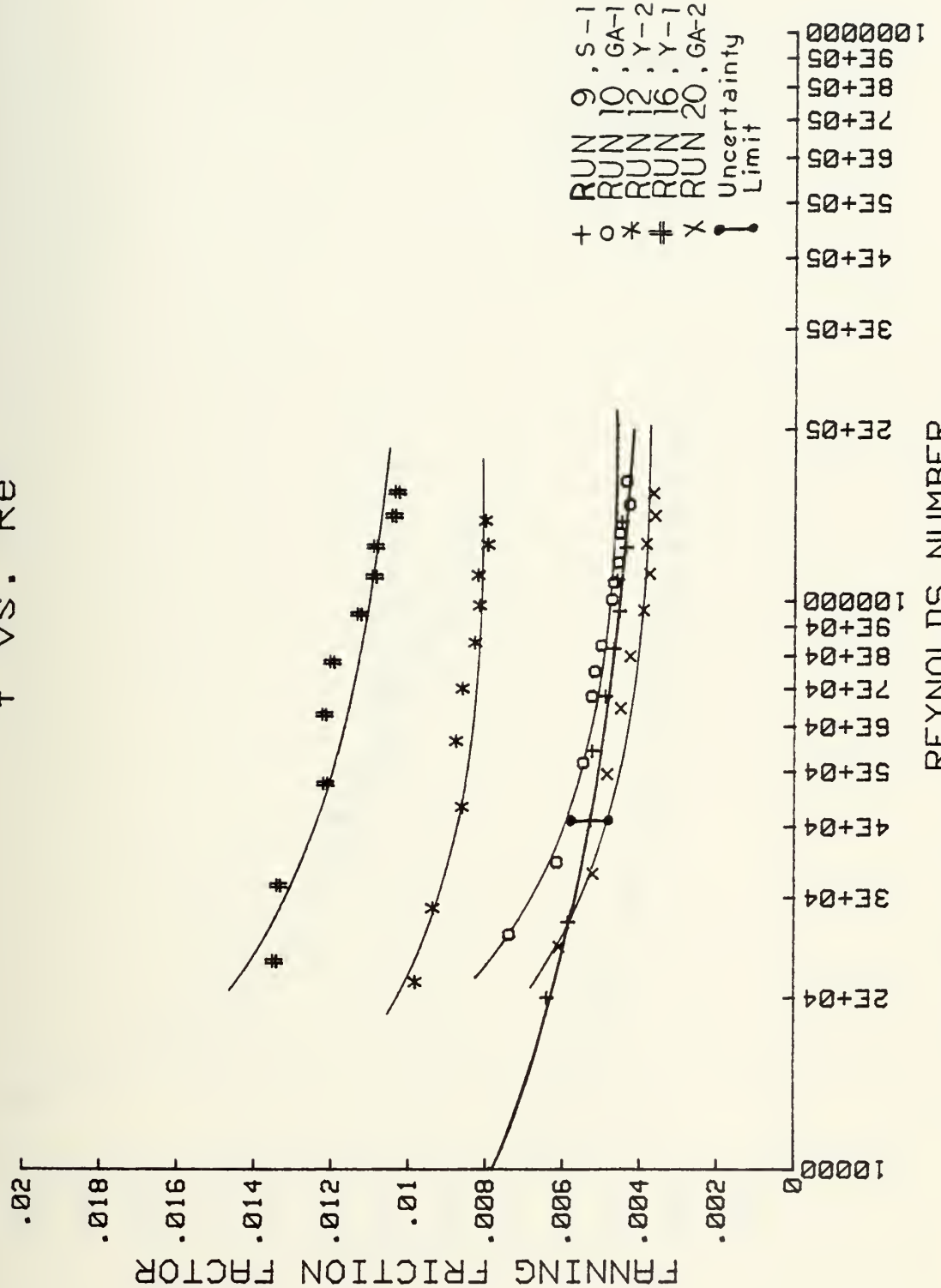

Figure 31. Friction Factor Versus Reynolds Number.

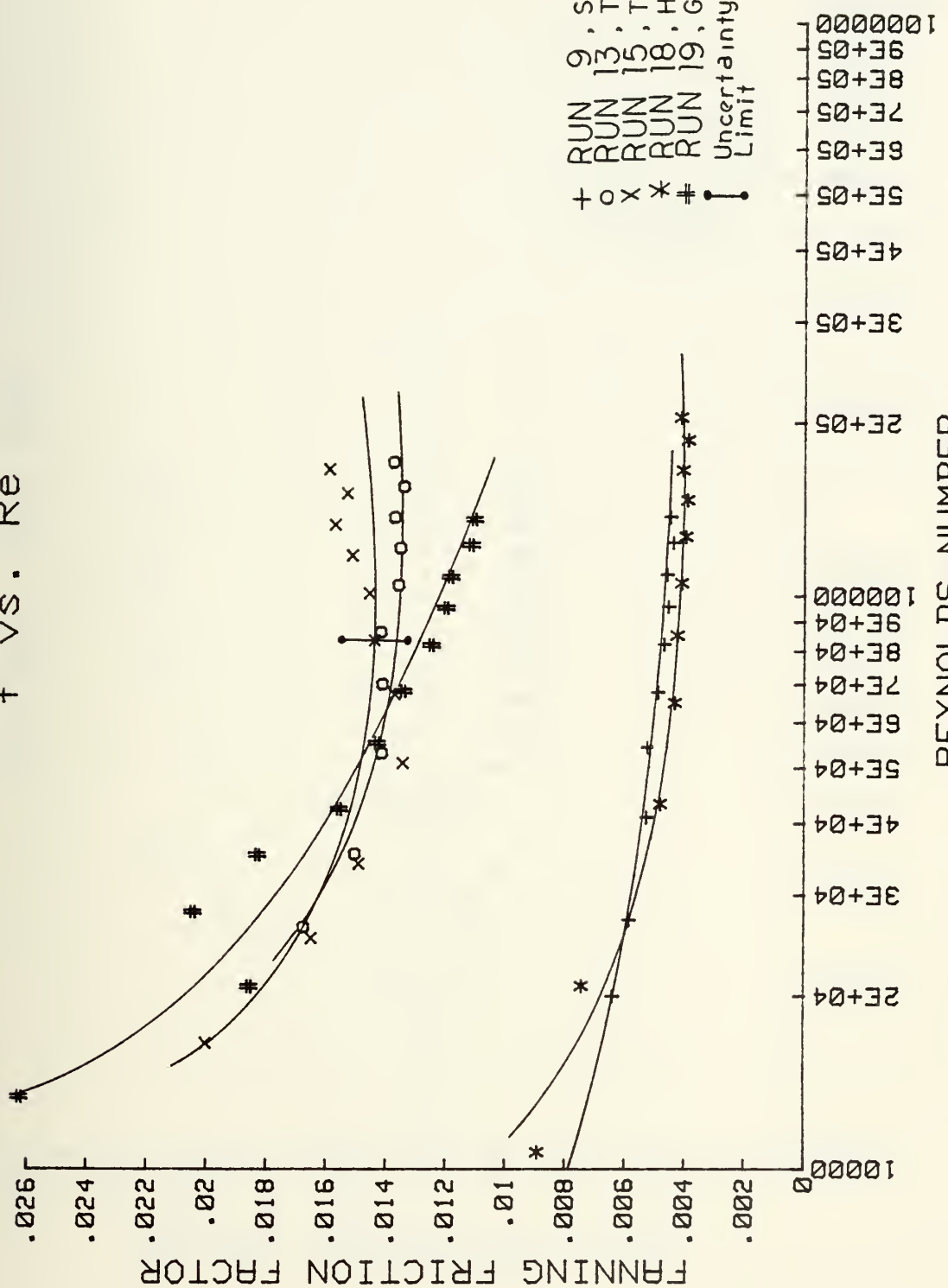

Figure 32. Friction Factor Versus Reynolds Number.

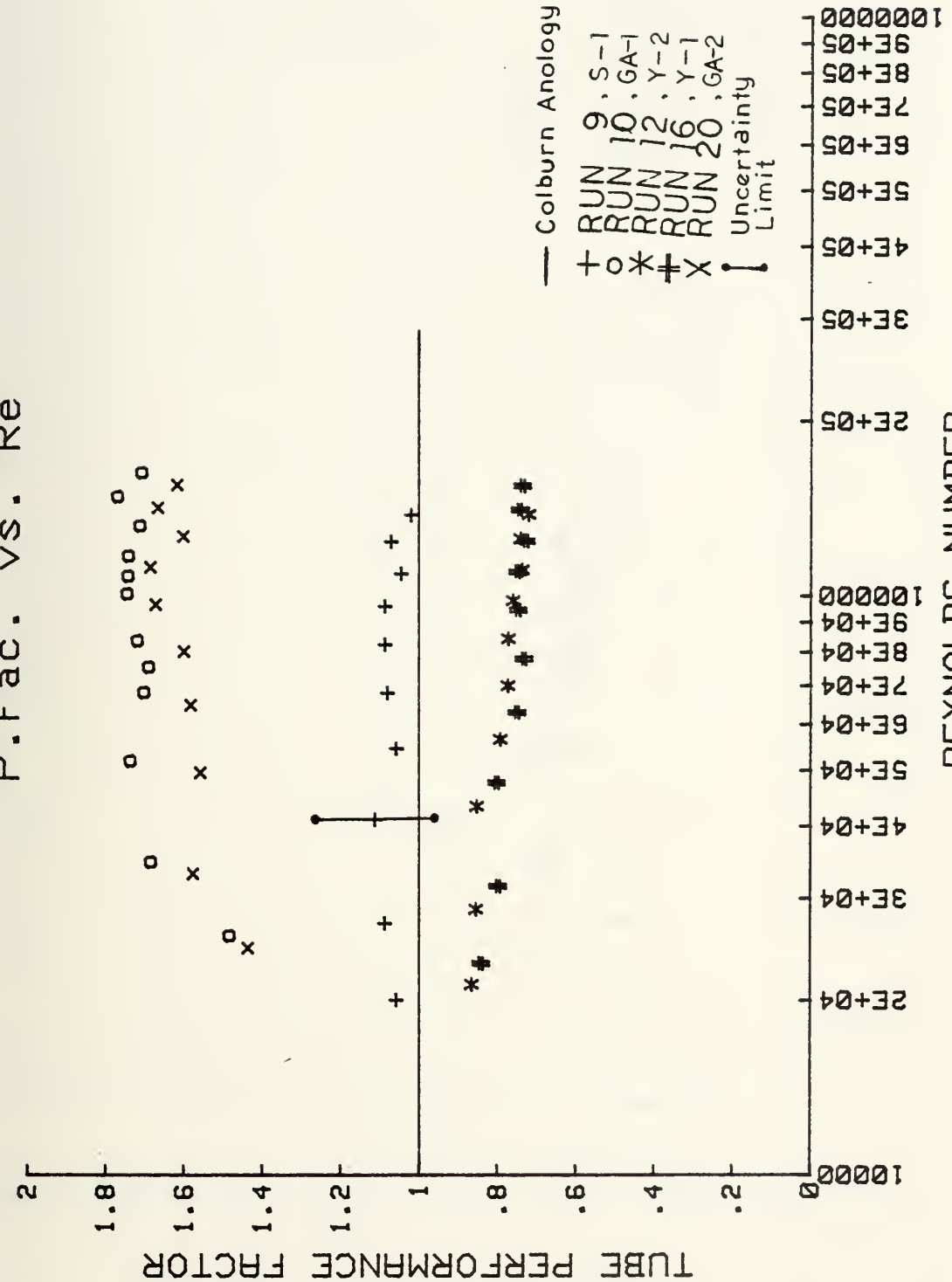

Figure 33. Tube Performance Factor Versus Reynolds Number.

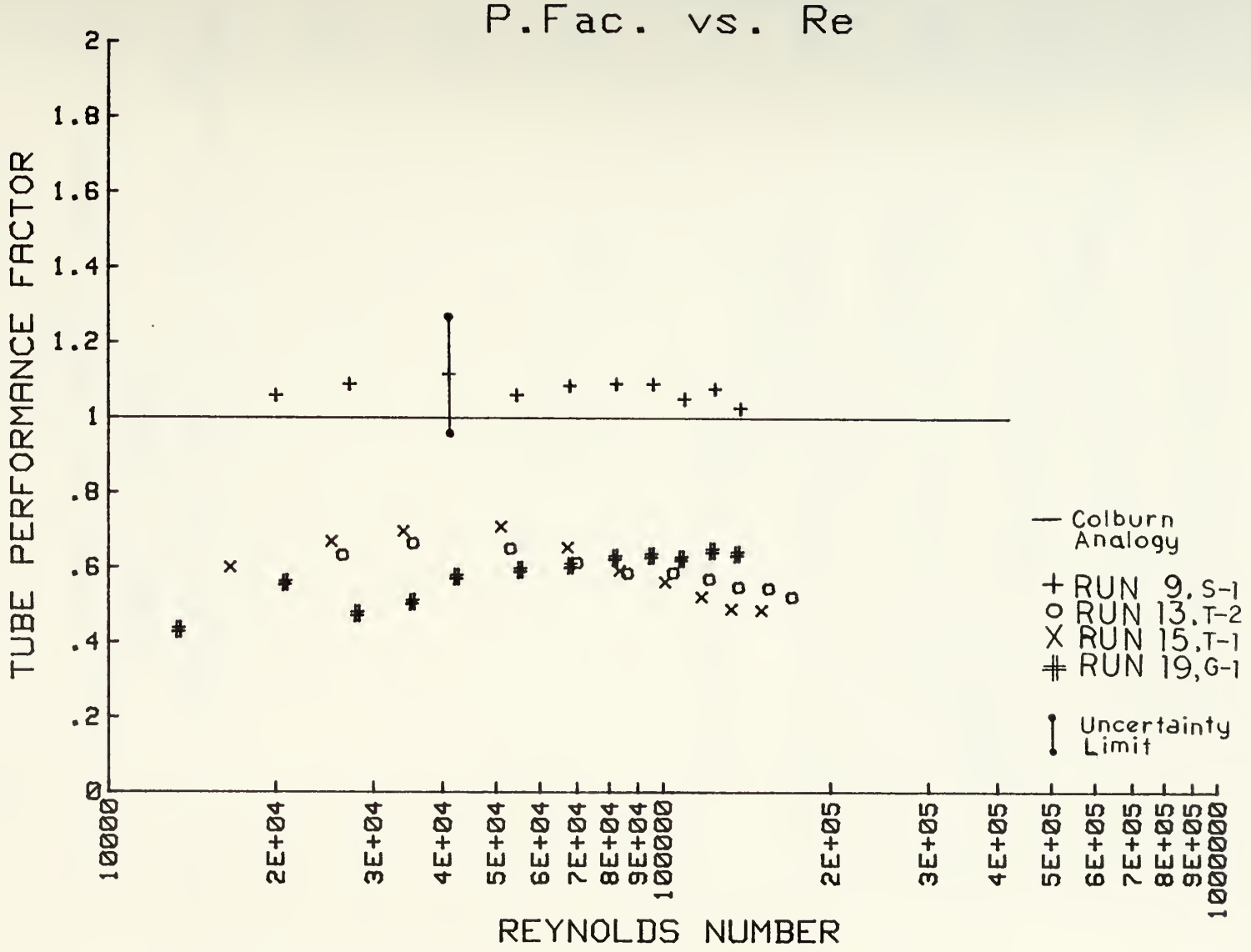

Figure 34. Tube Performance Factor Versus Reynolds Number.

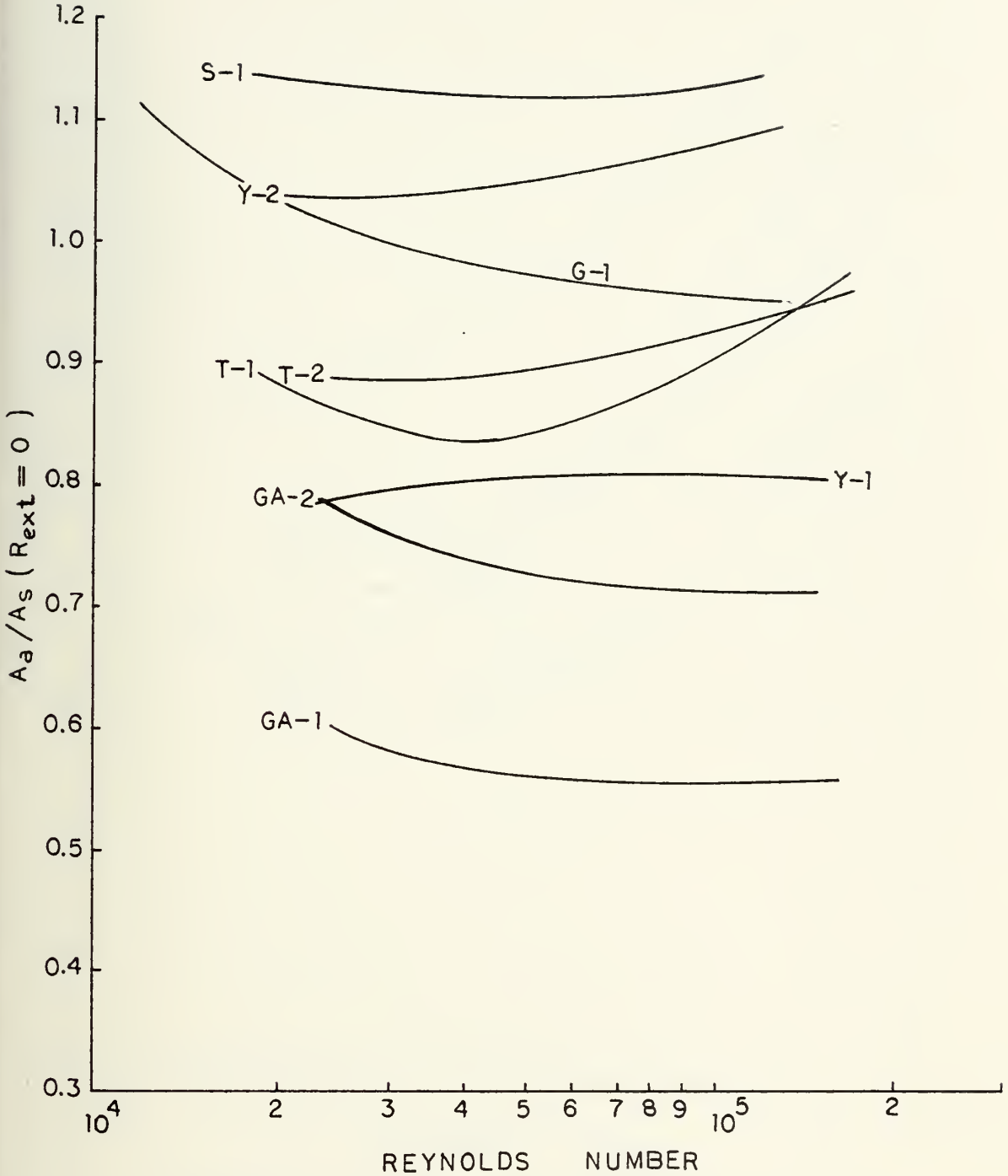

Figure 35. Area Ratio Versus Reynolds Number for $R_{ext}=0$.

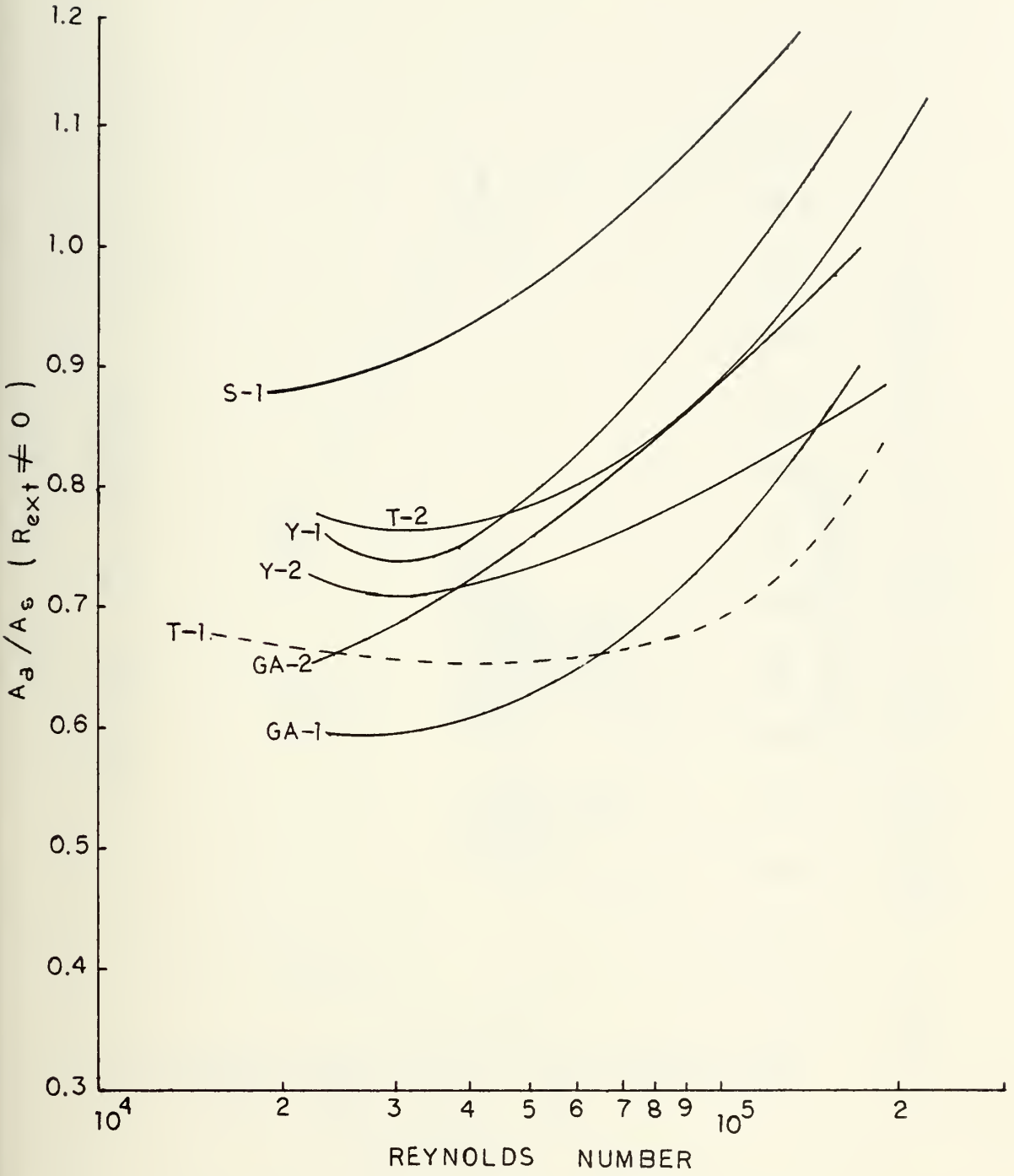

Figure 36. Area Ratio Versus Reynolds Number for $R_{ext} \neq 0$.

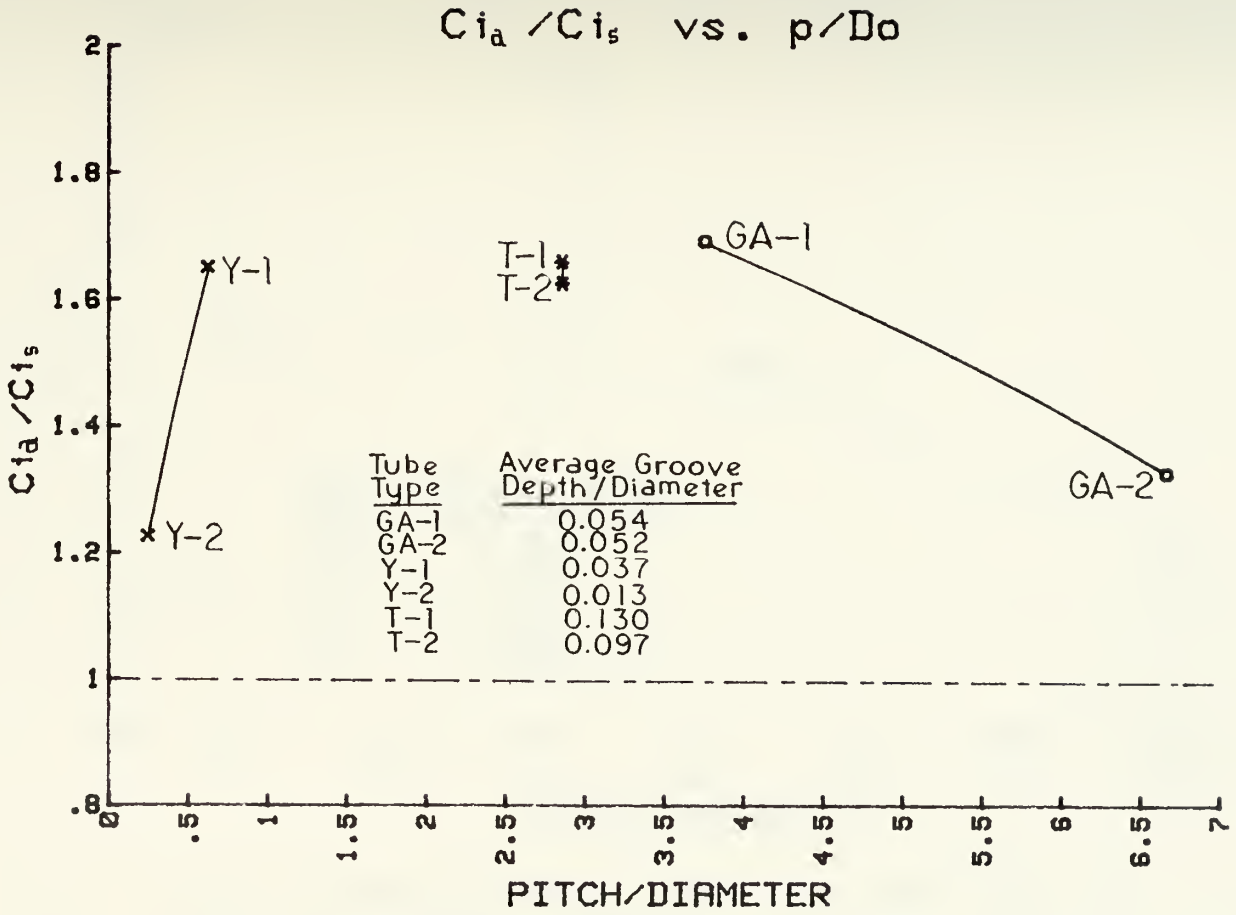

Figure 37. Comparative Effect of Tube Pitch (Helix Angle) on Inside Heat Transfer Coefficient.

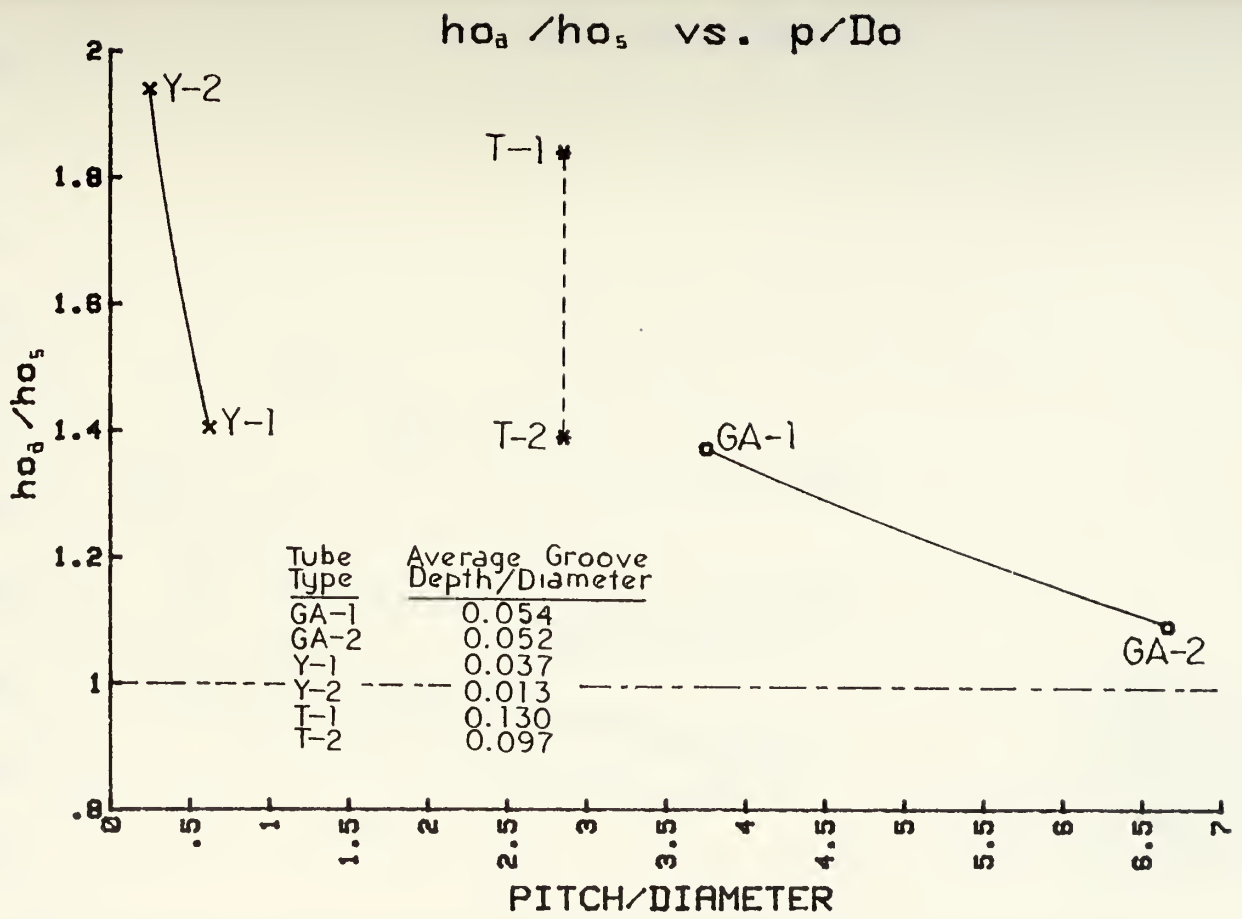

Figure 38. Comparative Effect of Tube Pitch (Helix Angle) on Outside Heat Transfer Coefficient.

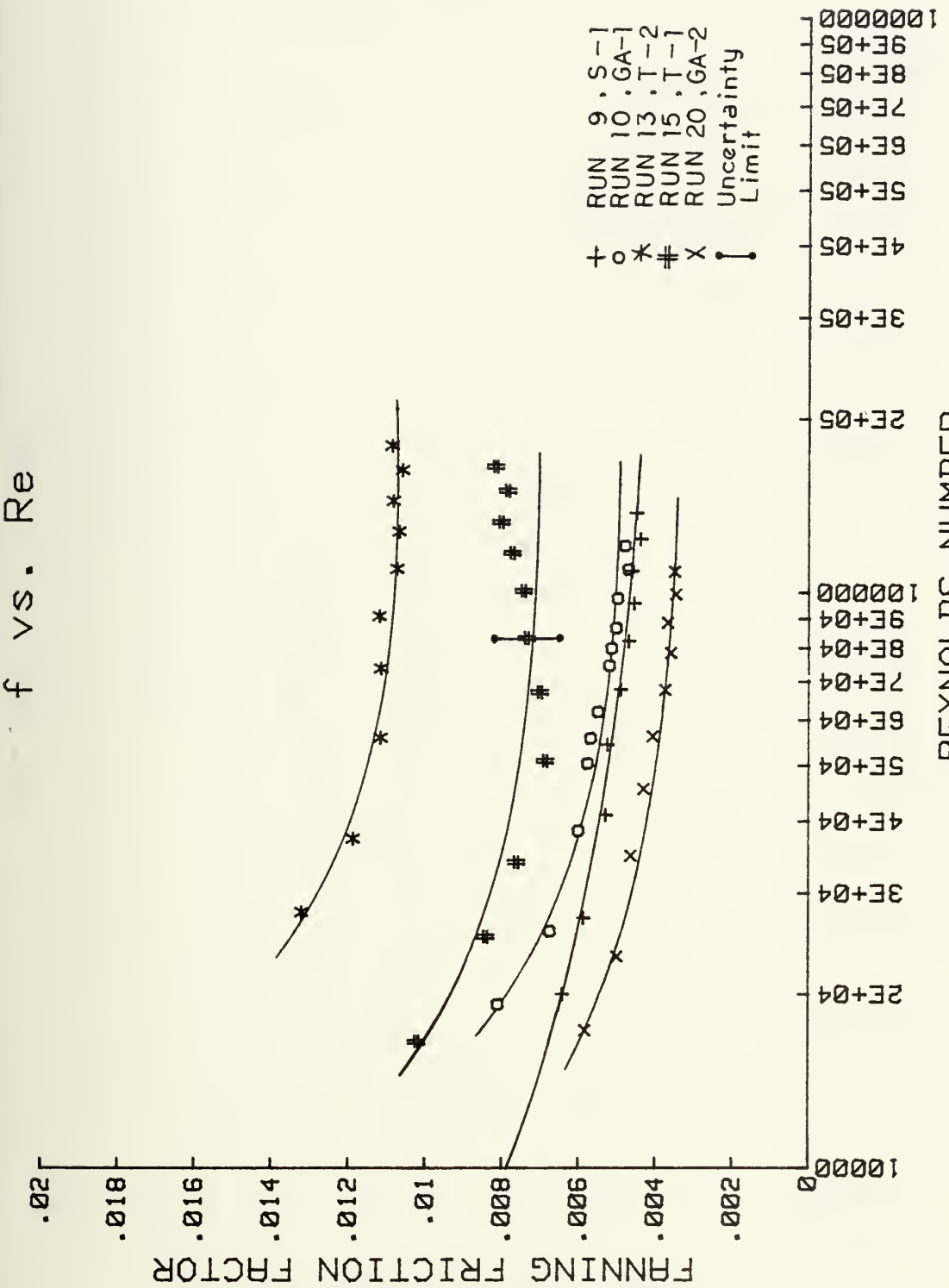

Figure 39. Friction Factor Versus Reynolds Number Based on D_h.

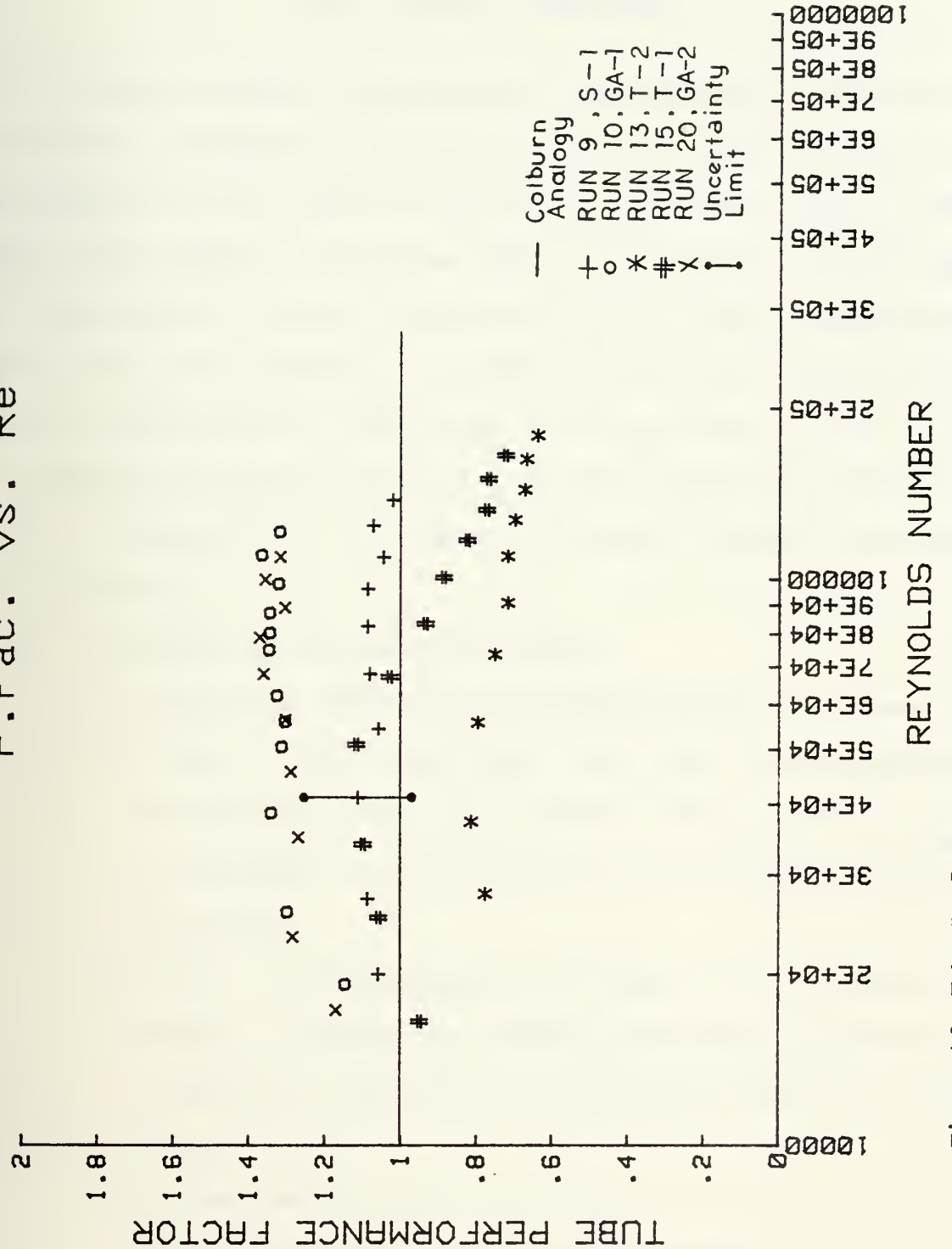

Figure 40. Tube Performance Factor Versus Reynolds Number Based on D_h.

APPENDIX A

TUBE CLEANING PROCEDURE

To insure filmwise condensation, the condenser tubes had to be prepared. Exterior and interior surfaces were cleaned to insure proper wetting characteristics and to insure that all deposits were removed. Titanium tube was prepared in accordance with the procedure given in Fenner [12]. Copper and copper-nickel tubes were prepared in accordance with the procedures given in Pence [10]. Stainless steel tubes and inside of the test condenser were prepared in accordance with the procedure given in Newton [23]. The steps in these cleaning procedures are as follows:

A. Titanium tubes cleaning process

1. Swab tube surface with acetone to remove grease.
2. Using a test tube brush, brush the inside surface of the tube with a 50 percent sulfuric acid solution. Also apply this solution to the outside surface of the tube.
3. Rinse inside and outside of tube with tap water.
4. Apply a 50 percent solution of sodium hydroxide (heated to 95°C) to the outside surface of the tube.
5. Rinse the tube with tap water.
6. Rinse thoroughly with distilled water.

B. Copper and copper-nickel tubes cleaning process.

1. Prepare a solution of equal parts of ethyl alcohol and a 50 percent solution of sodium hydroxide, and heat to 85°C.

2. Apply this solution to the surface of the test tube.
3. Drain and rinse the test tube with tap water.
4. Rinse thoroughly with distilled water.

To remove any deposits on the inside surface of the test tube a solution of 50 percent hydrochloric acid is used. The acid solution is applied by brush and the test tube is then rinsed thoroughly with tap water. After rinsing with tap water the tube is then rinsed with distilled water.

C. Stainless steel tubes cleaning process.

1. Prepare a Alconox detergent solution and heat to $90^{o}C$.
2. Apply this solution to the inside and outside surfaces of the test tube.
3. Drain and rinse the test tube with distilled water.
4. Spray with alcohol.
5. Rinse with distilled water.
6. Spray with acetone.
7. Rinse with distilled water.

To remove any deposits on the inside surface of the test tube use the process as outlined above for the copper and copper-nickel tubes.

APPENDIX B

OPERATING PROCEDURES

1. LIGHT-OFF PROCEDURE

A. Boiler Operation

(1) Energize main circuit breaker located in power panel P-2.

(2) Turn key switch on - located on right side of main control board.

(3) Energize circuit breaker on left side of main control panel by depressing start button.

(4) Energize individual circuit breakers on left side of main control panel. The following list identifies each circuit breaker:

(a) #1 - Feed pump
(b) #2 - Outlets
(c) #3 - Hot water heater (feedwater tank)
(d) #4 - Condensate pump
(e) #5 - Boiler
(f) #6 - Cooling tower
(g) #7 - Cooling water pump

(5) Insure water level is up in the feedwater tank, and turn on switch to energize heater.

(6) Check valve alignment for recirculating water (FW-1).

(7) Turn on the switch to the feed pump to recirculate water in the feedwater tank.

(8) Energize instrumentation (See section #1).

(9) Energize cold trap refrigeration unit, insure that flammable stowage locker exhaust fan is on, and start vacuum pump.

(10) After feedwater tank has reached a temperature of 60°C, insure water level in boiler is avove low level mark and energize boiler.

(11) Open valve FW-4 (Set rotameter to 15-25% flow).

2. OPERATION

A. Cooling water system

(1) Open valves CW-1 and CW-2 two turns.

(2) Open valve CW-4; then energize pump No. 1 and pump No.2.

(3) Open valve CW-2, and open valve CW-1 (set flow-meter to 40-50% flow).

(4) Open valves CW-5 and CW-6 to obtain desired cooling water flow rate.

(5) Adjust valve CW-4 to obtain desired flow rate.

(6) Vent both sides of the 3.66 m. manometer.

(7) Open valve DS-1 (Begin flow to secondary condenser).

B. Steam System

(1) Boiler operation

(a) When boiler has reached the desired pressure (approximately 3 psig) open valve MS-1.

(b) Insure valve MS-6 is open.

(c) Open valve MS-3 to obtain desired steam flow rate to test condenser. Open valve MS-4 as necessary to maintain boiler pressure at desired level (approximately 5 psig).

(2) House steam operation

(a) Follow steps (1) through (4), (8), (9) and (11) as outlined above for boiler operations.

(b) Insure valves MS-1 is closed and MS-6 is open.

(c) Close valve MS-3 and open valve MS-4.

(d) Open valve MS-2 (approximately 1 turn).

(e) After 5-10 minutes open valve MS-3 to obtain desired steam flow rate to test condenser, and close valve MS-4.

(f) Adjust valve MS-2 approximately 5 psig.

C. Condensate and feedwater system

(1) Using boiler

(a) To collect drains in test condenser hotwell operate with valve C-1 closed. After test run has been completed, open valve C-1 and condensate will drain into secondary condenser hotwell.

(b) The condensate pump is operated intermittently, when level in secondary condenser hotwell dictates. When pump is secured, keep valve C-2 closed. When pump is required, start pump and then open valve C-2. In this mode keep valve C-3 closed. When pump is not required, close valve C-2 and stop pump.

(c) While feed pump is running (continuous operation) valve FW-1 must be throttled so that a positive flow is insured (about 20% percent

flow). Valve FW-2 is a solenoid valve which is actuated by the boiler controls.

(d) When boiler is energized, valve FW-3 must be fully opened.

(e) Make-up is added to the system through the top of the feedwater tank by removing anode.

(2) Using house steam

(a) As using boiler, the condensate pump is operated intermittently, when level in secondary condenser hotwell dictates. When pump is secured, keep valves C-2 and C-3 closed. When pump is required, start pump and then open valve C-3, in this mode keep valve C-2 closed.

(b) Keep feed pump closed.

3. SECURING SYSTEM

A. Using boiler

(1) Close valves MS-3 and MS-4. Secure power to boiler and then close valve MS-1.

(2) Close valve FW-4.

(3) Pump condensate from secondary condenser hotwell to feedwater tank. Secure valve C-2.

(4) Secure vacuum pump and refrigeration unit.

(5) Secure power to heater (switches on side and stand).

(6) Secure flow to secondary condenser.

(7) Bottom blow boiler to remove deposits. Repeat twice, blowing from high water mark to low water mark each time.

(8) Secure pump No. 1 and pump No. 2, and close valves CW-4, CW-5 and CW-6.

(9) Secure instrumentation.

(10) Secure power to feed pump.

(11) De-energize individual circuit breakers.

(12) De-energize circuit breaker on control panel; depress stop button. Turn key switch off.

B. Using house steam

(1) Open valve MS-4, then close valve MS-3.

(2) Close valve MS-2.

(3) Close valve FW-4.

(4) Pump condensate from secondary condenser hotwell to house condensate return. Secure valve C-3.

(5) Follow steps (4), (6), (8), (9), (11) and (12) as outlined above for using boiler.

4. SECONDARY SYSTEMS

A. Vacuum system

Vacuum is established by a mechanical vacuum pump and is controlled by a vacuum regulator mounted on steam return line (near valve MS-6). The vacuum pump is separated from the condenser system by a refrigerated cold trap to prevent moisture from entering the pump. The cold trap hotwell is drained intermittently, when level in cold trap hotwell dictates.

B. Desuperheater

Valve FW-4 controls flow of feedwater ($60^{o}C$) to spray nozzles. Optimum flow level is between 15 and 20

percent flow on rotameter when using boiler and between 20 and 30 percent flow on rotameter when using house steam.

5. SAFETY DEVICES

A. Emergency power shut-off

To secure all power to the system in an emergency depress the red button on the right of the main control panel next to the key switch.

B. Boiler

There are three lights on the boiler

(1) The white light will light indicating that the electrical circuit for the boiler has been energized and that all controls are working properly.

(2) The amber light will light whenever the element is operating and will go out whenever it shuts off (when boiler reaches pressure).

(3) The red light will also light and will remain on at all times unless for some reason, the heating element overheats, it will then be shut off automatically by the thermostatic control on the heater. As soon as the red light goes out this means that the heating element and the boiler have failed safe.

(4) The mercury switch mounted on the main control panel secure power to the heating elements of the boiler when the steam pressure exceeds 25 psig. Power is restored to the heating elements when the pressure drops to approximately 15 psig.

(5) A low water level limit switch is contained within the boiler, and when the water level inside the boiler drops below a present level, power is secured to the boiler and will not be restored until the water level is above the present height.

(6) The relief valve mounted on the boiler is set to lift at 30 psig.

Section 1:

ENERGIZE INSTRUMENTATION

A. Multichannel pyrometer

B. Autodata 9 recorder and amplifier

C. Program Autodata using following procedure:

SET TIME:

(1) All alarms and output switches off

(2) Set date/time on thumbwheels (24 hour clock)

(3) Set the display switch to "time"

(4) Lift "set time" switch

ASSIGNING MULTIPLE CHANNELS:

(1) Set display switch to "off"

(2) Check that all alarms and output switches are still off.

(3) Set the scan switch to "continuous".

(4) Lift the slow switch.

(5) Set the first channel thumbwheels to "000" and last channel thumbwheels to "001".

(6) To assign channel "0" and "1" depress and hold the 10V and HI RES buttons for at least one scan and

lift scan start switch to start scanning.

(7) Set the last channel thumbwheels to "039" before setting the first channel thumbwheels to "001".

(8) Depress the "skip" button to skip channels 1 through 39.

(9) Set the last channel thumbwheels to "054" before setting the first channel thumbwheels to "040".

(10) To assign channels 40 thru 54 depress and hold the T/^{o}C and HI RES buttons for at least one complete scan.

INTERVAL SCAN:

(1) Set thumbwheels to interval desired between scans (usually one minute).

(2) Depress to "stop/enter" switch.

(3) Set the display switch to "interval".

(4) Depress the "set interval" switch.

(5) Set the scan switch to "interval"/

(6) Set the first channel thumbwheels to "000".

(7) Set the last channel thumbwheels to "054".

(8) Lift the "scan start" switch.

Use the following as needed/desired:

(1) Printer on/off.

(2) Slow switch.

(3) Single channel display.

APPENDIX C

SAMPLE CALCULATIONS

A sample calculation is performed here to illustrate how the data reduction program [11] progresses to the results. The GENERAL ATOMIC, 45° spiral angle - AISI 409 tube, Run number 10 at 70 percent flow (25.94 GPM) was selected at random to perform this analysis.

The water property calculations are shown in section 1. Section 2 of this appendix corresponds to the calculations performed for plain end inside diameter and section 3 corresponds to the calculations performed for hydraulic diameter.

INPUT PARAMETERS

Tube	GENERAL ATOMIC, AISI 409
Run Number	10
Tube inside diameter, Pain end (D_i)	0.01925 m.
Tube outside diameter, (D_o)	0.0202999 m.
Enhanced section length (L_{ts})	0.97155 m.
Smooth end length (L_s)	0.428625 m.
Enhanced section cross sectional flow area, (A_c)	0.000331 m^2
Outside nominal surface area (A_n)	0.0619596 m^2
Tube thermal conductivity, (kW)	22 W/m.°C
Wall resistance, (Rw)	24.5×10^{-6} m^2°C/w
Tube hydraulic diameter, (D_h)	0.0162814 m.
Inside wetted perimeter, (P_{wi})	0.08128 m.
Outside wetted perimeter, (P_{wo})	0.084328 m.

Cooling water in, (Tc_i)	$20.9^{\circ}C$
Cooling water out, (Tc_o)	$24.225^{\circ}C$
Average cooling water temperature (T_b, T_{br})	$22.5625^{\circ}C$, $295.7125^{\circ}K$ $72.6125^{\circ}F$, $532.2825^{\circ}R$
Steam vapor temperature, (T_v)	$67.65^{\circ}C$
Tube wall temperature, (T_w)	$301.75^{\circ}K$
Tube pressure drop, (P_m)	21.9118 kPa
% Flow	70
Tube inlet contraction factor Tube outlet expansion factor	Kc Ke } Kc + Ke = 0.070
Condensation rate, (Q_{con})	$0.032871\ m^3/hr$
Saturation temperature	$60.555^{\circ}C$

Section 1, Water Properties

$$k = 0.59303069 + (0.0019248784)(T_b) - (0.70238534\times10^{-5})(T_b)^2 - (2.0913612\times10^{-10})(T_b)^3$$

$$k = 0.59303069 + (0.0019248784)(22.5625) - (0.70238534\times10^{-5})(22.5625)^2 - (2.0913612\times10^{-10})(22.5625)^3$$

$$k = 0.63288275\ w/m.^{\circ}C$$

$$\rho = 1001.434664 - (0.21175821)(T_b) - (0.0023913147)(T_b)^2$$

$$\rho = 1001.434664 - (0.21175821)(22.5625) - (0.0023913147)(22.5625)^2$$

$$\rho = 995.43953\ kg/m^3$$

$$\mu = (4.1335979\times10^{-4})\exp\left[(0.0046066532)(T_{br}) + (4759.5941)/(T_{br}) - 10.59252566\right]$$

$$\mu = (4.1335979\times10^{-4})\exp\left[(0.004606532)(532.2825) + (4759.5941)/(532.2825) - 10.59252566\right]$$

$\mu = 9.2115311 \times 10^{-4}$ kg/m.sec = 3.3161512 kg/m.hr

$c_p = 4.2092198 - (0.0013594085)(T_b) + (1.3948397 \times 10^{-5})(T_b)^2$

$c_p = 4.2092198 - (0.0013594085)(22.5625) + (1.3948397 \times 10^{-5})(22.5625)^2$

$c_p = 4.1856488$ kJ/kg.^{o}C

$\dot{m} = (GPM)\ (0.00006309)\ (\rho)$

$\dot{m} = (25.94)(0.00006309)(995.43953)$

$\dot{m} = 1.6290911$ kg/sec = 5864.7281 kg/hr

$$Pr = \frac{\mu c_p}{k}$$

$$Pr = \frac{(9.2115311 \times 10^{-4})(4.1856488 \times 10^{3})}{0.63288275}$$

$Pr = 6.092$

Section 2, Plain-End-Tube Reduction

1. Determination of cooling water velocity

$$v = \frac{4\dot{m}}{\rho \pi D_i^{\,2}}$$

$$v = \frac{(4)(5864.7281)}{(995.43953)(\pi)(0.01925)^2}$$

$v = 20243.316$ m/hr

$v = 5.62314$ m/sec.

2. Determination of mass flow rate per unit area

$$G = \frac{4\dot{m}}{\pi D_i^{\,2}} = \rho v$$

$G = (995.43953)(20243.316)$

$G = 20,150,997.$ kg/m^{2}hr

$G = 5597.499$ kg/m^{2}sec

3. Determination of Reynolds Number

$$Re = \frac{D_i G}{\mu}$$

$$Re = \frac{(0.01925)(5597.499)}{(9.2115311 \times 10^{-4})}$$

$$Re = 116,974.9$$

4. Determination of Overall Heat Transfer Coefficient

$$U_n = \frac{\dot{m} c_p}{A_n} \ln\left[\frac{T_v - Tc_i}{T_v - Tc_o}\right]$$

$$U_n = \frac{(1.6290911)(4.1856488 \times 10^3)}{(0.0619596)} \ln\left[\frac{(67.65-20.9)}{(67.65-24.225)}\right]$$

$$U_n = 8119.55 \ w/m^2.{}^oC$$

5. Determination of Corrected Overall Heat Transfer Coefficient

$$U_c = \frac{1}{\frac{1}{U_n} - Rw}$$

$$U_c = \frac{1}{\frac{1}{8119.55} - 24.5 \times 10^{-6}}$$

$$U_c = 10,135.86 \ \ w/m^2.{}^oC$$

6. Determination of Friction Factor

$$f_s = \frac{0.046}{(Re)^{0.2}}$$

$$f_s = \frac{0.046}{(116,974.9)^{0.2}}$$

$$f_s = 0.00445799$$

(a) Smooth End Pressure Drop

$$\Delta P_s = \frac{4 f_s G^2 \left(\frac{L_s}{D_i}\right)}{\rho 2 g_c}$$

$$\Delta P_s = \frac{(4)(0.00445799)(5597.499)^2 \left(\frac{0.428625}{0.01925}\right)}{(995.43953)(2)}$$

$$\Delta P_s = 6.24869 \text{ kPa}$$

(b) Cooling Water Velocity At Test Section

$$v_{ts} = \frac{\dot{m}}{\rho A_c}$$

$$v_{ts} = \frac{(5864.7281)}{(995.43953)(0.000331)}$$

$$v_{ts} = 17{,}779.385 \text{ m/hr}$$

$$v_{ts} = 4.94427 \text{ m/sec}$$

(c) Expansion And Contraction Pressure Drop

$$\Delta P_{e/cn} = \frac{v_{ts}^2}{2 g_c}(K_c + K_e)$$

$$\Delta P_{e/cn} = \frac{(995.43953)(4.94427)^2}{(2)} (0.070)$$

$$\Delta P_{e/cn} = 0.8517 \text{ kPa}$$

(d) Test Section Pressure Drop

$$\Delta P_{ts} = \Delta P_m - \Delta P_s - \Delta P_{e/cn}$$

$$\Delta P_{ts} = 21.9118 - 6.2469 - 0.8517$$

$$\Delta P_{ts} = 14.8114 \text{ kPa}$$

$$f = \frac{\Delta P_{ts}\ 2g_c\ \rho}{4G^2 \left(\frac{L_{ts}}{D_i}\right)}$$

$$f = \frac{(995.43953)(14.8114 \times 10^3)(2)}{(4)(5597.499)^2 \quad \frac{0.97155}{0.01925}}$$

$$f = 0.00466185$$

7. Determination of Wilson Plot Parameters

(a) Ordinate

$$Y = \frac{1}{U_n}$$

$$Y = \frac{1}{8119.55} = 1.231595 \times 10^{-4} \text{ m}^2\text{°C/W}$$

(b) Abscissa

$$X = \frac{1}{(Re)^{0.8}\ (Pr)^{1/3} \left(\frac{\mu}{\mu_w}\right)^{0.14}}$$

$$\mu_w = (4.1335979 \times 10^{-4}) \exp \left[(0.004606532)(T_{wr}) + (4759.5941)/(T_{wr}) - 10.59252566 \right]$$

$$\mu_w = (4.1335979\text{x}10^{-4})\exp\left[\ (0.004606532)(543.15) + (4759.5941)/(543.15) \ -10.59252566\ \right]$$

$$\mu_w = 8.0979128\text{x}10^{-4} \text{ kg/m.sec}$$

$$X = \frac{1}{(116,974.9)^{0.8}(6.092)^{1/3}\left[\frac{9.2115311\text{x}10^{-4}}{8.0979128\text{x}10^{-4}}\right]^{0.14}}$$

$$X = 4.743567\text{x}10^{-5}$$

8. Determination of Sieder-Tate Coefficient

$C_i = \frac{D_o}{MK}$, where M = slope of linear regression subroutine

M = 0.7747896, from linear regression subroutine

$$C_i = \frac{(0.0202999)}{(0.7747896)(0.63288275)}$$

$$C_i = 0.0413987$$

9. Determination of Inside Heat Transfer Coefficient

$$h_i = \frac{C_i}{D_i} k\ (Re)^{0.8}(Pr)^{1/3}\left(\frac{\mu}{\mu_w}\right)^{0.14}$$

$$h_i = \left(\frac{0.0413987}{0.01925}\right)(0.63288275)(116,974.9)^{0.8}(6.092)^{1/3}\left(\frac{9.2115311}{8.0979128}\right)^{0.14}$$

$$h_i = 28,692.88 \text{ W/m.}^{2o}\text{C}$$

10. Determination of Outside Heat Transfer Coefficient

$$h_o = \frac{1}{\frac{1}{U_n} - Rw - \frac{D_o}{D_i h_i}}$$

$$h_o = \frac{1}{\frac{1}{8119.55} - 24.5\times10^{-6} - \frac{(0.0202999)}{(0.01925)(28,692.88)}}$$

$$h_o = 16,153.3 \ W/m^2.{}^oC$$

11. Determination of Nusselt Number

$$Nu = \frac{h_i D_i}{k}$$

$$Nu = \frac{(28,692.88)(0.01925)}{(0.63288275)}$$

$$Nu = 872.733$$

12. Determination of Stanton Number

$$St = \frac{Nu}{RePr}$$

$$St = \frac{(872.733)}{(116,974.9)(6.092)}$$

$$St = 1.224698\times10^{-3}$$

13. Determination of Performance Factor

$$TPF = \frac{2j}{f}$$

$$j = (St)(Pr)^{2/3} = (1.224698\times10^{-3})(6.092)^{2/3}$$

$$j = 4.085096\times10^{-3}$$

$$TPF = \frac{(2)(4.085096\times10^{-3})}{(0.00466185)}$$

$$TPF = 1.75256$$

14. Determination of Heat Transfer Rate

$$TRAN1 = \dot{Q}\rho\left[c_{pv}\ (T_v - T_{sat}) + h_{fg} + c_{pl}\ (T_{sat} - T_{con})\right]$$

$$\rho = 1001.434664 - (0.21175821)(T_{con}) - (0.0023913147)(T_{con})^2$$

$$\rho = 1001.434664 - (0.21175821)(51.7) - (0.0023913147)(51.7)^2$$

$$\rho = 984.09498\ kg/m^3$$

$$TRAN1 = (3.2871x10^{-2})(984.09498)\left[1.9175544\ (67.65-60.555) + (2357.6336) + 4.1868\ (60.555-51.7)\right]$$

$$TRAN1 = 7.7904706x10^{4}\ kJ/hr$$

$$TRAN1 = (7.7904706x10^{4})(2.77731x10^{-4})$$

$$TRAN1 = 21.6366\ kW$$

$$TRAN2 = \dot{m}c_p\ (Tc_o - Tc_i)$$

$$TRAN2 = (5864.7281)(4.1856488)\left[24.225-20.9\right]$$

$$TRAN2 = 8.1621x10^{4}\ kj/hr$$

$$TRAN2 = (8.1621x10^{4})(2.77731x10^{-4})$$

$$TRAN2 = 22.6687\ kW$$

15. Determination of Area Ratios

(a) $R_{ext}=0$

$$Re_s = \left[\frac{0.027\ f\ Re^3}{0.046\left(Nu/(Pr^{1/3})(\mu/\mu_w)^{0.14}\right)}\right]^{0.5}$$

$$Re_s = \left[\frac{(0.027)(0.00466185)(116974.9)^3}{(0.046)\left(872.733\Big/(6.092^{1/3})\left(\frac{9.2115311x10^{-4}}{8.0979128x10^{-4}}\right)^{0.14}\right)}\right]^{0.5}$$

$$Re_s = 96603.056$$

$$f_s = \frac{0.046}{(Re_s)^{0.2}}$$

$$f_s = \frac{0.046}{(96603.056)^{0.2}}$$

$$f_s = 0.0046319052$$

$$\frac{A_a}{A_s} = \frac{(Re_s)^3 (f_s)}{(Re)^3 (f)} = \frac{(96603.056)^3 (0.0046319052)}{(116974.9)^3 \ (0.00466185)}$$

$$\frac{A_a}{A_s} = 0.55962$$

(b) $R_{ext} \neq 0$

$F_1 = 1.0$ (fouling correction)

$F_2 = 0.89$ (material correction for AISI 409 steel)

$F_3 = 1.02$ (temperature correction factor inlet cooling water)

$C' = 2922$ (for smooth tube) ; $C = 2652.59$

$U_a = U_n / F_3 = 8119.55 / 1.02$

$U_a = 7960.343 \ W/m^2.{}^oC$

$$v_s = \left[\frac{f v^3 C}{0.0046 U_a} \left(\frac{\rho D_i}{\mu} \right)^{0.2} \right]^{1/2.3}$$

$$v_s = \left[\frac{(0.00466185)(5.62314)^3 (2652.59)}{(0.046)(7960.343)} \left(\frac{(995.43953 \times 0.01925)}{(9.2115311 \times 10^{-4})} \right)^{0.2} \right]^{1/2.3}$$

$v_s = 5.175541 \ m/s$

$U_s = C(v_s)^{0.5} = 2652.59(5.1755411)^{0.5}$

$U_s = 6034.593 \ W/m^2.{}^oC$

$$\frac{A_a}{A_s} = \frac{U_s}{U_a} = \frac{6034.593}{7960.343}$$

$$\frac{A_a}{A_s} = 0.75808$$

Section 3, Tube Reduction Based Upon Hydraulic Diameter

1. Determination of Cooling Water Velocity

v_{ts} = 4.94427 m./sec

2. Determination of Mass Flow Rate Per Unit Area

$$G = \frac{\dot{m}}{A_c} = \frac{(5864.7281)}{(0.000331)}$$

G = 17,718,212. $kg/m^2.hr$

G = 4921.7256 $kg/m^2.sec$

3. Determination of Reynolds Number

$$Re = \frac{D_h G}{\mu}$$

$$Re = \frac{(0.0162814)(17,718,212)}{(3.3161512)}$$

Re = 86,991.599

4. Determination of Overall Heat Transfer Coefficient

U_n = 8,119.55 $W/m^2.^oC$

5. Determination of Corrected Overall Heat Transfer Coefficient

U_c = 10,135.86 $W/m^2.^oC$

6. Determination of Friction Factor

ΔP_{ts} = 14.8114 kPa

$$f = \frac{\Delta P_{ts} 2 g_c \rho}{4G^2 \left(\frac{L_{ts}}{D_h}\right)}$$

$$f = \frac{(995.43953)(14.8114 \times 10^3)(2)}{(4)\ (4921.7256)^2 \left(\frac{0.97155}{0.0162814}\right)}$$

$f = 0.0051$

7. Determination of Wilson Plot Parameters

(a) Ordinate

$$Y = \frac{1}{U_n}$$

$$Y = 1.231595 \times 10^{-4} \quad \frac{m^2 . {}^{o}C}{W}$$

(b) Abscissa

$$X = \frac{1}{(Re)^{0.8} (Pr)^{1/3} \left(\frac{\mu}{\mu_w}\right)^{0.14}}$$

$$X = \frac{1}{(86,991.599)^{0/8} (6.092)^{1/3} \left(\frac{9.2115311}{8.0979128}\right)^{0.14}}$$

$X = 6.0117 \times 10^{-5}$

8. Determination of Sieder-Tate Coefficient

$$C_i = \frac{A_n D_h}{P_w L_{ts} M k}$$

$$C_i = \frac{(0.0619596)(0.0162814)}{(0.08128)(0.97155)(0.61141126)(0.63288275)}$$

$C_i = 0.0330137$

9. Determination of Inside Heat Transfer Coefficient

$$h_i = \frac{C_i k}{D_h} (Re)^{0.8} (Pr)^{1/3} \left(\frac{\mu}{\mu_w} \right)^{0.14}$$

$$H_i = \frac{(0.0330137)(0.63288275)}{(0.0162814)} (86,991.599)^{0.8} (6.092)^{1/3} \left(\frac{9.2115311}{8.0799128} \right)^{0.14}$$

$$h_i = 21,346.776 \ W/m^2.{}^oC$$

10. Determination of Outside Heat Transfer Coefficient

$$h_o = \frac{1}{\frac{Pw_o L_{ts}}{A_n U_n} - \frac{Pw_o}{P_{bar}} Rw - \frac{Pw_o}{Pw_i h_i}}$$

$$h_o = \frac{1}{\frac{(0.084328)(0.97155)}{(0.0619596)(8119.55)} - \frac{(0.084328)}{(0.082804)} (24.5x10^{-6}) - \frac{(0.084328)}{(0.08128((21346.771)}}$$

$$h_o = 11,198.192 \ W/m^2.{}^oC$$

11. Determination of Nusselt Number

$$N_u = \frac{h_i D_h}{k}$$

$$N_u = \frac{(21,346.776)(0.0162814)}{(0.63288275)}$$

$$N_u = 549.1624$$

12. Determination of Stanton Number

$$St = \frac{Nu}{RePr} = \frac{(549.1624)}{(86,991.599)(6.092)}$$

$$St = 1.0362477x10^{-3}$$

13. Determination of Tube Performance Factor

$$TPF = \frac{2j}{f}$$

$$j = StPr^{2/3}$$

$$j = (1.0362477 \times 10^{-3})(6.092)^{2/3}$$

$$j = 0.0034565$$

$$TPF = \frac{(2)(0.0034565)}{(0.0051)}$$

$$TPF = 1.35549$$

APPENDIX D

UNCERTAINTY ANALYSIS

The basic equations used in this section are reproduced from Reilly [11]. The general form of the Kline and McClintock [24] "Second Order" equation is used to compute the probable error in the results. For some resultant, R, which is a function of primary variables x_1, x_2, ...x_n, the probable error in R, R is given by:

$$\delta R = \left[\left(\frac{\delta R}{\delta x_1}\,\delta x_1\right)^2 + \left(\frac{\delta R}{\delta x_2}\,\delta x_2\right)^2 + \ldots + \left(\frac{\delta R}{\delta x_n}\,\delta x_n\right)^2 \right]^{1/2} \qquad \text{(D1)}$$

where x_1, x_2,... x_n are the probable errors in each of the measured variables.

1. Uncertainty In Overall Heat Transfer Coefficient, U_n

The overall heat transfer coefficient is given by equation (5) in chapter III as:

$$U_n = \frac{\dot{m}c_p}{A_n} \ln\left(\frac{T_v - Tc_i}{T_v - Tc_o}\right) \qquad (5)$$

By applying equation (D-1) to equation (5) the following equation results:

$$\frac{\delta U_n}{U_n} = \left[\left(\frac{\delta A_n}{A_n}\right)^2 + \left(\frac{\delta c_p}{c_p}\right)^2 + \left(\frac{\delta \dot{m}}{\dot{m}}\right)^2 + \left(\frac{\delta T_v (Tc_i - Tc_o)}{(T_v - Tc_i)(T_v - Tc_o) \ln \frac{T_v - Tc_i}{T_v - Tc_o}}\right)^2 + \left(\frac{\delta T_{c_i}}{(T_v - Tc_i) \ln \frac{T_v - Tc_i}{T_v - Tc_o}}\right)^2 + \left(\frac{\delta Tc_o}{(T_v - Tc_o) \ln \frac{T_v - Tc_i}{T_v - Tc_o}}\right)^2 \right]^{1/2} \qquad \text{(D2)}$$

The following are the values assigned to the variables:

$\delta c_p = 0.0042$ kJ/kg.^{o}C

$\delta \dot{m} = 0.01\ \dot{m}$ kg/sec

$\delta T_v = 1.0\ ^{o}$C

$\delta Tc_i = 0.1\ ^{o}$C

$\delta Tc_o = 0.1^{o}$C

$\delta D_o = 0.00025$ m.

$\delta L_{ts} = 0.0015$ m.

$$A_n = \pi D_o L_{ts}$$

$$\frac{\delta A_n}{A_n} = \left[\left(\frac{\delta D_o}{D_o} \right)^2 + \left(\frac{\delta L_{ts}}{L_{ts}} \right)^2 \right]^{1/2}$$

$$\frac{\delta A_n}{A_n} = \left[\left(\frac{0.00025}{0.0202999} \right)^2 + \left(\frac{0.0015}{0.97155} \right)^2 \right]^{1/2}$$

$$\frac{\delta A_n}{A_n} = 0.0124$$

$$\frac{\delta U_n}{U_n} = \left[(0.0124)^2 + \left(\frac{0.0042}{4.1856488} \right)^2 + \left(\frac{0.01\ \dot{m}}{\dot{m}} \right)^2 + \left(\frac{(1.0)(-3.325)}{(46.75)(43.425)\ \ln \frac{46.75}{43.425}} \right)^2 + \left(\frac{(0.1)}{(46.75)\ \ln \frac{46.75}{43.425}} \right)^2 + \left(\frac{(0.1)}{(43.425)\ \ln \frac{46.75}{43.425}} \right)^2 \right]^{1/2}$$

$$\frac{\delta U_n}{U_n} = 0.0506$$

$$U_n = 8119.55 \pm 410.85\ \ W/m^2.^{o}C$$

2. Uncertainty In Inside Heat Transfer Coefficient, h_i

The probable error in the inside heat transfer coefficient is given by:

$$\frac{\delta h_i}{h_i} = \left[\left(\frac{\delta k}{k}\right)^2 + \left(\frac{\delta D_i}{D_i}\right)^2 + \left(\frac{0.8\delta Re}{Re}\right)^2 + \left(\frac{0.333\delta Pr}{Pr}\right)^2 + \left(\frac{\delta C_i}{C_i}\right)^2 + \left(\frac{0.14\delta(\mu/\mu_w)}{\mu/\mu_w}\right)^2\right]^{1/2} \quad \text{(D3)}$$

where:

$\delta k = 0.030$ W/m.°C

$\delta D_i = 0.00025$ m.

$\delta Pr = 0.10$

$\delta\left(\frac{\mu}{\mu_w}\right) = 0.050$

The probable error in the Reynolds number is given by:

$$\frac{\delta Re}{Re} = \left[\left(\frac{\delta G}{G}\right)^2 + \left(\frac{\delta \mu}{\mu}\right)^2 + \left(\frac{\delta D_i}{D_i}\right)^2\right]^{1/2} \quad \text{(D4)}$$

where,

$$\frac{\delta G}{G} = \left[\left(\frac{0.01\dot{m}}{\dot{m}}\right)^2 + \left(2\frac{\delta D_i}{D_i}\right)^2\right]^{1/2} \quad \text{(D5)}$$

$$\frac{\delta G}{G} = \left[(0.01)^2 + \left(\frac{(2.0)(0.00025)}{0.01925}\right)^2\right]^{1/2}$$

$$\frac{\delta G}{G} = 0.0278$$

Since $\delta\mu = 0.15$ kg/m.hr. then

$$\frac{\delta Re}{Re} = \left[(0.0278)^2 + \left(\frac{0.15}{3.3161512}\right)^2 + \left(\frac{0.00025}{0.01925}\right)^2 \right]^{1/2}$$

$$\frac{\delta Re}{Re} = 0.0547$$

$$Re = 116975 \pm 6399$$

The probable error in the coefficient C_i is given by:

$$\frac{\delta C_i}{C_i} = \left[\left(\frac{\delta D_o}{D_o}\right)^2 + \left(\frac{\delta Slope}{Slope}\right)^2 + \left(\frac{\delta k}{k}\right)^2 \right]^{1/2} \qquad (D6)$$

where

$\delta D_o = 0.00025$

$\delta k = 0.030$ W/m.$^\circ$C

$\delta slope = 0.035$ slope

$$\frac{\delta C_i}{C_i} = \left[\left(\frac{0.00025}{0.0202999}\right)^2 + (0.035)^2 + \left(\frac{0.030}{0.63288275}\right)^2 \right]^{1/2}$$

$$\frac{\delta C_i}{C_i} = 0.06$$

$$C_i = 0.0413987 \pm 0.00248$$

Using the above information, the probable error in the inside heat transfer coefficient can be calculated as:

$$\frac{\delta h_i}{h_i} = \left[\left(\frac{0.030}{0.63288275}\right)^2 + \left(\frac{0.00025}{0.01925}\right)^2 + (0.8 \times 0.0547)^2 + \left(\frac{0.333 \times 10}{6.092}\right)^2 + (0.06)^2 + \left(\frac{0.14 \times 0.050}{1.1375192}\right)^2 \right]^{1/2}$$

$$\frac{\delta h_i}{h_i} = 0.0894$$

$$h_i = 28693 \pm 2565 \text{ W/m}^2.^\circ\text{C}$$

3. Uncertainty In The Outside Heat Transfer Coefficient, h_o

The probable error in the outside heat transfer coefficient is given by:

$$\frac{\delta h_o}{h_o} = \left\{ \left[\frac{\delta U_n}{U_n^2 \left(\frac{1}{U_n} - Rw - \frac{D_o}{D_i h_i} \right)} \right]^2 + \left[\frac{\delta R_w}{\left(\frac{1}{U_n} - Rw - \frac{D_o}{D_i h_i} \right)} \right]^2 + \left[\frac{\left(\frac{D_o}{D_i h_i} \right) \left(\frac{\delta h_i}{h_i} \right)}{\frac{1}{U_n} - Rw - \frac{D_o}{D_i h_i}} \right]^2 \right\}^{1/2} \quad \text{(D7)}$$

where:

$\frac{\delta U_n}{U_n} = 0.0506$

$\frac{\delta h_i}{h_i} = 0.0894$, and

Assuming $\delta Rw = 0.10Rw$, then $\delta Rw = 2.45 \times 10^{-6}\ m^2\ ^oC/W$

Also, $\left(\frac{1}{U_n} - Rw - \frac{D_o}{D_i h_i} \right) = 6.1907 \times 10^{-5}\ m^2.^oC/W$

with this information:

$$\frac{\delta h_o}{h_o} = \left\{ \left[\frac{0.0506}{(8119.55)(6.1907 \times 10^{-5})} \right]^2 + \left[\frac{2.45 \times 10^{-6}}{6.1907 \times 10^{-5}} \right]^2 + \left[\frac{0.0000368)(0.0894)}{6.1907 \times 10^{-5}} \right]^2 \right\}^{1/2}$$

$\frac{\delta h_o}{h_o} = 0.121$

$h_o = 16153 \mp 1955\ W/m^2C$

4. Uncertainty In Tube Performance Factor, 2j/f

Since the Colburn Analogy defines j as $StPr^{2/3}$, the probable error in the Tube Performance Factor 2j/f is given by:

$$\frac{\delta TPF}{TPF} = \left[\left(\frac{St}{St}\right)^2 + \left(\frac{2}{3}\ \frac{\delta Pr}{Pr}\right)^2 + \left(\frac{\delta f}{f}\right)^2 \right]^{1/2} \qquad \text{(D8)}$$

where

$$\frac{\delta St}{St} = \left[\left(\frac{\delta Nu}{Nu}\right)^2 + \left(\frac{\delta Re}{Re}\right)^2 + \left(\frac{\delta Pr}{Pr}\right)^2 \right]^{1/2} \qquad \text{(D9)}$$

$$\frac{\delta Nu}{Nu} = \left[\left(\frac{\delta h_i}{h_i}\right)^2 + \left(\frac{\delta D_i}{D_i}\right)^2 + \left(\frac{\delta k}{k}\right)^2 \right]^{1/2} \qquad \text{(D10)}$$

Assuming $\delta\Delta P_{ts} = 0.02\ \Delta P_{ts}$, $\delta\rho = 0.01\rho$ the following numerical values result:

$$\frac{\delta f}{f} = \left[(0.02)^2 + (2x0.0278)^2 + \left(\frac{0.0015}{0.97155}\right)^2 + (0.01)^2 + \left(\frac{0.00025}{0.01925}\right)^2 \right]^{1/2}$$

$$\frac{\delta f}{f} = 0.061$$

$$\frac{\delta Nu}{Nu} = \left[(0.105)^2 + \left(\frac{0.00025}{0.01925}\right)^2 + \left(\frac{0.030}{0.63288275}\right)^2 \right]^{1/2}$$

$$\frac{\delta Nu}{Nu} = 0.116$$

$$\frac{\delta St}{St} = \left[(0.116)^2 + (0.0547)^2 + \left(\frac{0.10}{6.092}\right)^2 \right]^{1/2}$$

$$\frac{\delta St}{St} = 0.129$$

$$\frac{\delta TPF}{TPF} = \left[(0.129)^2 + \left(\frac{2}{3} \times \frac{0.10}{6.092}\right)^2 + (0.061^2) \right]^{1/2}$$

$$\frac{\delta TPF}{TPF} = 0.143$$

$$TPF = 1.75256 \pm 0.2506$$

5. Uncertainty In The Area Ratios

(a) $R_{ext} = 0$

Using equation (26) the probable error in the area ratio ($R_{ext} = 0$) is given by:

$$\frac{\delta(A_a/A_s)}{A_a/A_s} = \left[\left(\frac{\delta Nu_s}{Nu_s}\right)^2 + \left(\frac{\delta Nu_a}{Nu_a}\right)^2\right]^{1/2} \qquad (D12)$$

where

$$\frac{\delta Nu_a}{Nu_a} = 0.116$$

in addition, from equation (28),

$$\frac{\delta Re_s}{Re_s} = \left[\left(\frac{1}{2}\frac{\delta f_a}{f_a}\right)^2 + \left(\frac{3}{2}\frac{\delta Re_a}{Re_a}\right)^2 + \left(\frac{1}{6}\frac{\delta Pr}{Pr}\right)^2 + \left(0.07\frac{\delta(\mu/\mu_w)}{(\mu/\mu_w)}\right)^2 + \left(\frac{1}{2}\frac{\delta Nu_a}{Nu_a}\right)^2\right]^{1/2}$$

$$\frac{Re_s}{Re_s} = \left[\left(\frac{1}{2} \times 0.061\right)^2 + \left(\frac{3}{2} \times 0.0547\right)^2 + \left(\frac{1}{6} \times \frac{0.10}{6.092}\right)^2 + \left(0.07 \times \frac{0.050}{1.1375192}\right)^2 + \left(\frac{1}{2} \times 0.116\right)^2\right]^{1/2}$$

$$\frac{\delta Re_s}{Re_s} = 0.105$$

and using equation (27)

$$\frac{\delta Nu_s}{Nu_s} = \left[\left(0.8 \frac{\delta Re_s}{Re_s} \right) + \left(\frac{1}{3} \times \frac{\delta Pr}{Pr} \right)^2 + \left(0.14 \times \frac{\delta (\mu/\mu_w)}{(\mu/\mu_w)} \right)^2 \right]^{1/2} \quad \text{(D13)}$$

$$\frac{\delta Nu_s}{Nu_s} = \left[(0.8 \times 0.105)^2 + \left(\frac{1}{3} \times \frac{0.10}{6.092} \right)^2 + \left(0.14 \times \frac{0.050}{1.1375192} \right)^2 \right]^{1/2}$$

$$\frac{\delta Nu_s}{Nu_s} = 0.0844$$

$$\frac{\delta (A_a/A_s)}{(A_a/A_s)} = \left[(0.0844)^2 + (0.116)^2 \right]^{1/2}$$

$$\frac{\delta (A_a/A_s)}{(A_a/A_s)} = 0.143$$

$$A_a/A_s (R_{ext=0}) = 0.55962 \pm 0.08$$

(b) $R_{ext} \neq 0$

From equation (32), the probable error in the area ratio ($R_{ext} \neq 0$) is given by:

$$\frac{\delta (A_a/A_s)}{(A_a/A_s)} = \left[\left(\frac{\delta U_s}{U_s} \right)^2 + \left(\frac{\delta U_a}{U_a} \right)^2 \right]^{1/2} \quad \text{(D14)}$$

where:

$$\frac{\delta U_a}{U_a} = 0.0506$$

and from equation (33)

$$\frac{\delta U_s}{U_s} = \frac{1}{2} \cdot \frac{\delta v_s}{v_s} \qquad \text{(D-15)}$$

Equation (29) can be used as follows:

$$\frac{\delta v_s}{v_s} = \left[\left(\frac{\delta Re_s}{Re_s} \right)^2 + \left(\frac{\delta D_i}{D_i} \right)^2 + \left(\frac{\delta \rho}{\rho} \right)^2 + \left(\frac{\delta \mu}{\mu} \right)^2 \right]^{1/2} \qquad \text{(D-16)}$$

$$\frac{\delta v_s}{v_s} = \left[(0.105)^2 + \left(\frac{0.00025}{0.01925} \right)^2 + (0.01)^2 + \left(\frac{0.15}{3.3161512} \right)^2 \right]^{1/2}$$

$$\frac{\delta v_s}{v_s} = 0.115$$

$$\frac{\delta (A_a/A_s)}{(A_a/A_s)} = \left[\left(\frac{1}{2} \times 0.115 \right)^2 + (0.0506)^2 \right]^{1/2}$$

$$\frac{\delta (A_a/A_s)}{(A_a/A_s)} = 0.077$$

$$A_a/A_s \ (R_{ext} \neq 0) = 0.758 \pm 0.058$$

BIBLIOGRAPHY

1. Search, H.T., A Feasibility Study Of Heat Transfer Improvement In Marine Steam Condensers, MSME, Naval Postgraduate School, Monterey, Ca., December 1977.

2. Bergles, A.E., Summary Of Augmentation Of Two Phase Heat Transfer, paper presented at ASHRAE Semi-Annual Meeting, Dallas, Texas, February, 1976.

3. Bergles, A.E., and Jensen, M.K., Enhanced Single-Phase Heat Transfer For Ocean Thermal Energy Conversion Systems, Report HTL-13 ISU-ERI-AMES-77314, ERI Project 1278, April, 1977.

4. Palen, J., Cham, B., and Taborek, J., Comparison Of Condensation Of Steam On Plain And Turbotec Spirally Grooved Tubes In A Baffle Shell-And-Tube Condenser, Heat Transfer Research, Inc., Report 2439-300/6, January 1971.

5. Eiessenberg, D.M., An Investigation Of The Variables Affecting Steam Condensation On The Outside Of A Horizontal Tube Bundle, PhD dissertation, University of Tennessee, December 1972.

6. Watkinson, A.P., Miletti, D.L., and Tarasoof, P., Heat Transfer And Pressure Drop Of Internally Finned Tubes, AICHE Symposium Series, No. 131, Vol. 69 1973.

7. Catchpole, J.P., and Drew, B.C.H., "Evaluation Of Some Shaped Tubes For Steam Condensers," Steam Turbine Condensers, NEL Report No. 619, pp. 68-82, August 1976.

8. Young, E.H., Withers, J.G., and Lampert, W.B., Heat Transfer Characteristics Of Corrugated Tubes In Steam Condensing Applications, AICHE Paper No. 3, August 1975.

9. Beck, A.C., A Test Facility To Measure Heat Transfer Performance Of Advanced Condenser Tubes, MSME, Naval Postgraduate School, Monterey, California, January 1977.

10. Pence, D.T., An Experimental Study Of Steam Condensation On A Single Horizontal Tube, MSME, Naval Postgraduate School, Monterey, Ca., March 1978.

11. Reilly, D.J., An Experimental Investigation Of Enhanced Heat Transfer On Horizontal Condenser Tubes, MSME, Naval Postgraduate School, Monterey, Ca., March 1978.

12. Fenner, J.H., An Experimental Comparison Of Enhanced Heat Transfer Condenser Tubing, MSME, Naval Postgraduate School, Monterey, Ca., September 1978.

13. Acurex Autodata, Autodata Nine Technical Manual.

14. Holman, J.P., Heat Transfer, 4th ed., Mc-Graw-Hill, 1976.

15. Wilson, E.E., A Basis For Rational Design Of Heat Transfer Apparatus, paper presented at the spring meeting of Mechanical Engineers, Buffalo, N.Y., June 1965.

16. Briggs, D.E., and Young, E.H., Modified Wilson Plot Techniques For Obtaining Heat Transfer Correlations For Shell And Tube Heat Exchangers, Heat Transfer-Philadelphia, Vol. 65, No. 92, 1969.

17. Subroutine, NPS Computer Facility, Least Squares Polynominal, fitting, LSQPL2, Programmed by D.E. Harrison,

18. Kays, W.M., and London, A.L., Compact Heat Exchangers, McGraw-Hill, 1964.

19. Colburn, A.P., Trans. AICHE, 29:174, 1933.

20. Department Of The Navy, Bureau Of Ships, Design Data Sheet, DDS-4601-1, October 1953.

21. Marto, P.J., An Experimental Comparison Of Enhanced Heat Transfer Condenser Tubing, NPS Paper.

22. Young, E.H., and Withers, J.G., Steam Condensing On Vertical Rows Of Horizontal Corrugated And Plain Tubes, Ind. Eng. Chem. Process Des. Develop., Vol. 10, No. 1, 1971.

23. Newton, W.H., Performance Characteristics Of Rotating Non-capillary Heat Pipes, MSME, Naval Postgraduate School, Monterey, Ca., 1971.

24. The Chemical Rubber Company, Handbook Of Tables For Applied Engineering Science, CRC Press, 1976.

INITIAL DISTRIBUTION LIST

	No. Copies
1. Defense Technical Information Center Cameron Station Alexandria, Virginia 22314	2
2. Library, Code 0142 Naval Postgraduate School Monterey, California 93940	2
3. Department Ghairman, Code 69 Department of Mechanical Engineering Naval Postgraduate School Monterey, California 93940	2
4. Professor Paul J. Marto, Code 69Mx Department of Mechanical Engineering Naval Postgraduate School Monterey, California 93940	10
5. Professor Robert H. Nunn, Code 69Nn Department of Mechanical Engineering Naval Postgraduate School Monterey, California 93940	1
6. Deniz Kuvvetleri Komutanligi Egitim Daire Baskanligi Bakanliklar, Ankara/Turkey	2
7. Deniz Harp Okulu Komutanligi Heybeliada, Istanbul/Turkey	1
8. LT. Huseyin Ciftci Tirnova Mahallesi, 48.sok. No.60 Gonen, Balikesir/Turkey	3
9. Mr. Charles Miller Naval Sea Systems Command (0331) 2221 Jefferson Davis Hwy, CP #6 Arlington, Virginia 20360	1
10. Dr. P.T. Gilbert Yorkshire Imperial Metals Limited P.O. Box No. 166 Leeds LS1 1RD England	1
11. Mr. Walter Aerni Naval Ship Engineering Center (6145) Washington, D.C. 20362	1

12. Mr. Wayne L. Adamson 1
Naval Ship Research and Development Center (2761)
Annapolis, Maryland 21402

13. Professor W. Roetezel 1
Hochschule der Bundeswehr Hamburg
Holstenhofweg 85.2 Hamburg 70
West Germany

14. Dr. David Eissenberg 1
Oak Ridge National Laboratory
Post Office Box Y
Oak Ridge, Tennessee 37830

15. Miss Eleanor J. Macnair 1
Ship Department
Ministry of Defence
Director-General Ships, Block B
Foxhill, Bath, Somerset
England

16. Professor A.E. Bergles 1
Department of Mechanical Engineering
Iowa State University
Ames, Iowa 50010

17. Dr. A.L. London 1
4020 Amaranta Avenue
Palo Alto, California 94306

18. Mr. Norman F. Sather 1
Argonne National Laboratory
9700 S. Cass Avenue
Argonne, Illinois 60439

19. Mr. Jack S. Yampolsky 1
Senior Technical Advisor
Advanced Projects Division
General Atomic Company
P.O. Box 81608
San Diego, CA 92138

20. Mr. M.K. Ellingsworth 1
Office of Naval Research
800 N. Quincy Street
Arlington, VA 22217

21. Mr. John Michele 1
Oak Ridge National Laboratory
Oak Ridge, TN 37830

Thesis
C478835 Ciftci 186668
c.2
An experimental study of filmwise condensation on horizontal enhanced condenser tubing.